Titre: Title:	Processing and Patterning of Conducting Polymer Films for Flexible, Stretchable and Healable Electronics
Auteur: Author:	Shiming Zhang
Date:	2017
Type:	Mémoire ou thèse / Dissertation or Thesis
Référence: Citation:	Zhang, S. (2017). Processing and Patterning of Conducting Polymer Films for Flexible, Stretchable and Healable Electronics [Thèse de doctorat, École Polytechnique de Montréal]. PolyPublie. https://publications.polymtl.ca/2812/

UNIVERSITÉ DE MONTRÉAL

PROCESSING AND PATTERNING OF CONDUCTING POLYMER FILMS FOR FLEXIBLE, STRETCHABLE AND HEALABLE ELECTRONICS

SHIMING ZHANG

DÉPARTEMENT DE GÉNIE CHIMIQUE

ÉCOLE POLYTECHNIQUE DE MONTRÉAL

THÈSE PRÉSENTÉE EN VUE DE L'OBTENTION

DU DIPLÔME DE PHILOSOPHIAE DOCTOR

(GÉNIE CHIMIQUE)

NOVEMBRE 2017

UNIVERSITÉ DE MONTRÉAL

ÉCOLE POLYTECHNIQUE DE MONTRÉAL

Cette thèse intitulée :

PROCESSING AND PATTERNING OF CONDUCTING POLYMER FILMS FOR FLEXIBLE, STRETCHABLE AND HEALABLE ELECTRONICS

présentée par: ZHANG Shiming

en vue de l'obtention du diplôme de: Philosophiae Doctor

a été dûment acceptée par le jury d'examen constitué de:

M. AJJI Abdellah, Ph. D., président

M. CICOIRA Fabio, Ph. D., membre et directeur de recherche

Mme SANTATO Clara, Doctorat, membre et codirectrice de recherche

M. SAVADOGO Oumarou, D. d'état, membre

M. LIPOMI Darren John, Ph. D., membre externe

DEDICATION

To my parents, my wife and my son.

ACKNOWLEDGEMENTS

I am grateful for all the support, guidance and help that I have received over the last 4 years at Polytechnique Montreal.

First, I would like to express my deepest thanks to my research director, Prof. Fabio Cicoira, for giving me the opportunity to work in the field of organic bioelectronics. Thank you for guiding, supporting, and encouraging me during my study in Montreal. Your passion for science and your personal involvement in my projects helped me to overcome many difficult moments. Thank you for offering me freedom on the projects, for putting so much confidence in me, and for entrusting me. Thank you for always be available to discuss the projects with me. Thank you for your concerns and what you have done on my family issues in the past four years, for which I will always be grateful. No success will be there without your continuous care of me.

I am thankful to my co-supervisor, Prof. Clara Santato, for her advices and moral support. Her patience and laboratory space were invaluable for my projects. Thank you for your encouragement and your support on me. I will always be grateful for your special care of my family.

I am grateful to the jury members, Prof. Abdellah Ajii, Prof. Oumarou Savadogo, Prof. Frédéric Lesage, Prof. Frédéric Sirois, and Prof. Darren Lipomi, for their time and interest in my work.

I am very grateful to NSERC for financial support through a Vanier Canada Graduate Scholarship, which motived me to set high standard for myself every single day.

Many thanks to all the collaborators, to John DeFranco of Orthogonal Inc. for discussions on the orthogonal photolithography, to Prof. Peter Grutter of McGill University for his invaluable input on the AFM/EFM characterizations on the stretchable electronics project, and his Ph.D. student Maddy Anthonisen for performing the AFM/EFM measurements and the useful discussions. I am also grateful to Keith Lewis, from SCS coating, for valuable instructions on Parylene deposition, to William Doak of Binghamton University on the design of tensile tester for the stretchable project, and to Richard Silverwood at Polytechnique for tensile tester measurements.

I am grateful to my all friends. Thanks Dr. Huiliang Wang (Stanford Univ) for input on the elastomer processing, Dr. Pei He (Manchester Univ) and Dr. Qingyu Cui (Michigan Univ) for endless discussions on the flexible devices, Qian Li (Youxin Pai Inc) for the time spent with me on the schematic image drawing, and Bo Zhang (Zhiyuan Electronics co., ltd.) for discussions and

design on the wireless communication devices. Thank Changsheng, Qinghua, Yinghao, Mengjiao, Hongliang for being my intimate friends in Polytechnique/UdeM.

I also want to thank some distinguished scientists for individual discussions at the conference which greatly inspired me. These thanks goes to Prof. Stephanie P. Lacour (EPFL), Prof. Zhenan Bao (Stanford Univ), Prof. Yonggang Huang (Northwest Univ), and many other scientists I met in the past years for invaluable discussions.

I am very grateful to technicians at Polytechnique: Daniel Pilon for his kind support on the Labview software for the device characterization, Christophe Clément and Alireza H. Mesgar for technical assistance in the clean room, and numerous discussions on my microfabrication issues, Josianne Lefebvre (XPS and ToF-SIMS), Nicole MacDonald (SEM), and Samir Elouatik (FTIR).

I have not yet thanked my colleagues at Polytechnique. I have to thank Gaia, Prajwal, Irina, Yang, Arun, Yasmina, Michelle, Tom, Come, Elizabeth, Shalin, Fanny, Camille, Hao, Olga, Laurie, Amel, Gabriel; and Francis, Frédéric, Eduardo, Zhaojing, Tian, Xu, Martin, Dominic, Guido, Tania, Jonathan, Julia, Sareh, and Dilek. It was a pleasure to work with you all. I enjoyed the time I spent with you in Montreal. I should be very grateful to life and to the chance I had to meet you.

And many thanks to Polytechnique Montreal for academic and administrative services.

Finally, I would like to thank my father Weijun Zhang, my mother Jingfang Xie, my brother Shidong Zhang and his family, for their support and for always being with me.

Thank you, Xiang, my wife, and Mark, my son, nothing matters without you.

RÉSUMÉ

L'électronique flexible, étirable et autoréparante a le potentiel de redéfinir l'apparence, la conception et la fabrication des appareils électroniques ayant un impact sur l'électronique personnelle, la peau électronique et les soins de santé. Le développement de l'électronique flexible, étirable et autoréparante à des fins biologiques et médicales fait appel à la biocompatibilité et la transparence des matériaux électroniques adaptable. Parmi ces matériaux, les polymères organiques conducteurs présentent des opportunités uniques. La recherche sur les propriétés électroniques, chimiques et mécaniques des polymères organiques conducteurs permet d'assurer leur intégration dans les appareils électroniques adaptable.

Cette thèse explore le traitement des polymères organiques conducteurs et le développement de nouvelles technologies de fabrication pour l'électronique flexible, étirable et autoréparante.

Nous avons premièrement recherché les effets de plusieurs additifs sur les propriétés fondamentales du polymère conducteur poly(3,4-éthylènedioxythiophène) polystyrène sulfonât (PEDOT:PSS). Nous avons démontré que les additifs jouent des rôles vitaux dans la détermination de la conductivité électronique de la couche mince, les propriétés mécaniques et la stabilité dans l'eau (essentielle aux applications biologiques). Nous avons trouvé que les couches minces déposées sur des substrats flexibles en plastiques ou sur des élastomères étirables démontrent une stabilité accrue dans l'eau en comparaison avec les couches minces sur des substrats rigides en verre. Des couches minces de PEDOT:PSS hautement conductrices, étirables et stables dans l'eau ont été obtenues en ajustant la composition chimique des couches et en contrôlant les conditions de traitement.

Pour la fabrication de dispositifs flexibles et étirables, un défi majeur apparait lors de la génération de patron de matériaux électroniques organiques dans le but de produire une électronique à haute résolution. L'application de la photolithograpie à cet effet n'est pas aussi facile, car les composés chimiques utilisés dans cette technique (photorésines, développeurs, décapant de résine) peuvent contaminer ou solubiliser les polymères organiques conducteurs. De plus, la génération de patrons d'électrodes métalliques pour les électroniques souples crée aussi un défi. En effet, l'adhésion des photorésines sur la surface des substrats souples (tels que les élastomères) sur lesquels les composants électroniques sont déposés est faible.

Nous avons pu fabriquer, avec une résolution micrométrique, des dispositifs qui peuvent soutenir des plis et des extensions afin de leur permettre de s'adapter à des surfaces courbées, souples et

élastiques. À cet effet, nous avons utilisé une photorésine récemment développée, qui est immiscible avec des matériaux organiques, pour générer des patrons de PEDOT:PSS. Des masques basés sur des couches minces (2 µm) de polymère ont été utilisées pour générer des patrons d'électrodes métalliques.

Ensuite, nous avons utilisé ces techniques pour fabriquer des transistors électrochimiques flexibles et étirables avec une résolution micrométrique. Nos dispositifs ont démontré une haute performance sous des conditions de pli et d'étirement et aussi une très bonne stabilité cyclique.

Les dispositifs électroniques souples doivent supporter la déformation mécanique à travers le temps, qui peut endommager les appareils et nuire à leur fonctionnalité. Le développement de matériaux autoréparants, pouvant restaurer la fonctionnalité de l'appareil après endommagement, permettrait d'améliorer grandement la longévité de l'électronique souple. En particulier, l'autoréparation des matériaux électroniques organiques est de première importance car elle peut être combinée avec la flexibilité et la biocompatibilité. Ainsi, cette propriété est très prometteuse pour la détection biologique, l'enregistrement neurologique et l'ingénierie tissulaire.

Nous avons exploré les propriétés d'autoréparation du PEDOT:PSS. Les couches de PEDOT:PSS, avec une épaisseur de plus de 1 µm, démontrent une autoréparation électronique instantanée après que de l'eau ait été appliquée à l'endroit endommagé. Le processus d'autoréparation des couches minces n'est pas affecté par le dommage répété et se réalise très rapidement après mouillage. L'autoréparation se fait même après exposition à la vapeur d'eau. Nous avons établi qu'une application possible pour les couches minces autoréparantes est de les utiliser dans des détecteurs d'eau ultrasensibles.

La fabrication avancée et les techniques de traitements étudiées dans cette thèse permettront de paver la voie pour le développement de microélectroniques organiques souples pour les appareils électroniques portatifs et de stockage d'énergie flexibles, les écrans flexibles et les détecteurs d'humidité. En particulier, le fait que les appareils puissent travailler de manière stable et s'auto réparer dans l'eau, mène à de futures applications dans la détection biologique, les interfaces neurales, l'administration de médicaments et l'ingénierie tissulaire.

ABSTRACT

Flexible, stretchable and healable electronics have the potential to redefine the appearance, design and fabrication of electronic devices, with a profound impact on personal electronics, electronic skin and healthcare. The development of flexible, stretchable and healable electronics, in particular for biological or healthcare applications, calls for biocompatible, transparent and conformable electronic materials, among which organic conducting polymers present unique opportunities. Investigation of the fundamental properties of organic conducting polymers, in order to control their electronic, chemical and mechanical properties is therefore of great importance for their integration into conformable organic electronic devices.

This thesis explores the processing of organic conducting polymer and the development of new fabrication technologies for flexible, stretchable and healable electronics.

We first investigate the effect of several additives on the fundamental properties of the conducting polymer, poly(3,4-ethylenedioxythiophene) polystyrene sulfonate (PEDOT:PSS). We demonstrate that the additives play vital roles in determining the films' electronic conductivity, mechanical properties, and water stability (essential for biologic applications). We find that films on flexible plastic and stretchable elastomer substrates show enhanced water stability compared with that of films on rigid glass substrates. Highly conductive, intrinsically stretchable and water-stable PEDOT:PSS thin films are finally obtained by adjusting the films' chemical composition and controlling the processing conditions.

For the fabrication of flexible and stretchable device, a major challenge is the patterning of organic electronic materials to produce electronics with high resolution. Applying conventional photolithographic techniques to this purpose is not straightforward, because the standard lithography chemicals (photoresists, developers, strippers) may contaminate or solubilize the organic material. In addition, the patterning of metallic electrodes for soft electronics is also challenging because photolithography is an inefficient method for directly patterning stretchable electronics, due to the poor adhesion of the photoresist on the surfaces of soft substrates (such as elastomers) on which electronic components are deposited.

We are able to pattern devices with microscale resolution that are able to sustain not only bending but also extensive stretching, so that they can accommodate on curved, soft, and elastic surfaces. To this purpose we use a recently developed photoresist, which is non-miscible with organic

materials, to pattern PEDOT:PSS and a ultrathin polymer film (< 2 μm) to pattern metallic electrode arrays on stretchable substrates. We use these technologies thereafter to develop both flexible and stretchable organic electrochemical transistors with microscale resolution. Our devices show high performance with unchanged electrical properties under extreme bending or stretching conditions, and also superior cyclic stabilities.

Soft electronics must endure mechanical deformation over time, which may damage devices and disable their functionality. The development of healable materials, which can repair themselves and restore the device functionality after damage could greatly improve the longevity of soft electronics. Particularly, healing of organic electronic materials is of primary importance because it can be combined with flexibility and biocompatibility, thus being very promising for long-term biological sensing, neurologic recording and tissue engineering applications.

We explore the healing property of PEDOT:PSS. PEDOT:PSS films (with thickness greater than 1 μm) show instantaneous electronic healing after water is applied to the damaged area. The healing process of the films is not affected by repeated damage to the film and occurs very rapidly, i.e. within 150 ms after wetting. Healing occurs even after exposure to water vapor. The potential of healable PEDOT:PSS thin films is demonstrated as ultrasensitive water detectors and as active materials for self-healing organic electronic devices.

The advanced fabrication and processing technologies investigated in this thesis pave the way for the development of soft organic microelectronics for personal wearable electronics, flexible energy storage devices, flexible display and humidity detectors. In particular, the fact that devices can work stably and can self-repair in water leads to further applications in biological sensing, neural interfaces, drug delivery, and tissue engineering.

TABLE OF CONTENTS

LIST OF FIGURES

LIST OF ABBREVIATIONS

AC	Activated carbons
Ag	Silver
AgCl	Silver chloride
Au	Gold
BJT	Bipolar junction transistor
CE	Counter electrode
CNT	Carbon nanotube
CTAB	Cetyltrimethylammonium bromide
D	Drain
DBSA	Dodecyl benzene sulfonic acid
DMSO	Dimethyl sulfoxide
ECoG	Electrocorticography
ECT	Electrochemical transistors
EDL	Electrical double layer
EEG	Electroencephalogram
EG	Electrolyte-gated
EIS	Electrochemical Impedance Spectroscopy
FET	Field-effect transistor
G	Gate
GO_x	Glucose oxidase
GOPS	Glycidoxypropyltrimethoxysilane
H_2O_2	Hydrogen peroxide
H_2SO_4	Sulfuric acid

HFE	Hydrofluoroethers
HOMO	Highest occupied molecular orbital
IL	Ionic liquid
LED	Light-emitting device
LUMO	Lowest unoccupied molecular orbital
MOSFET	Metal–oxide–semiconductor field-effect transistor
NaCl	Sodium chloride
OECTs	Organic electrochemical transistors
OLEDs	Organic light-emitting diodes
OTFTs	Organic thin-film transistors
OSCs	Organic solar cells
PBS	Phosphate-buffered saline
PDMS	Poly(dimethylsiloxane)
PEDOT:PSS	Poly(3,4-ethylenedioxythiophene):polystyrenesulfonate
PET	Polyethylene terephthalate
PLGA	Poly(L-lactide-co-glycolide)
Pt	Platinum
RE	Reference electrode
RIE	Reactive ion etching
S	Source
SiO_2	Silicon dioxide
STEC	Stretchability and electrical conductivity
WE	Working electrode

LIST OF SYMBOLS

A_g	Gate area
C_c	Channel capacitance per unit area
C_g	Gate capacitance per unit area
C	Capacitance
Cr	Chromium
E	Electrical field
e^-	Electron
G	Transconductance
I_{ds}	Source-drain current
I_{on}	ON-state current
I_{off}	OFF-state current
I_g	Gate-source current
I_{gs}	Gate-source current
l	Drift length
K	Boltzmann constant
L	Length
M^+	Cations
n	Electron density
T	Temperature
t	Time
τ_e	Transit time
Ti	Titanium
u	Mobility

v	Velocity
V	Voltage
V_{ds}	Drain-source voltage
V_g	Gate-source voltage
V_{gs}	Gate-source voltage
V_{sol}	Gate voltage drop on the channel
W	Width

LIST OF APPENDICES

CHAPTER 1 INTRODUCTION AND OBJECTIVES

1.1 Organic electronics and organic bioelectronics

Organic materials have been traditionally considered as insulators. Therefore, most electronic devices, such as transistors or light emitting devices, for a long time have been exclusively based on inorganic materials. In the 1970s, the discovery that polymers can show electrical conductivity that can be increased up to seven orders of magnitude upon chemical doping, altered scientists' understanding of organic materials[1]. This breakthrough observation was recognized by awarding Alan J. Heeger, Alan G. MacDiarmid and Hideki Shirakawa the Nobel Prize in Chemistry in 2000 "*for the discovery and development of conductive polymers*". Since then, conductive polymers have become the cornerstone of a new type of electronics: organic electronics. Organic electronic materials have the advantages of light weight, superior flexibility, solution processability and biocompatibility[2]. These unique properties open new fields for applications such as flexible displays, flexible solar cells, wearable healthcare devices and disposable electronics[2]. One example, organic light-emitting diodes (OLEDs), has already entered the market for small-area displays and lighting applications[3,4].

Inorganic electronic materials normally conduct only electronic charge carriers, while organic conducting polymers conduct both electronic and ionic charge carriers (mixed conduction)[5]. Since 2007, the mixed conduction behavior in organic conducting polymers has received great attention, especially for biological applications. The interplay between electronic and ionic signals, i.e., ion-to-electron conversion, is at the basis of the new field of organic bioelectronics[6]. Organic bioelectronics deal with devices operating at the interface between biology and human-made electronics, with possible applications in sensing, diagnostics and healthcare[7].

Among the most exciting examples of organic bioelectronics devices are organic electrochemical transistors (OECTs). The first OECT, based on polypyrrole, was developed in 1984 by Wrighton's group[8]. In 2002, a solution-processable and air-stable conducting polymer, poly(3,4-ethylenedioxythiophene)-poly(styrene sulfonic acid) (PEDOT:PSS), was introduced as a channel material into OECTs[9]. Since then, dozens of groups across Europe, America, Asia and Australia have become active in OECT research[10]. Hundreds of peer-reviewed publications per year, along

with multiple international symposia, indicate both that the potential of OECTs has not been fully exploited and research on OECTs is in its infancy with many challenges still to be overcome.

1.2 Motivations and objectives of this thesis

Human body is soft, while electronics on silicon are not. Realizing soft electronic devices that overcome this fundamental mechanical mismatch will permit applications that are impossible to achieve with rigid devices. In addition, self-healing is a unique property of the human skin but is not attainable in most electronic materials. Self-healing electronic materials represent a very interesting and important area of research especially for soft electronics because soft electronic devices must endure mechanical deformation over time, which may damage devices and disable their functionality. In particular, healable OECTs will inarguably increase device longevity and improve long-term device reliability. Given the rapid growth of wearable electronics, establishing technologies for soft and healable OECTs will also promote their integration with such systems.

The primary objective of this thesis is to develop flexible, stretchable and healable electronic materials and devices, e.g., OECTs, for applications in sensing, diagnostics and healthcare. In working towards this goal, it is of paramount importance to investigate the processing of conducting polymers to achieve flexibility, stretchability and healability and to develop new device fabrication technologies on substrates that are unconventional for electronics, such as polyethylene terephthalate (PET) and poly(dimethylsiloxane) (PDMS).

Therefore, the main specific objectives of this thesis are:

(1) Processing flexible, stretchable and healable PEDOT:PSS films. A better understanding of fundamental properties of PEDOT:PSS is essential to control device performance, and also of great fundamental interest for other research topics, since PEDOT:PSS is the most successful conductive polymer in terms of practical applications.

(2) Developing new technologies for patterning PEDOT:PSS and metallic electrode arrays on flexible and stretchable substrates, and fabricating flexible and stretchable micro-OECTs.

In Chapter 2, the history, working mechanism, figures of merit, and applications of OECTs are discussed. Chapter 2 also contains the introduction to PEDOT:PSS processing, with special attention paid to electrical and mechanical properties. Finally, the existing technologies for PEDOT:PSS patterning and research progress in flexible and stretchable OECTs are reviewed.

Chapters 3 to 6 are reprints of four articles resulting from the work for this thesis.

-**Article 1**: Shiming Zhang, Prajwal Kumar, Amel Sarah Nouas, Laurie Fontaine, Hao Tang, Fabio Cicoira, Solvent-induced changes in PEDOT: PSS films for organic electrochemical transistors, APL Materials, 2015, 3 (1), 014911.

-**Article 2**: Shiming Zhang, Elizabeth Hubis, Camille Girard, Prajwal Kumar, John DeFranco, Fabio Cicoira, Water stability and orthogonal patterning of flexible micro-electrochemical transistors on plastic, Journal of Materials Chemistry C, 2016, C 4 (7), 1382-1385.

-**Article 3**: Shiming Zhang, Elizabeth Hubis, Gaia Tomasello, Guido Soliveri, Prajwal Kumar, Fabio Cicoira, Patterning of stretchable organic electrochemical transistors, Chemistry of Materials, 2017, 29 (7), 3126–3132.

-**Article 4**: Shiming Zhang and Fabio Cicoira, Water-enabled healing of conducting polymer films, Advanced Materials, 2017, DOI: 10.1002/adma.201703098.

In **Article 1**, we systematically study how additives affect film conductivity and identify glycerol as the best conductivity enhancer. We investigate film stability on glass and reveal a thickness loss after the sample is immersed in polar solvents. The thickness loss can be prevented by adding a crosslinking agent in the suspension before coating. Then, in **Article 2**, we observe that films processed on plastic PET substrates show better long-term water-stability than films on glass substrates. We perform orthogonal photolithography to pattern PEDOT:PSS on PET and fabricate flexible micro-OECTs featuring high performance and excellent water stability. In **Article 3**, we investigate the additives' effect on film stretchability. By engineering a wrinkle device structure, introducing a new metallic micro-patterning method and using stretchable hydrogel as electrolyte, we assemble a fully stretchable organic transistor. In **Article 4**, we demonstrate that PEDOT:PSS can show electrical healing properties by increasing film thickness. The rapid-healing property is utilized to demonstrate a self-healing organic transistor and a wireless water detector.

Following these four articles, supplementary methods and results for this thesis are presented.

In Chapter 8, the results of this thesis are discussed as a whole, supported by the literature review and the published articles. Finally, conclusions are drawn and perspectives on future work are given in Chapter 9.

CHAPTER 2 LITERATURE REVIEW

Nowadays, smart cellphones, flat panel displays, computers, sensors, memories and other electronic products play an indispensable role in daily life. Information display products link every corner of the world via internet and various electronic devices. In modern society, they are an ever-present extension of our corporeal fabric and help us to deal with a myriad of daily tasks. Key components inside these devices are semiconductor-based logic devices, such as complementary metal-oxide semiconductors (CMOSs) and bipolar junction transistors (BJTs) for high-speed logic calculation, field-effect transistors (FET) and light-emitting diodes (LED) for information processing and display[11]. For decades (1930s-1970s) these devices have been based on inorganic materials, which show high performance, high stability and, importantly, can be processed with mature fabrication technologies.

Generally speaking, polymers are insulators. In 1977, Alan J. Heeger, Alan G. MacDiarmid and Hideki Shirakawa discovered that conductivity of the semiconducting polymer polyacetylene can increase seven orders of magnitude upon oxidization (reaching the order of 10^3 S/cm[1)] by exposing it to halogen. This breakthrough observation was recognized by the Nobel Prize in Chemistry for 2000 "*for the discovery and development of conductive polymers*". The combination of metal and polymer properties in a conducting polymer opens new opportunities in many applications, particularly in the electronics industry. In addition, conducting polymers are generally not thermoplastics and do not melt at high temperatures. Since 1977, conducting polymers have become the cornerstone of a new type of electronics: organic electronics[12]. In addition to polyacetylene, a series of conducting polymers, including polythiophene, polypyrrole, and polyaniline[13] (Figure. 2.1), and the low-energy-gap light-emitting polymers polyphenylene vinylene were reported from the 1970s to 1980s[14], which greatly promoted research on organic electronics.

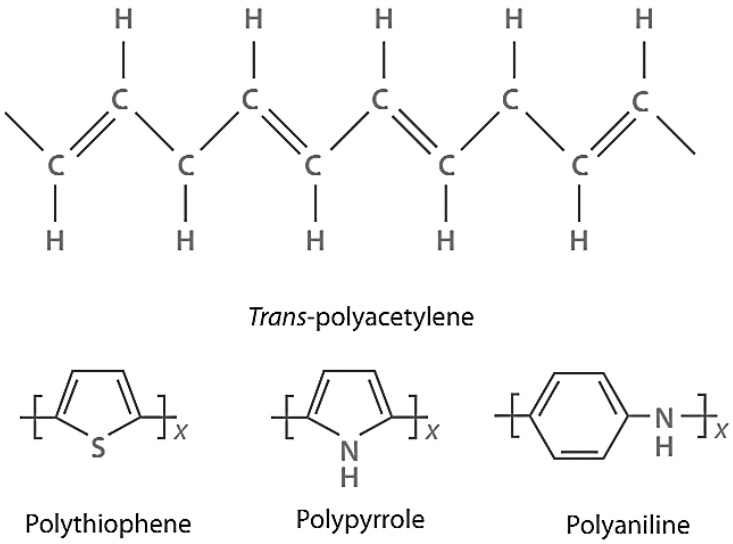

Figure 2.1. Chemical structures of some conducting polymers[13]. Reprinted with permission.

2.1 Why some polymers conduct electricity

2.1.1 Chemical bonds in conducting polymer

The general electronic configuration of conducting polymer *trans*-polyacetylene is $1s^2$, $2s^2\ 2p^2$, the ground state electronic configuration of carbon is $1s^2$, $2s^2\ 2p_x^1 2p_y^1 2p_z^0$, and the excited state electronic configuration of carbon is $2s^1\ 2p_x^1 2p_y^1 2p_z^1$. The $2s^1$ and $2p_x^1$, $2p_y^1$ orbitals of carbon undergo sp^2 hybridizations and form three sp^2 hybrid orbitals in a planar structure (Figure. 2.2), the three sp^2 hybrid orbitals and one pure $2p_z^1$ orbital having one electron each. In polyacetylene, σ (sp^2-sp^2) bonds are observed between two adjacent carbon atoms[15]. The remaining one pure $2p_z^1$ orbital of one carbon atom overlaps sideways with the corresponding $2p_z^1$ orbital of another carbon atom and thus forms one π bond[16] (Figure. 2.2). According to energy bond theory, the energy difference between the occupied binding orbitals and the unoccupied anti-binding orbitals of the σ bonds is quite large and well beyond the visible spectral range. Correspondingly, they have a large gap between the highest occupied molecular orbital (HOMO) and the lowest unoccupied molecular orbital (LUMO), leading to insulating properties[16]. However, the π bonds have a much smaller difference between the homo and LUMO, leading to strong absorption in or near the visible spectral range and to semiconducting properties[15,16].

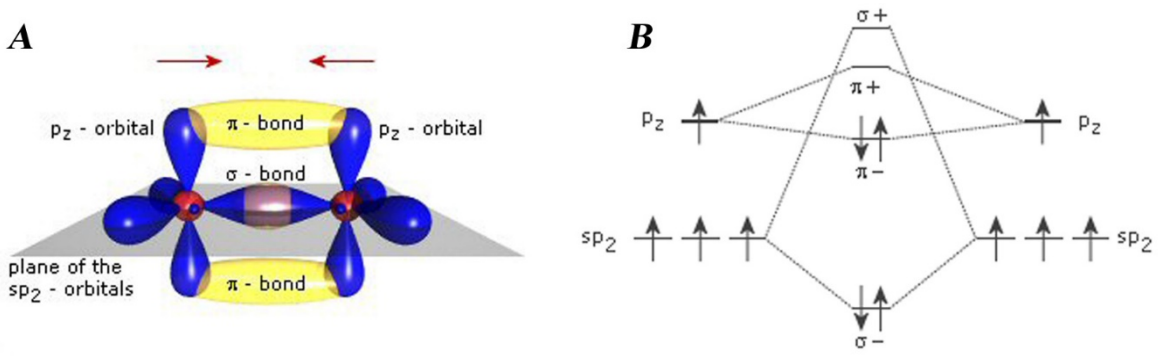

Figure 2.2. (A) Illustration of π bond and σ bond, and (B) the energetic difference of the π bond and the σ bond, in *Trans*-Polyacetylene[16].

2.1.2 Electron delocalization in conjugated backbones

When polymers have a conjugated backbone (for example, *Trans*-Polyacetylene), the $2p_z^1$ orbital in the π-bonds overlap with each other, allowing the electrons to be more easily delocalized. Electrons do not belong to a single carbon atom but are shared between a group of atoms so they are able to move freely in the chain[16]. However, the conductivity due to the delocalization of electrons between the π-bonds is still limited due to relatively low carrier densities.

2.1.3 Doping is the key

The key to obtaining high conductivity of conducting polymer is chemical doping. While doping in inorganic materials is achieved by controllably introducing impurity atoms (electron donors or acceptors) via covalent interaction to replace the atoms of a pure crystalline semiconductor, doping in organic semiconductors mostly uses strong oxidizing agents to remove electrons from polymer chains, leaving "holes" in the form of positive charges that can move along the conjugated chain[17]. When the polymer is synthesized in the presence of the dopant molecules (a negative charge/anion in most cases), the dopants remove electrons from the polymer chains. The dopant molecule attracts an electron from the polymer chain and becomes negatively charged. The positively charged polymer molecule is termed a radical cation, or polaron[17] (Figure. 2.3). In this case, when an electrical field is applied, these positively charged carriers can move inside the polymer, thus allowing charges to pass though the polymer in the form of polarons. The conductivity of the

polymer is proportional to the number of polarons, i.e., to the amount of dopant used during synthesis of the polymer.

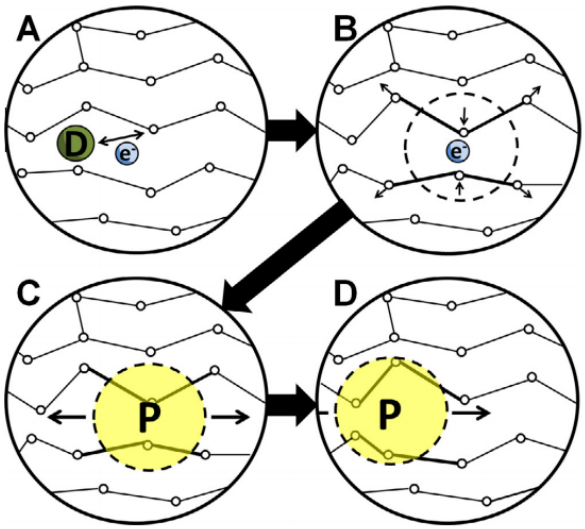

Figure 2.3. A demonstration of the electrical conductivity of conducting polymers. (A) Dopants add an electron to (or remove it from) the polymer chain, thus creating a delocalized charge. (B) It is energetically favorable to localize this charge and surround it with a local distortion of the crystal lattice. (C) A charge surrounded by a lattice distortion is called a polaron (a radical ion associated with a lattice distortion). (D) The polaron is able to travel freely along the polymer chain, leading to a conductive increase[17].

2.2 The conducting polymer PEDOT:PSS

Since the work of Shirakawa, McDiarmid and Heeger[1], conducting polymers have been investigated intensively. Combining advantageous properties such as solution processability and flexibility of conducting polymers with high electrical conductivity could initiate a revolution in technology. Researchers in Bayer AG showed that, despite its high conductivity up to 10^5 S/cm, polyacetylene is not stable for technical applications, for which a high conductivity with unchanged performance at 120℃ over 1000 h in room atmosphere is required[18]. They noticed that doped polypyrrole or polythiophene has higher stability than doped polyacetylene and attributed this difference to the stabilizing effect on the positive charges on the conjugated chains by nitrogen or sulfur[18]. Then, during the second half of the 1980s, they introduced stabilizing alkylenedioxy

substituents into the thiophene system and realized a conducting polymer, polythiophene derivative, poly(3,4-ethylenedioxythiophene), i.e., PEDOT[19], with very good air stability (Figure 2.4).

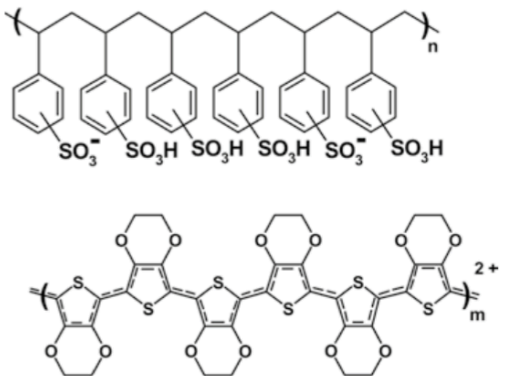

Figure 2.4. Chemical structure of PEDOT:PSS. The positive charges on the PEDOT chain are compensated for by negative sulphonate ions on the PSS chain[19]. Reprinted with permission.

PEDOT exhibited very interesting properties, such as high conductivity, electrochromism, transparency in thin oxidized films and a very high stability in the oxidized state[19]. However, PEDOT is insoluble in most solvents, which significantly limits its applications. The solubility problem was subsequently circumvented by using a water-soluble polyelectrolyte, poly(styrene sulfonic acid) (PSS) in the 1990s, as the charge-balancing dopant during polymerization to yield PEDOT:PSS[20]. The electronic and ionic transport in this polymer can be balanced by controlling the processing condition[21]. Depending on the processing conditions, PEDOT and PSS form segregated phases of sizes ranging from about three to tens of nanometers[22]. This combination resulted in a water-soluble polyelectrolyte system with good film forming properties, high conductivity, high visible light transmissivity, as well as excellent stability. PEDOT:PSS can be heated at 100℃ for over 1000 h in air with only a small change in conductivity[19]. Given its advantageous properties, PEDOT:PSS has become the most successful conducting polymer. Several PEDOT:PSS formulations are presently available in the form of aqueous suspensions from two European companies: Haraeus (formerly Baytron, Germany) and Agva Gevaert (Belgium). With PEDOT:PSS, researchers have been able to promote research on organic electronics and

develop new applications. Although initially mostly used as an antistatic coating film, PEDOT:PSS has found several new applications over the past few years, e.g., transparent electrodes, hole transport layers in OLED displays and organic solar cells, electrolytic polymer capacitors, screen-printed electronics, wearable electronics and bioelectronics etc. (Figure 2.5)[23].

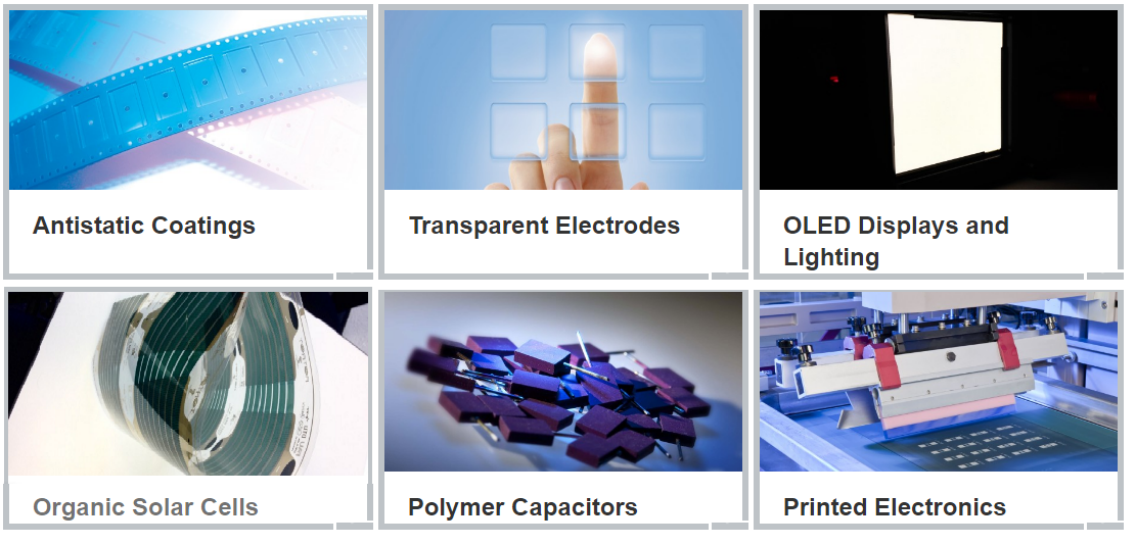

Figure 2.5. Several applications of the commercial Haraeus Clevios™ PEDOT:PSS products[23].

2.3 PEDOT:PSS processing

The as-received PEDOT:PSS suspensions have electrical conductivities ranging from 10^{-4} to 10^{-1} S/cm, depending on the PEDOT/PSS ratio. A high PEDOT/PSS ratio leads to a high conductivity. In this thesis, we selected Haraeus Clevios™ PEDOT:PSS PH1000 due to its high conductivity. Several properties of PEDOT:PSS film, such as electrical conductivity, wettability, adhesion, mechanical property, need to be modified by adding co-solvents into the suspension before coating in order to meet the requirements of different applications.

2.3.1 Electrical conductivity

Solvents added to PEDOT:PSS suspension to increase its conductivity are called secondary dopants or conductivity enhancers[24], which will evaporate during the baking process. Many groups have studied PEDOT:PSS processing over the past decades to understand the effect of the additive

on film conductivity. The highest conductivity, up to 4380 S/cm, has been obtained by treating the film with H_2SO_4[25]. The following materials are these most widely used as conductivity enhancers: i) high boiling point polar organic compounds or additives: such as ethylene glycol (EG), dimethyl sulfoxide (DMSO) and sorbitol[26]; ii) surfactants: such as dodecylbenzenesulfonic acid (DBSA)[26], sodium dodecyl sulfonate[27], and fluorosurfactant such as Zonyl-FS300 (Zonyl)[28,29]; and iv) ionic liquids[30]. The common properties of these additives are: i) they are all water soluble; and ii) they have polar molecular groups. Despite numerous studies on the role of these compounds, the mechanism of the conductivity improvement in these films remains unclear. Kim et al. proposed that high dielectric constant solvents could induce a screening effect between $PEDOT^+$ and PSS^-, thus reducing the columbic interactions between these two units[31]. Bao et al. also suggested the charge screening effect of ionic additives results in a morphological change to form more crystalline PEDOT nanofibrillar structures[30]. Ouyang et al. argued that the conductivity enhancement was attributed to the effect of the secondary dopants on the conformation of the conductive $PEDOT^+$ chains[32]. The $PEDOT^+$ chain could be released from following the structure of the PSS^- chain after adding the dopants, which leads to more direct carrier transport paths along the straighter PEDOT chains. The same group first added H_2SO_4 into PEDOT:PSS and obtained a high conductivity of 2400 S/cm[33]. They proposed the introduction of H_2SO_4 contributes H^+ to the film and neutralizes PSS^- by $H^+ + PSS^- = PSSH$. This results in the replacement of some PSS^- with HSO_4^- as the counter anions of PEDOT. Lee et al. reported that when PEDOT:PSS is further treated with 100% H_2SO_4, more than 70% of the PSS was removed from the pristine PEDOT:PSS[25]. In this case, conformational change of PEDOT happens because PEDOT chains don't need to follow the coiled PSS^- (via columbic interaction). The removal of PSSH further leads to reduction of the energy barrier width for the interchain and inter-domain charge hopping, whereas the conformational change of PEDOT makes the positive charges on PEDOT more delocalized as coil conformation causes localization of positive charges on the PEDOT chains. Such a reorientation, for the first time, results in the formation of highly crystallized PEDOT nanofibril and obtains extremely high conductivity of 4380 S/cm (Figure 2.6)[25]. H_2SO_4 treatment also decreases the PEDOT:PSS adhesion on hydrophilic substrates, due to the more hydrophobic film property (more PEDOT and less PSS), and thus facilitates its transfer onto hydrophobic elastomer substrates for transfer printing[34]. It is notable that the addition of H_2SO_4 should be performed after film formation, otherwise it will cause severe phase separation between PEDOT and PSS in the suspension[35]. Such

a separation between PEDOT and PSS can obtain high conductive PEDOT films, but disables the solution processability of PEDOT by separating out PEDOT plates in the suspension. While mild conductivity enhancers such as glycerol, EG, DMSO can be added directly into the suspension. Due to their more gentle separation process in the suspension, they are supposed to trigger the separation of the PEDOT and PSS, mainly during the water evaporation process (baking or vacuum)[24].

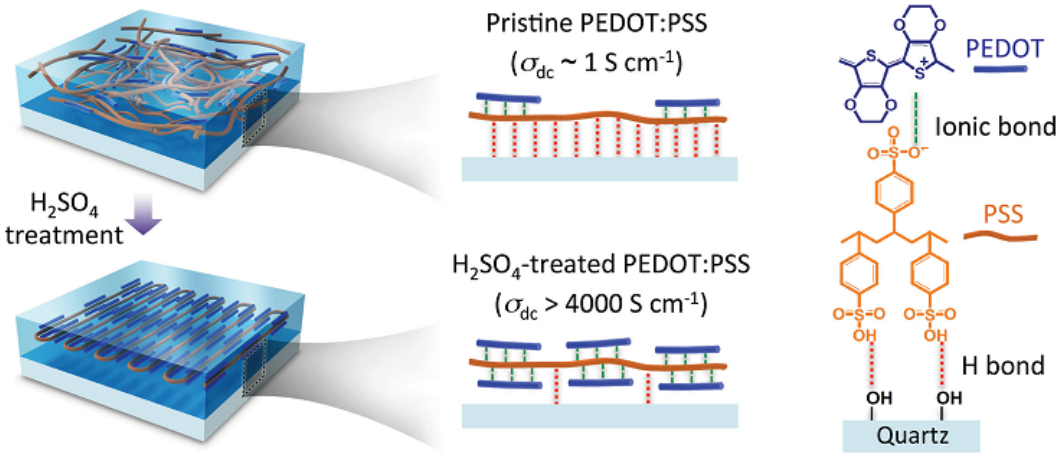

Figure 2.6. Improved conductivity of H_2SO_4-treated PEDOT:PSS due to removal of70% PSS (100% H_2SO_4) and formation of well-crystallized PEDOT nanofibrils[34]. Reprinted with permission.

A consensus for the conductivity increase is that conductivity enhancers cause a re-arrangement in the morphology of the films upon drying. The re-arrangement results in larger and straighter $PEDOT^+$ grains and increased phase separation between the conducting $PEDOT^+$ and the insulating PSS^-, leading to a better $PEDOT^+$-$PEDOT^+$ connecting network in the film[21] (Figure. 2.7). Since both $PEDOT^+$ and PSS^- chains are charged it is reasonable to assume that the high polarity of the secondary dopant is necessary to interact with the ionic charges of the polyanion and the polycation. This has also been described as a screening between the two oppositely charged polymer chains, which allows the chains to orient. In most cases, the conductivity enhancers are then thermally removed and leave the films in a thermodynamically favorable state[24]. The separation process is

similar to a hydrophobic effect as the hydrophobic PEDOT group tends to push aside the surrounding PSS and aggregate with the neighbor PEDOT upon water evaporation.

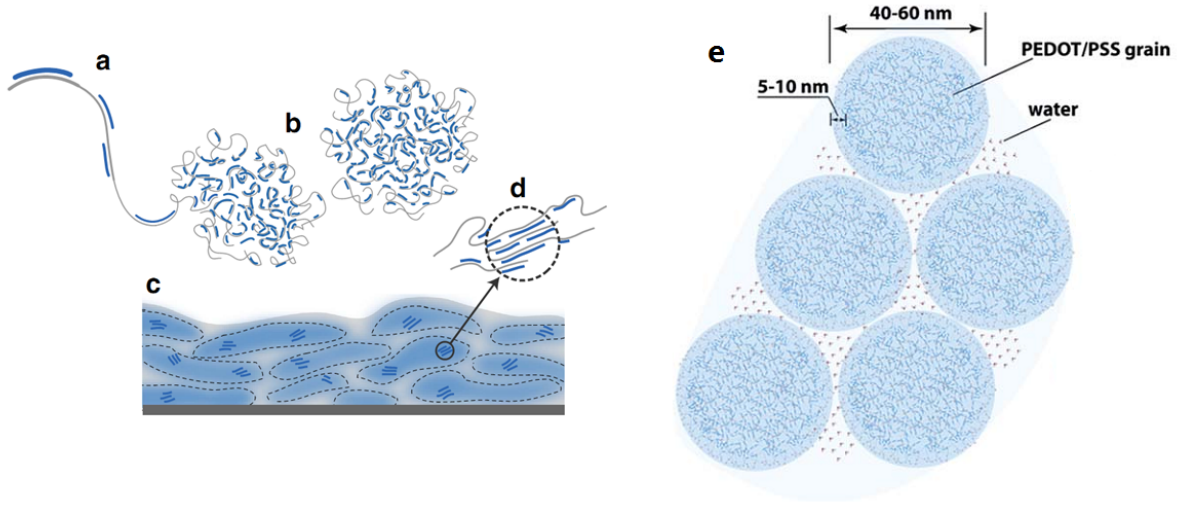

Figure 2.7. Commonly described microstructure of PEDOT:PSS (a) PEDOT synthesis on PSS template, (b) formation of colloidal gel particles in dispersion and (c) resulting film with PEDOT:PSS-rich (blue) and PSS-rich (grey) phases. (d) Aggregates/crystallites support enhanced electronic transport[21]. (e) The typical diameter of PEDOT/PSS grains is 40–60 nm, with a PSS-rich shell thickness of 5–10 nm[36]. Reprinted with permission.

2.3.2 Film forming properties

In certain cases, some amphiphilic additives (mostly surfactant), such as DBSA[26], Zonyl-FS300 (Zonyl)[28] and Triton X-100[37] (Figure 2.8), are mixed with the PEDOT:PSS aqueous suspension to improve its film forming ability. For example, Vosgueritchian et al. reported that mixing with the fluorosurfactant Zonyl significantly increases PEDOT:PSS wettability on hydrophobic surfaces due to the amphiphilic nature of the Zonyl, which is composed of both a hydrophobic (fluorinated) and hydrophilic (ethylene glycol) segment. Additives used to increase the PEDOT:PSS wettability usually also increase the film stretchability when the concentration is optimized. For example, we observed the sole addition of DBSA to PEDOT:PSS not only increases film wettability, but also increases the film conductivity, as well as the stretchability. However, adding more than 2% DBSA induces a phase separation in the suspension (similar to the case of adding H_2SO_4). Further

increases in the DBSA concentration causes a gel-like structure, and makes PEDOT:PSS suspension impossible to be solution processed.

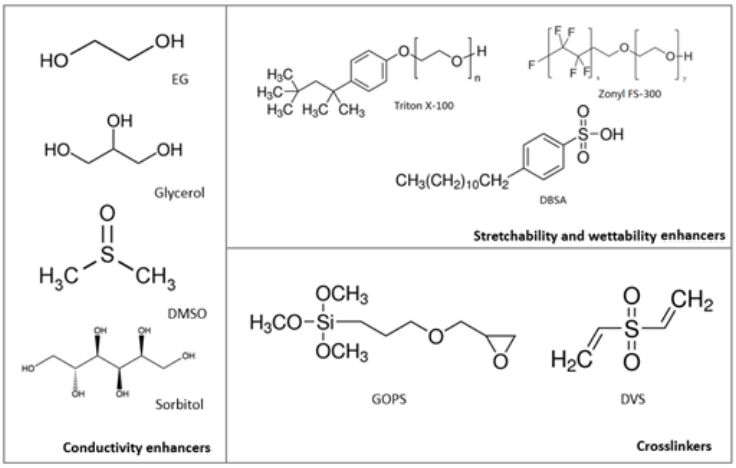

Figure 2.8. Additives used to improve specific properties of PEDOT:PSS.

PEDOT:PSS films easily delaminate from hydrophilic substrates such as glass and silicon, upon water immersion[38]. Therefore for in-water applications, it is necessary to use a crosslinking agent (such as glycidoxypropyltrimethoxysilane, GOPS) to improve adhesion on substrates and promote long-term resistance to dissolution and delamination, while maintaining effective charge-transport performance[26] (Figure 2.8). GOPS is a silane with a polar and reactive epoxide functional group and silanol group after hydrolysis in water. GOPS is compatible with aqueous PEDOT:PSS suspension and can form a network structure after spin-coating. Silanol groups produced from hydrolysis of GOPS react with a surface hydroxyl group on glass or silicon to form siloxane linkage or hydrogen bonding. In addition, GOPS can form a network structure through self-condensation reaction between silanol groups[26,39-41]. PEDOT:PSS mixed with GOPS is insoluble in any solvent after spin-coating, while pristine PEDOT:PSS is slightly soluble in water. However, GOPS has the disadvantage of decreasing both ionic and electronic mobility in the film[42]. Recently, it has been reported that divinylsulfone is able to crosslink PEDOT:PSS at room temperature without deteriorating film conductivity[43]. It looks very promising as a replacement for GOPS (Figure. 2.8).

2.3.3 Flexibility and stretchability

Without doubt, flexibility is a desirable advantage of conducting polymer with respect to Si electronics. Silicon is held together by covalent bonds, where each atom shares valence electrons with four neighbors. In contrast, conducting polymer consists of macromolecular blocks within which atoms are covalently bonded to each other, however these blocks are held together via weak van der Waals or electrostatic interactions. The prevalence of van der Waals interactions in "soft" conducting polymer defines the key difference with the "hard" silicon[5]. We reported that PEDOT:PSS on plastic PET can undergo extreme bending of hundreds of cycles with negligible effect on conductivity, indicating excellent intrinsic flexibility of PEDOT:PSS[38]. We also developed a flexible device on ultrathin parylene films. Moving beyond flexible to more advantageous stretchable forms opens new possibilities for wearable, implantable and conformable electronics. However, the intrinsic stretchability of the pristine PEDOT:PSS is only ~5% which limits its applications[30]. With this motivation, in 2012, Lipomi et al. optimized the processing condition on PDMS and increased PEDOT:PSS stretchability to 30% by blending with 1% fluorosurfactant Zonyl, without cracks occurring in the film[44]. They expected that Zonyl would function as a typical plasticizer in the film by increasing the free soft volume (that can absorb strain) in the film and weakening intermolecular forces between the polymer chains[45]. In 2015, Li et al. reported that the PEDOT:PSS stretchability can be improved after blending with a series of polymers such as poly(ethylene glycol), poly(ethylene oxide) or poly(vinyl alcohol)[46]. The stretchability of a thick PEDOT:PSS film was increased from 2% to 55% when blending with poly(vinyl alcohol). They proposed the polymers can mix well with PSS so that they increase soft areas in the polymer matrix[46]. In 2015, Oh et al. obtained a stretchable dough by blending PEDOT:PSS with the surfactant Triton X-100 to form nanofibril microstructures. They proposed the increased stretchability originated from the formation of softer matrix due to the good miscibility of Triton X-100 with PSS[47]. In 2017, Wang et al. demonstrated highly stretchable PEDOT:PSS films by incorporating a series of ionic stretchability enhancers such as ionic compounds and ionic liquids (Figure 2.9)[30]. With these enhancers the conductivity can reach the remarkable value of 4100 S/cm, while remaining above 100 S/cm under 600% strain, with a fracture strain of 800%. They suggested that the stretchability enhancers mix well with PEDOT:PSS and are able to further soften the PSS. Besides, the charge screening effect of the ionic additives leads to more crystalline and more interconnected PEDOT nanofibrillar structures,

thus increasing conductivity. Because the PEDOT phase becomes more crystalline with additives, they suspect the soft additive molecules reside in the more disordered PEDOT regions, which further softens the material, and gives rise to a nanofiber PEDOT network embedded in a soft matrix of the additives, which is a desirable morphology for high stretchability[30].

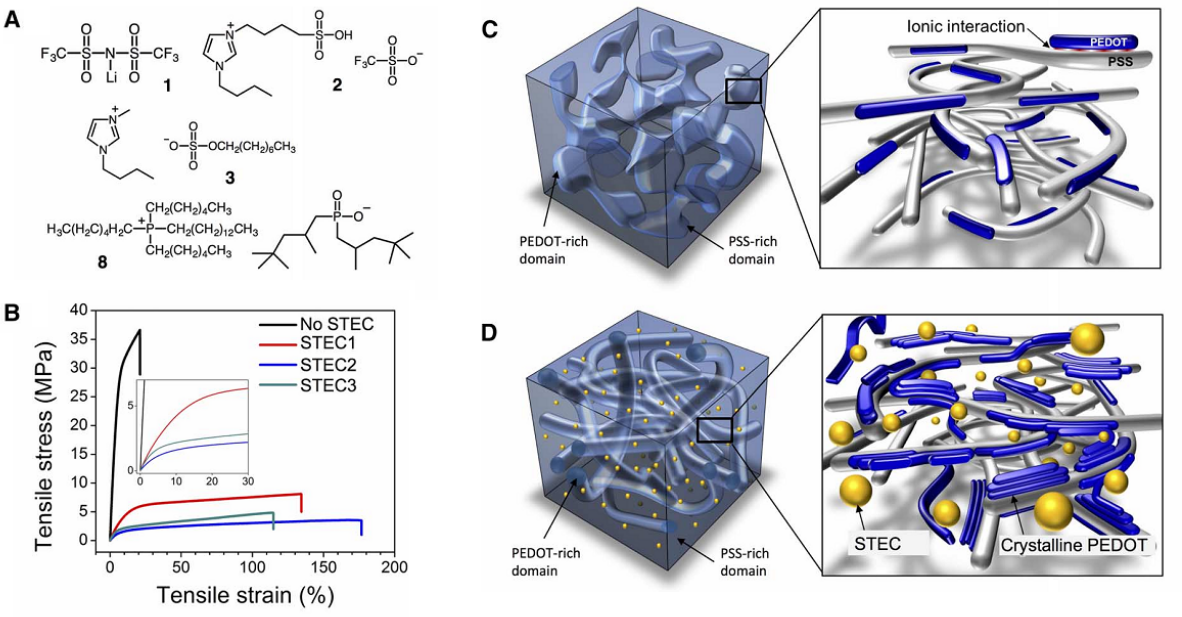

Figure 2.9. Chemical structures and schematic representation. (A) Representative stretchability and electrical conductivity enhancers. (B) Strain-stress curves of PEDOT:PSS with and without stretchability and electrical conductivity (STEC) enhancers. (C and D) Schematic diagram representing the morphology of (C) a typical PEDOT:PSS film versus that of (D) a stretchable PEDOT film with STEC enhancers[30]. Reprinted with permission.

In addition to increasing the stretchability of PEDOT:PSS thin films, many groups were able to make stretchable PEDOT:PSS gels by blending with elastomer[48] or hydrogel[49], and stretchable PEDOT fibers by wet spinning[50]. We recently demonstrated highly stretchable PEDOT:PSS nanofibers via electrospinning. These efforts are paving the way for the development of stretchable interconnects for wearable electronics applications.

2.3.4 Self-healing

Self-healing electronic materials can repair damage caused by frequent bending or external agents. Therefore, they are highly desirable, increasing reliability and longevity of electronic devices[51]. Although the self-healing abilities of non-conjugated polymer networks have been frequently reported, very few works are dedicated to investigating the self-healing ability of conjugated polymers[52]. In 2015, Oh et al. reported self-healing of PEDOT:PSS in the form of a dough by blending PEDOT:PSS with 80% (weight ratio) plasticizer Triton X-100. They proposed the reason for the healing is because the capillary shear force from PEDOT:PSS film to the damaged area was larger than the critical shear stress[47].

2.4 PEDOT:PSS patterning

Conventional photolithography materials, such as photoresist, developer and strippers, are not suitable for patterning organic electronic materials, because they can dissolve or contaminate the organic semiconductors[53,54]. Therefore, although simple patterns can be obtained with conventional lithography[9,22], alternative strategies need to be found to pattern PEDOT:PSS.

Several alternative methods for patterning organic semiconductors are being investigated. Direct printing technologies such as ink-jet printing, screen printing and roll-to-roll printing can be used for features larger than approximately 10-20 um[55,56]. While transfer printing and soft lithography using an elastomer stamp increase the resolution, they require critical control of the adhesion between the carrier stamp and donor/acceptor substrates, which sometimes produces low yield due to variation in the contact area[57,58]. Moreover, lateral collapse of relief structures and sagging of recessed structures of the stamp will result in complete failure of the pattern[59].

A decade before, DeFranco et al. introduced thin parylene film (< 2 um) to pattern PEDOT:PSS[53]. The parylene film can be pre-deposited on glass by chemical vapor deposition and subsequently patterned by conventional photolithography. Deposition of PEDOT:PSS on the patterned parylene layer, followed by a parylene peeling off process, leads to high resolution PEDOT:PSS patterns. The advantage of this method is that the seamless parylene shadow-masking avoids PEDOT:PSS exposure to solvents used in photolithography and thus ensures an unchanged film property after patterning. Since then, parylene patterning has become a widely used method to pattern PEDOT:PSS, especially for the fabrication of OECTs[60].

In any case, direct photolithography is one of the most favored technologies for high resolution patterns due to well-established techniques in the industry. Aiming to develop photolithographic materials that are compatible with organic electronic materials, the groups of Malliaras and Ober proposed a new photolithography chemistry based on fluorinated materials, i.e., hydrofluoroethers (HFE)[54]. HFEs are chemically "orthogonal" to organic compounds, so that organic semiconductors are insoluble and are not swollen in HFEs (Figure 2.10). Thus, this method is named orthogonal photolithography. Despite several demonstrations on rigid substrates[61], this technology is still in its early stage. It is, therefore, necessary to investigate its reliability and optimize photolithographic processes on different substrates to facilitate further applications.

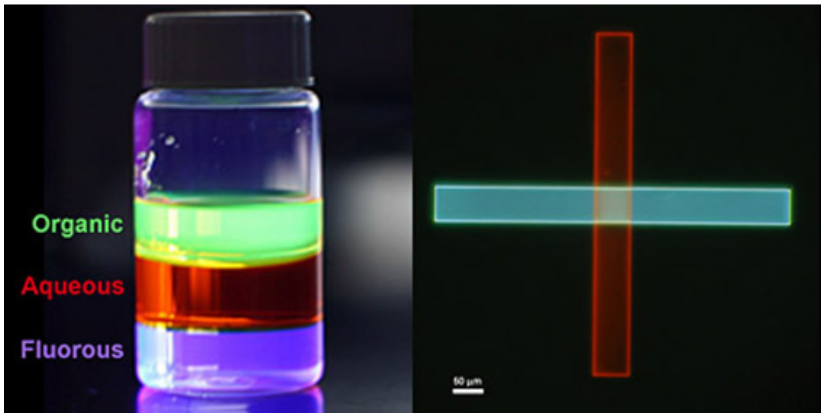

Figure 2.10. The immiscibility of fluorous, aqueous, and organic liquids (shown above, left) enables patterning of two overlapping stripes of light-emitting polymers, with the use of a fluorinated photoresist (shown above, right)[61]. Reprinted with permission.

2.5 The transistor

A transistor is a semiconductor device used to amplify or switch electronic signals and electrical power. Integration of billions of transistors is at the core of industrial electronics, such as processors and memories.[62]. The invention of the transistor is considered to be one of the most important inventions of the 20th century. William Shockley, John Bardeen and Walter Brattain were awarded the Nobel Prize in Physics in 1956, "*for their researches on semiconductors and their discovery of the transistor effect*".

2.5.1 Field-effect transistor

The most successful and widely used transistor is the metal-oxide semiconductor field-effect transistor (MOSFET)[62]. Generally speaking, the most used FETs control current flow in the semiconductor through electrostatic interactions (Figure. 2.11). Two distinct advantages of inorganic (such as silicon) FETs are their excellent stability and fast response speed (up to THz due to high mobility), which permit commercial applications in high frequency communications and high speed data processing. In the past 60 years, inorganic FETs have garnered extraordinary success in industry because of advances in the development of semiconductor materials and well-established manufacturing processes. We have witnessed the rapid development of inorganic FETs. From the initial 10 um process developed by Intel in 1971, to the 14 nm process in 2014, and then to the 10 nm process in 2017[63], FETs have dominated the development of the electronics industry.

2.5.2 Electrochemical transistor

An electrochemical transistor (ECT) uses electrolyte as the gating medium[7]. When a gate bias is applied to the electrolyte, ions migrate into the semiconductor and trigger an electrochemical reaction, or doping/dedoping process (Figure. 2.11), which modulates film conductivity[7]. Metal oxides and conducting polymers are well-known candidates for channel materials in electrochemical transistors.

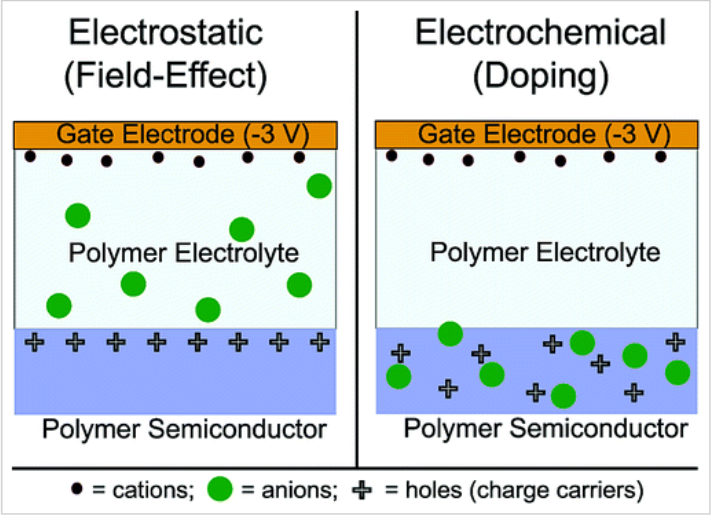

Figure 2.11. Cross-sections of polymer EG transistors showing the difference between (a) electrostatic FET and (b) electrochemical doping ECT[7]. Reprinted with permission.

Using electrolytes as gating media leads to low voltage operation. At electrolyte/solid interfaces a major component of charge separation can arise from the response of the free charges in the electrolyte to the electric field produced by a charge that is bound to the surface. This inhomogeneous region of electrolyte near a charged surface is called an electrical double layer[64] (EDL, Figure. 2.12). At a given potential, the electrode–solution interface is characterized by a double-layer capacitance typically in the range of 10 to 40 mF/cm^2 due to the extremely thin EDL thickness[65]. This value is 10–1,000 times greater than that of conventional solid dielectrics such as SiO_2.

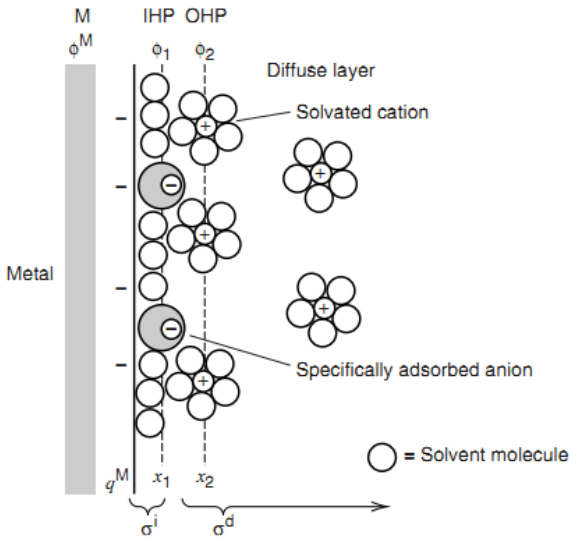

Figure 2.12. Proposed model of the double-layer region under conditions where anions are specifically adsorbed. The solution side of the double layer is thought to be made up of several "layers." That closest to the electrode, the inner layer, contains solvent molecules and sometimes other species (ions or molecules) that are said to be specifically adsorbed. This inner layer is also called the compact, Helmholtz, or Stern layer. The locus of the electrical centers of the specifically adsorbed ions is called the inner Helmholtz plane (IHP), which is at a distance x_1. The total charge density from specifically adsorbed ions in this inner layer is σ^1 (uC/cm^2). Solvated ions can approach the metal only to a distance x_2; the locus of centers of these nearest solvated ions is called the outer Helmholtz plane (OHP)[66]. Reprinted with permission.

2.6 Organic electrochemical transistors (OECTs)

In 1984, seven years after the discovery of conducting polymers, White et al. reported a microelectrode array based on polypyrrole[8] that functioned as a transistor when in contact with an electrolyte solution. This is considered to be the first demonstration of an OECT. They noticed that only a very small gate signal was needed to oxidize (on) or reduce (off) the channel material. Although rather neglected in the beginning due to the material instability and complex fabrication process, OECTs have recently received renewed attention in the emerging area of organic bioelectronics, especially after the introduction of water-stable PEDOT:PSS as channel material in 2002[9], which makes OECTs able to work in aqueous environments, including the human body.

OECTs consist of source and drain electrodes and a channel containing a conducting polymer (e.g., PEDOT: PSS) in ionic contact with the gate *via* an electrolyte solution (Figure. 2.13)[67]. PEDOT:PSS OECTs working in depletion mode: the PEDOT:PSS channel is highly conductive initially and the conductivity decreases upon the application of a gate voltage. When a gate voltage is applied, ions redistribute in the electrolyte and migrate into the conducting polymer. For example, application of positive voltage at the gate pushes cations into PEDOT:PSS and reduces its conductivity via the following redox process[67]:

$$PEDOT^{+}PSS^{-} + M^{+} + e^{-} = PEDOT^{0} + M^{+}\ PSS^{-} \quad (1)$$

Where $PEDOT^{+}$ refers to the oxidized state (conductive), $PEDOT^{0}$ refers to the reduced state (nonconductive), M^{+} is a cation from the electrolyte, and e^{-} is the electron from the drain. The doping ($PEDOT^{+}$)/dedoping ($PEDOT^{0}$) is an electrochemical process that is driven by the applied potential at the gate. Removing the gate bias causes the cations to diffuse back from the channel to the electrolyte, along with a re-doping process, thus restoring the conductivity.

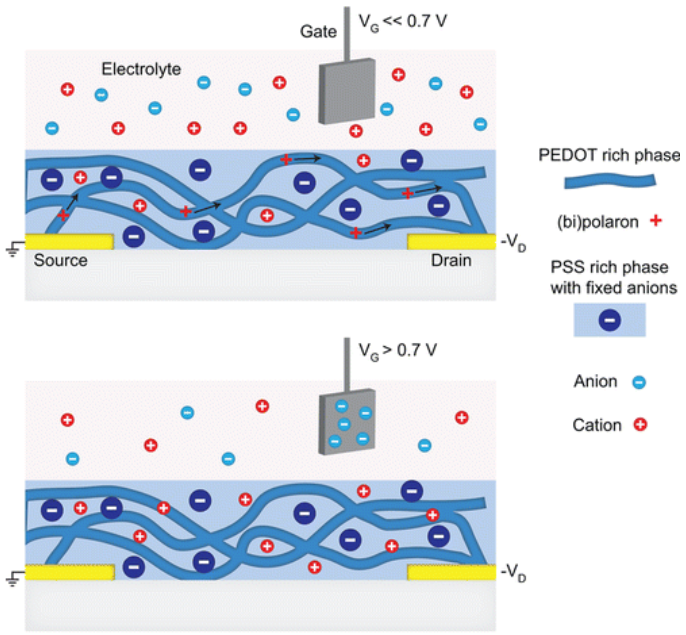

Figure 2.13. PEDOT:PSS-based OECTs. A conductive channel is formed for gate voltages that cause the PEDOT to be in the doped state (top). By reversing the gate potential, the PEDOT can be undoped by electrochemical reaction in the film, rendering the channel nonconductive (bottom). The ionic transport in and out of the film is facilitated by the gate electrode, either by charging and discharging of the EDL of the electrode (shown) or by electrochemical reactions[67]. Reprinted with permission.

2.7 Figures of merit of OECTs

2.7.1 Transfer and output characteristics

Plots of source-drain current (I_{ds}) versus gate voltage (V_{gs}) with constant source-drain voltage (V_{ds}) are named transfer characteristics. Plots of I_{ds} versus V_{ds} with constant V_{gs} are named output characteristics. Transfer and output plots are used to extract the most important figures of merit of the transistors.

2.7.2 ON/OFF ratio

The ON/OFF ratio is defined as the ratio of on-state current (e.g., I_{on} at zero V_{gs} for a PEDOT:PSS OECT) to off-state current (e.g., I_{off} at a positive V_{gs} for a PEDOT:PSS OECT), which can be

obtained from transfer characteristics. A high ON/OFF ratio indicates a good switching property. For PEDOT:PSS OECTs the key to obtaining a high ON/OFF ratio is to minimize the I_{off} at maximum V_{gs} which requires effective or complete dedoping of PEDOT:PSS. OECTs can show a high ON/OFF up to 10^5 (completely dedoped) with a subthreshold slope of 75 mV dec^{-1}[68].

2.7.3 Transconductance

Like other transistors, OECTs convert a modulation in the ΔV_{gs} to a modulation in the ΔI_{ds}. The parameter that determines this conversion is called transconductance, mathematically defined as $g_m = \Delta I_{ds} / \Delta V_{gs}$. The transconductance is the main transistor parameter that governs signal amplification: a voltage amplifier (with gain >1) can be built by connecting OECT in series with a resistor R[68].

Transconductance is the key figure of merit that leads to the success of OECT applications in organic bioelectronics. PEDOT:PSS OECTs can reach transconductance as high as 4 mS, which is 300 times more than solid state silicon transistors and exceeds that of all other electrolyte-gated transistors[69]. Compared to electrolyte-gated FETs where the electrostatic coupling of the gate to the channel is described by the capacitance per unit area of the gate dielectric (interfacial doping), the electrochemical coupling of the gate to channel in an OECT is described by capacitance per volume (volumetric doping, 100 times larger than interfacial doping)[70]. That is, OECTs permit ions to be injected into the PEDOT:PSS film and modulate electronic charge transport in the bulk (thus a lower interface impedance). As such, the transconductance of OECTs can be linearly increased not only by increasing W/L (attainable in FET), but also by increasing channel thickness (not attainable in FET)[71].

With high transconductance, OECTs can easily obtain a high gain exceeding 10[68]. If an OECT is used to record the signal, it will thus increase the signal to noise ratio (noise from the processing setups) from $^{signal}/_{noise}$ to $n \times {}^{signal}/_{noise}$, thus ensuring its practical application for signal sensing and recording.

2.7.4 Response time

OECTs consist of two circuits: the ionic one, where ions are transported between the electrolyte and the channel, and the electronic one, where holes are transported in the PEDOT:PSS channel

between the source and the drain. Accordingly, both ion transport in the ionic circuit and hole transport in the PEDOT:PSS channel affect the response time of OECTs. Khodagholy et al, revealed that hole transport time (~10^{-1} cm^2 V^{-1} S^{-1}) in a microscale OECT is 10-100 times faster than the ionic transport time (~10^{-3} cm^2 V^{-1} S^{-1}), and therefore the latter one is the limiting factor of the response time[69]. In particular, the OECT has a temporal response time with a time constant of ~100 us, resulting in a cut-off frequency of ~1 kHz. Decreasing the channel thickness can further decrease the response time by reducing ionic transport time into the bulk[70]. Other factors limiting the OECTs' response time are the distance between the gate and channel[72] and the channel length[67].

2.7.5 Mobility

Mobility indicates the ability of an ionic or electronic charge (hole in case of PEDOT:PSS) to move in response to a given electrical field. Both high ion and hole mobilities are required to obtain a fast response OECT. The ionic drift mobility in PEDOT:PSS was estimated by Stavrinidou et al. based on a planar electrolyte/PEDOT:PSS junction (Figure. 2.14a)[42]. They assumed voltage only drops on the dedoped part (high resistance) of a PEDOT:PSS film and the injected cations in the dedoped region are equal to the sulfonate density, thus the cation diffusion rate is v = dl/dt =uE=uV/l, in which u is the ion mobility and V is the applied voltage. By monitoring the propagation of dedoping front, cation mobility in the PEDOT:PSS film was calculated by l^2=2uVt, where V is the applied bias and t is time, and μ, the cation mobility, can be obtained with a value ~10^{-3} $cm^2/V^{-1}s^{-1}$.

The hole mobility in PEDOT:PSS can be estimated by using the model developed by Bernards et al.[71], who observed that driving an OECT at constant I_g results in a linear I_{ds} change with time, i.e., $dI_{ds}/dt = -I_g/\tau_e$ where τ_e is the transit time that is described by $v\tau_e$= L, where v is the hole velocity (uE), E is the electrical field (V_{ds}/L) and L is the channel length (Figure. 2.14b). Thus, at a fixed V_{ds}, the hole mobility (u) in PEDOT:PSS film can be extracted by gating OECT with constant I_g and measuring its response time, τ_e. The calculated hole mobility in PEDOT:PSS film is 10^{-2} ~ 10^{-1} $cm^2/V^{-1}s^{-1}$, which is about 10 times higher than the ion mobility.

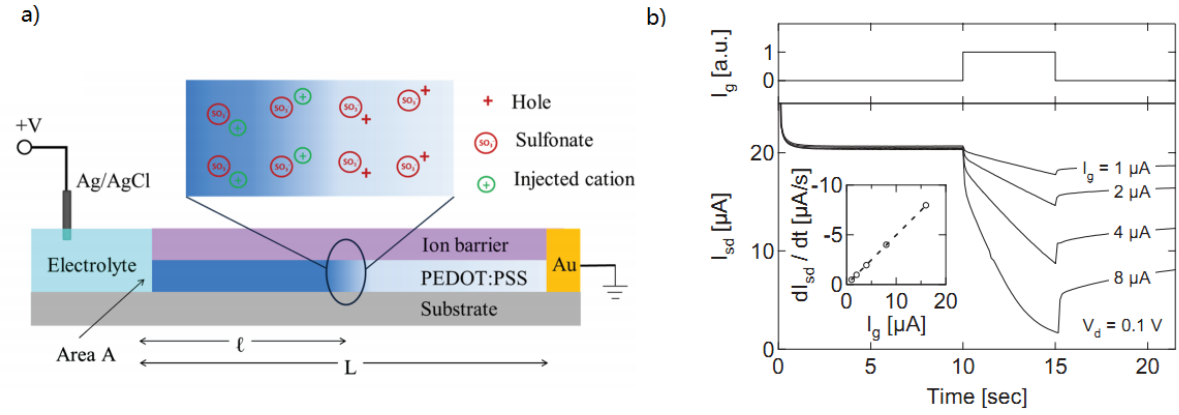

Figure 2.14. a) Schematic of the device indicating the charge distribution around the dedoping front according to the model (not to scale), the drift length of injected ions, the total length, L, of the PEDOT:PSS film, and the area, A , of the electrolyte/conducting polymer junction[42]. Reprinted with permission. b) Experimental transient response of an OECT under application of a constant gate current[71]. Reprinted with permission.

2.8 Applications of organic electrochemical transistors (OECT)

2.8.1 Non-faradic sensing

The non-faradic sensing, i.e., no faradic reaction at the gate electrode, using PEDOT:PSS OECT is first demonstrated as a humidity sensor[73] (Figure. 2.15a). The proton conductivity of the electrolyte Nafion is heavily affected by water content. The change of humidity between 30% RH and 80% RH will cause an I_{ds} change due to the increased proton conductivity in the Nafion membrane and thus an increased dedoping process in the PEDOT:PSS channel. This is also the first demonstration of using OECT as a transducer (ion to electron).

Cicoira et al. reported the use of a PEDOT:PSS OECT for monitoring micelle formation of cetyltrimethylammonium bromide (CTAB) in aqueous solution[74] (Figure. 2.15b). Normally, modulation in OECTs mostly depends weakly on the electrolyte concentration (such as sodium chloride, NaCl). However, they noted when the CTAB concentration is higher than the critical micelle concentration, a significant increase in OECT modulation occurs due to the more efficient

dedoping of micelle ions with respect to the dissociated ions. Thus OECTs can be used to sense the micelle formation process of CTAB.

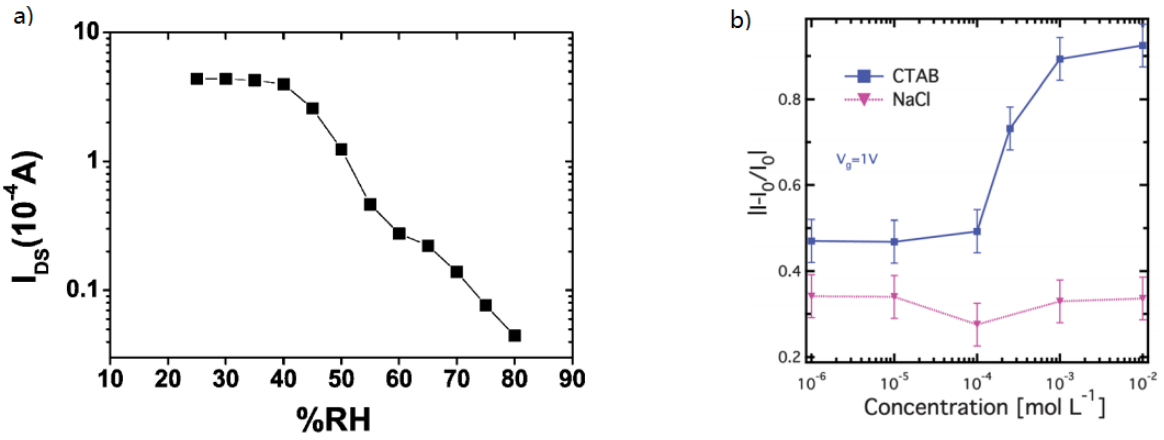

Figure 2.15. (a) I_{ds} measurements in an OECT at variable relative air humidity[73]. Reprinted with permission. (b) OECT modulation, where I is the OFF current and the I0 is the ON current (V_g= 0V), versus molar concentration of CTAB and NaCl aqueous solutions at V_g = 1 V[74]. Reprinted with permission.

2.8.2 Faradic sensing

Faradic sensing, i.e., a faradic reaction taking place at the gate, was first studied by Bernards et al., who reported an enzymatic sensing of glucose and elucidated the underlying mechanism[75]. When a positive V_g is applied in an OECT, the voltage drop between the gate and the channel depends on the ratio between the channel and gate capacitance (C_c) / (C_g). Let $\gamma = C_c/C_g$, it can be shown that

$$V_{sol}= \frac{Vg}{1+\gamma} \quad (2)$$

When charge transfer occurs between the electrolyte and the gate (i.e., faradic process), V_{sol} will be affected. In the case of electron flow from the electrolyte to the gate electrode, following Nernst equation, V_{sol} will be pulled up a value of ($\frac{kT}{ne}$ ln [analyte] + constant) to:

$$V_{sol}= \frac{Vg}{1+\gamma} + (\frac{kT}{ne} \ln [\text{analyte}] + \text{constant}) \quad (3)$$

where k is Boltzmann's constant, T is the temperature, e is the fundamental charge, n is the number of electrons transferred during the reaction and [analyte] is the analyte concentration. Thus, changing the analyte concentration will change the V_{sol} which, in turn, changes the I_{ds} in OECT and thus analyte concentration is sensed.

Since Bernards et al. reported the use of OECTs to sense a faradic process at the gate many groups have shown interest in sensing species based on their concentration-dependent faradic reactions at the gate[76-78]. In particular, with this methodology, the Yan's group reported many examples, by facilitating the faradic process via the gate modulation with enzyme, graphene, carbon nanotube (CNT) and Pt nanoparticles, to sense biomaterials such as glucose[79], DNA[80], dopamine[81] and saliva[82].

2.8.3 Cell sensing and in vivo recording

Cell sensing and in-vivo recording are a direct use of OECT to sense biological signals. They represent the most important exploration of OECTs for real medical diagnosis and therapy. In the past decade, great advances have been made in this field. In 2009, Berggren's group reported control of the adhesion and growth of epithelial cells with OECTs[83]. OECTs show the ability to affect the spreading and position of the cell density along the OECT channel by controlling gate- and drain-voltage levels. In 2010, Yan's group first demonstrated the use of PEDOT:PSS OECTs as cell-based biosensors to monitor cell activities[84]. The electrostatic interaction between cells and PEDOT:PSS can result in a conductivity change of the OECT. In 2012, Owens' group reported the use of OECT to monitor in-situ barrier tissue integrity[85]. The presence of cells with tight junctions slows the OECT response compared with the response when no cells are present. In 2013, Dion et al. successfully demonstrated the first in-vivo application of PEDOT:PSS OECT for recording eElectrocorticography (ECoG) signals in the brain of the rat[86]. They proved that OECTs showed a superior signal-to-noise ratio due to local amplification (high transconductance) of OECT. In 2014, Owens' group demonstrated that OECTs are able to sense epithelial cells with high-resolution time-lapse images[87]. In the same year, Biscarini's group also demonstrated that OECTs fabricated on resorbable bioscaffold poly(L-lactide-co-glycolide) (PLGA) can be used to record electrocardiographic (ECG) signal[88]. In 2015, Rivnay et al. further exploited the use of thick OECT for highly sensitive electroencephalography (EEG) recordings in the human body[70]. In the same

year, the Berggren's group demonstrated the first example of electronic functionality added to plants by using OECT and reported integrated organic electronic analog and digital circuits in the plant[89]. And, in 2017, Owens' group successfully introduced OECT in sensing lactate in tumor cell cultures[90]. The detailed historical diagrams are summarized in Figure. 2.16.

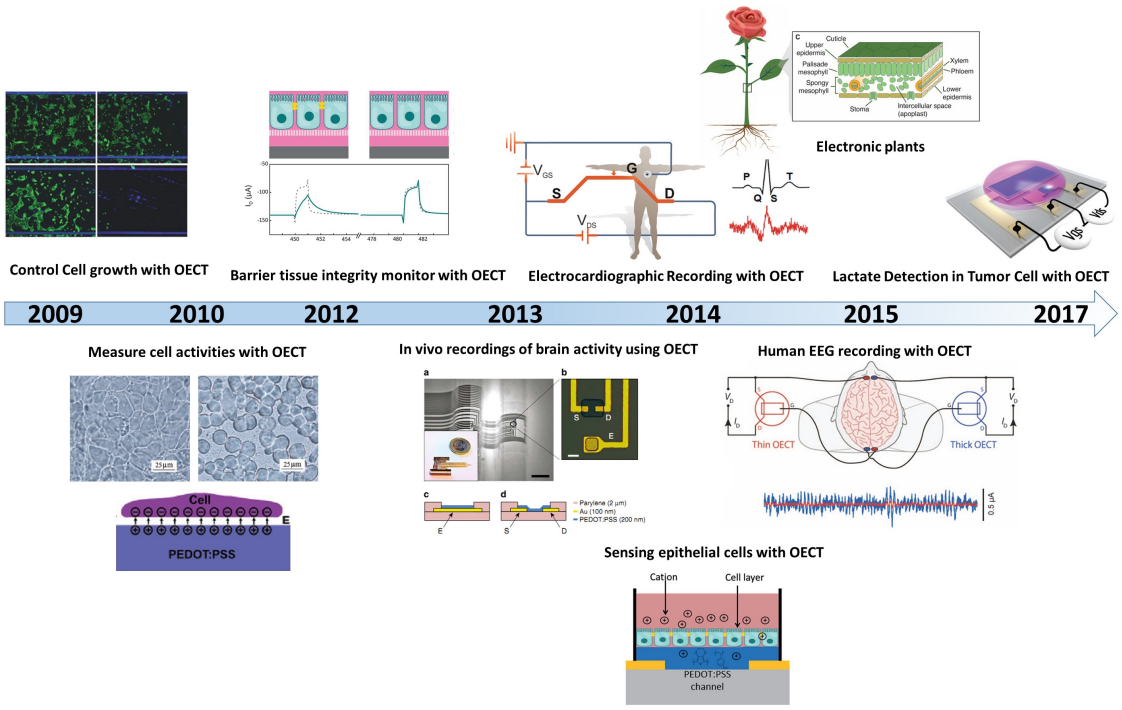

Figure 2.16. OECTs research progress in cell sensing and in vivo recording[70,83-90]. Reprinted with permissions.

2.9 Strategies for stretchable electronics

Stretchable electronic devices have received increasing attention in recent years due to their great potential in wearable electronics, electronic skin, bio-implanted electronics, human-activity monitoring, and personal healthcare[91-93]. In the past decade, rapid developments in both materials design and device engineering in stretchable electronics have contributed to significant progress in stretchable light-emitting diodes, transistors, solar cells, energy harvesters, biological sensors, and energy-storage devices et al[91,94,95].

In general, three different strategies can be used to develop stretchable electronic devices: the bulking method[96], geometric structuring[91,93] and intrinsically stretchable materials[97] (Figure. 2.17).

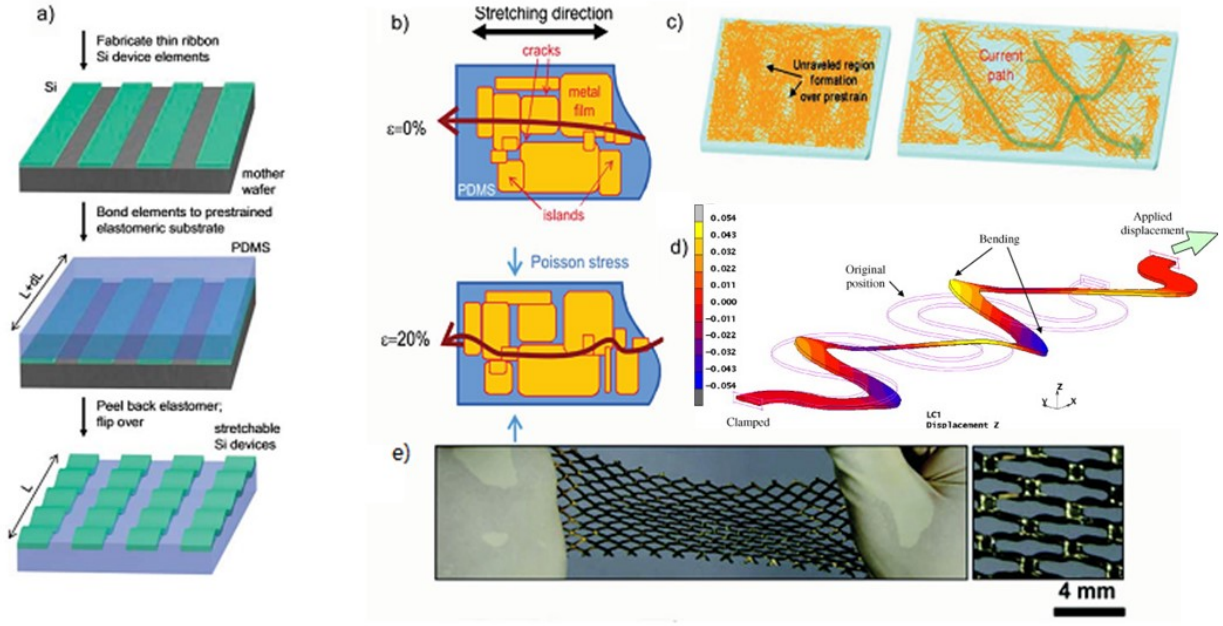

Figure 2.17. (a) Bulking method (out of plane): a schematic illustration of the process for building stretchable single-crystal Si devices on elastomeric substrates[98]; Reprinted with permission. And various geometric structuring methods to impart stretchability at different length scales using in-plane films: b) A percolating pathway in an Au film, consisting of micron-sized cracks under applied strain; c) A percolating pathway in a nanowire film; d) Out-of-plane deformation of a serpentine metal interconnect. Adapted with permission; and e) Distortion of a substrate patterned on the device level[91]. Reprinted with permission.

The bulking method was first developed in 1998 when Whiteside et al. observed that deposition of a high-modulus thin film (e.g., Au) onto a restrained elastomeric substrate (PDMS) results in the formation of a wrinkled (buckled) film structure upon relaxation of the elastomer[96]. The released substrate can be stretched to the value of the prestrain without inducing considerable strain in the active components. Geometric structuring is similar to buckling but is based on the formation of cracks or patterns in the film which can distort under strain while retaining percolative electrical conduction[93]. In 2006, Rogers' group obtained bulked (wavy) ultrathin single-crystal Si ribbons upon releasing the prestrained PDMS substrates, thus introducing the buckling method to fabricate stretchable electronic devices[98]. Since then, the Rogers group has pioneered many techniques to make buckled or geometric structuring devices from traditional high-performance inorganic

semiconductors and conductors, such as a hemispherical electronic eye camera[99], and epidermal electronics[100]. They also investigated the theoretical physics behind the stretchable electronic device and developed stretchable devices with more complex structures, e.g., with the "kirigami" approach[101]. The group of Takao Someya also pioneered the fabrication of stretchable organic light-emitting diodes[102], active matrix[103] and ultra-lightweight transistors[104].

Intrinsically stretchable devices have specific advantages since they allow more intimate contact with the targets, such as human skin, and can be processed via cost effective and simple fabrication processes by direct printing onto elastomeric substrates[91,95]. In general, it is more challenging to achieve intrinsically stretchable electronic devices due to the brittle and rigid nature of the conductors. Currently, well-known intrinsically stretchable materials are mostly nanostructured, for example, CNTs[105], silver nanowires[106] and nanofibers[50,107]. However, these materials are considered challenging to handle in large-scale and high fidelity fabrication processes.

CHAPTER 3 ARTICLE 1: SOLVENT-INDUCED CHANGES IN PEDOT:PSS FILMS FOR ORGANIC ELECTROCHEMICAL TRANSISTORS

This article has been published in the journal "APL Materials" in 2015. This article reports processing PEDOT:PSS thin films for organic electrochemical transistors (OECTs) applications. The supporting information for this article is reprinted in Appendix A of this thesis.

3.1 Authors

Shiming Zhang, Prajwal Kumar, Amel Sarah Nouas, Laurie Fontaine, Hao Tang, Fabio Cicoira

Department of Chemical Engineering, Polytechnique Montreal, Montreal,

Québec H3C 3J7, Canada, Email : fabio.cicoira@polymtl.ca

3.2 Abstract

Organic electrochemical transistors based on the conducting polymer poly(3,4-ethylenedioxythiophene) doped with poly(styrenesulfonate) (PEDOT:PSS) are of interest for several bioelectronic applications. In this letter, we investigate the changes induced by immersion of PEDOT:PSS films, processed by spin coating from different mixtures, in water and other solvents of different polarities. We found that the film thickness decreases upon immersion in polar solvents, while the electrical conductivity remains unchanged. The decrease in film thickness is minimized via the addition of a cross-linking agent to the mixture used for the spin coating of the films.

3.3 Introduction

Organic electronic devices have attracted particular attention in recent decades because they are easy to process over large areas, exhibit electronic properties that can be tuned via chemical synthesis, and are compatible with flexible and low-weight substrates[2,108]. Besides established applications such as organic light-emitting diodes, organic solar cells, and organic field-effect transistors[109,110], the past few years have seen the rise of organic bioelectronics, which exploits the coupling of devices based on conducting polymers with biological systems[6]. Among organic

bioelectronic devices, organic electrochemical transistors (OECTs) are investigated because they can be operated at low voltages (below 1 V) and are able to act as ion to electron converters[8,22,73,75,79,111]. OECTs consist of source and drain electrodes and a channel containing a conducting polymer in ionic contact with a gate electrode via an electrolyte solution. The gate voltage modulates the current flowing in the channel between the source and drain electrodes[71,112]. OECTs have been used as sensors for chemical and biological species, such as hydrogen peroxide[113], glucose[77], neurotransmitters[114], chloride ions[111], DNA[80], as well as to establish controlled cell gradients on conducting polymer surfaces[83], monitor tissue integrity[85], and record in vivo brain activity[86]. They have been integrated with microfluidic channels for lab-on-a-chip applications[115], and are also the fundamental unit of other newly emerging devices, such as ion transistors and organic electronic ion pumps[22,116].

The majority of OECTs are currently based on the conducting polymer poly(3,4-ethylenedi-oxythiophene) doped with polystyrene sulfonate (PEDOT:PSS). PEDOT:PSS is a heavily doped p-type semiconductor, where holes on the $PEDOT^+$ chains are compensated by sulfonate anions on the PSS^- chains (dopant)[69]. The application of a positive gate bias causes cation inclusion into the PEDOT:PSS channel[71]. These cations compensate the sulfonate anions in the film and de-dope

$PEDOT^+$, thereby decreasing the source-drain current. PEDOT:PSS films are typically obtained by spin coating from commercially available aqueous suspensions, which need to be mixed with other chemical compounds to increase film electrical conductivity, which in films processed from pristine PEDOT:PSS suspensions is typically as low as 1 S/cm[75,77,117]. Mixing with other chemical compounds is also necessary to facilitate film processing and to improve film mechanical stability. The compounds employed to increase film conductivity are often named secondary dopants. However, as there is no evidence that they change the doping level of PEDOT[118], it is more appropriate to name them conductivity enhancement agents[119]. The conductivity increase upon addition of conductivity enhancement agents is likely due to the fact that they alter the film morphology during drying, leading to lower energy barrier for charge carrier transport between individual PEDOT:PSS clusters[119]. Despite the widespread use of PEDOT:PSS in organic electronics, little attention has been so far dedicated to the behaviour of PEDOT:PSS films in water, which is a universal solvent for bioelectronic applications. In this letter, we investigate the variation of the thickness, chemical composition, and electrical properties of PEDOT:PSS films after immersion in water and in other solvents with different polarities. These studies are of paramount

importance for the development of devices working at the interface with biological systems and living tissues, where the release of substances needs to be strictly controlled.

3.4 Experimental part

PEDOT:PSS films were deposited on glass substrates by spin coating from mixtures containing all or part of the following components: a PEDOT:PSS aqueous suspension (Clevios™ PH1000, Haraeus Electronic Materials), the surfactant dodecyl benzene sulfonic acid (DBSA), which facilitates film processing, one conductivity enhancing agent among glycerol, sorbitol, ethylene glycol (EG), and dimethyl sulfoxide (DMSO), to increase film electrical conductivity, and the crosslinking agent 3-glycidoxypropyltrimethoxysilane (GOPS), to improve film mechanical stability and adhesion to the substrate[42,76]. The Clevios PH1000 PEDOT:PSS aqueous suspension has a PEDOT:PSS content of 1.1 w/w %, with a PEDOT to PSS ratio of 1:2.5 (i.e., ∼0.3 w/w % PEDOT and ∼0.8 w/w % PSS)[42]. Therefore, the amounts of conductivity enhancement agents added to the suspension can, as it is the case for the range of ∼2 w/w % and 40 w/w % investigated in this work, significantly exceed the initial amount of PEDOT:PSS. After spin coating, the films were baked at 140 °C for 1 h. The film thickness was measured with a Dektak 150 profilometer. The film electrical conductivity was obtained by four point probe measurements according to the model developed by Smits[120]. Additional experimental details are available in the supplementary material.

3.5 Results and discussions

To gain insight into the effect of the various additives, we first investigated films obtained from a mixture of Clevios PH1000 and DBSA. Although DBSA is widely used as an additive (surfactant) to facilitate film processing from PEDOT:PSS suspensions[69,71,86], its effect on film conductivity has not been investigated yet. By measuring the electrical conductivity of PEDOT:PSS films processed from mixture with different DBSA contents, we found that DBSA significantly affects film conductivity (inset of Figure. 3.1). The highest conductivity (∼500 S/cm) is observed for a mixture containing 2 v/v % DBSA. However, we found that concentrations of DBSA higher than ca. 0.5 v/v % induce a phase separation in the mixture, which makes processing by spin coating more difficult and results in a poor film quality. Therefore, for the following studies, we kept the DBSA concentration at 0.5 v/v % and used conductivity enhancing agents, such as glycerol,

sorbitol, EG, and DMSO, to achieve high film conductivity. Although conductivity enhancing agents have been used for decades for the processing of PEDOT:PSS films, their role is still under debate. Kim et al. proposed that these compounds could induce screening effects, thus reducing the coulombic interactions between $PEDOT^+$ and PSS^- and therefore enhancing the charge carrier hopping rate and conductivity in the PEDOT:PSS films[31]. Inganas et al. considered conductivity enhancing agents to act as plasticizers, which would aid the reorientation of the PEDOT:PSS chains during the baking process to form more connection pathways between $PEDOT^+$ chains[121]. Ouyang et al. attributed the conductivity enhancement to an effect on the conformation of the $PEDOT^+$ chains[32]. Leo et al.[122] and Jonsson et al.[123] assumed that removal of insulating PSS^- is the prime reason for the conductivity improvement after the introduction of conductivity enhancing agents. It has been reported recently that the conductivity of PEDOT:PSS films can be increased up to about 4000 S/cm, a value comparable to that of indium tin oxide, via a post-treatment with sulphuric acid[25]. However, sulphuric acid is a strong and corrosive acid, which limits its application in bioelectronics.

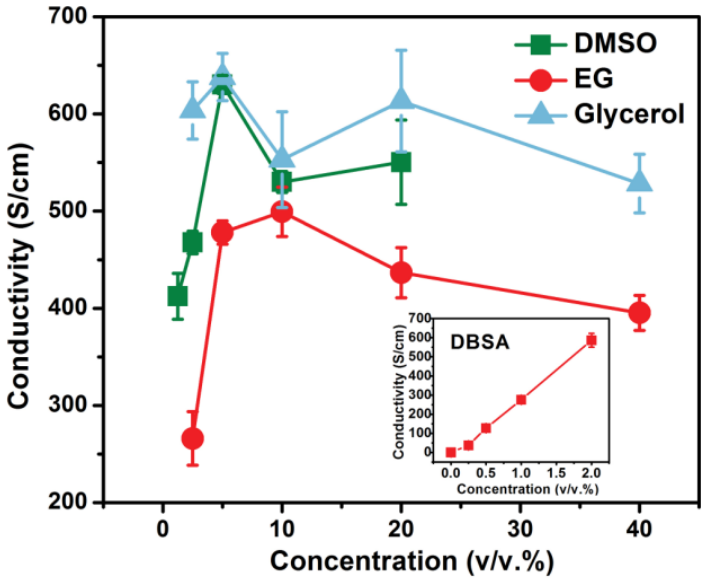

Figure 3.1. Electrical conductivity of PEDOT:PSS films processed from mixtures containing Clevios PH1000, 0.5 v/v % DBSA, and different v/v % concentrations of conductivity enhancing agents (DMSO, EG, glycerol). The inset shows the electrical conductivity variation versus increasing DBSA concentrations in absence of conductivity enhancing agents. The films thickness is about 150 nm. The error bars correspond to the standard deviations of three samples.

Figure. 3.1 shows the effect of the conductivity enhancing agents EG, DMSO, and glycerol (data for sorbitol are shown in Figure. S1 in the supplementary material) on the conductivity of films processed from mixtures of Clevios PH1000 and DBSA (0.5 v/v %). The highest conductivity, of 600–700 S/cm, is observed for glycerol (5 v/v %), DMSO (5 v/v %), and sorbitol (2.5 wt. %). Considering the lower toxicity of glycerol with respect to DMSO and EG and its ease of process as compared to sorbitol, we employed it as the conductivity enhancing agent in our experiments.

The mixture used to process our films contains 94.5 v/v % of Clevios PH1000, 5 v/v % of glycerol, and 0.5 v/v % of DBSA. Most of the glycerol is expected to be removed after baking, based on water-glycerol temperature-composition phase diagrams obtained at atmospheric pressure[124]. This hypothesis is supported by XPS analysis (shown in Figure. S2), which shows that our films processed from pristine Clevios PH1000 and from Clevios PH1000/glycerol mixtures show similar carbon to sulphur (C/S) and oxygen to sulphur (O/S) ratios. As the addition of glycerol to Clevios PH1000 leads to a significant increase of the amount of C and O in the liquid mixture, a significant presence of glycerol in the film would result in an increase of C/S and O/S ratios, with respect to films processed from pristine Clevios PH1000 (from ∼2.7 to ∼16 for the C/S ratio and from ∼7.5 to ∼21 for the O/S ratio). The significant removal of glycerol after baking is further validated by weighing experiments carried out with an analytical balance (see Figure. S3 in supplementary material).

As all organic bioelectronic devices work in aqueous environment, we first investigated the changes of PEDOT:PSS film properties after immersion into deionized water. We found that water immersion induces a considerable decrease in film thickness and, as a consequence, an increase in sheet resistance (see Table S1 in supplementary material). Inspired by this observation, we measured the change in thickness and conductivity of PEDOT:PSS films after immersion for 10 minutes in solvents with different polarity parameters, namely, iso-propanol (polarity parameter 3.9), acetone (5.1), and Milli-Q deionized water (10.2)[125]. The polarity parameter, as defined by Snyder[126], is a measure of the ability of a solvent to interact with various polar test solutes. Interestingly, we observed (Figure. 3.2) that solvents with higher polarity parameter induce a larger thickness decrease. The decrease ratio is nearly independent of the initial film thickness. The

decrease in thickness does not significantly affect the film electrical conductivity (see Table S1 in the supplementary material).

To gain insight into the mechanism of the thickness decrease of PEDOT:PSS films after immersion in water, we analyzed the film chemical composition before and after immersion in water by XPS, focusing in particular on the relative intensities of the characteristic $PEDOT^+$ and PSS^- peaks. Figure. 3.3(a) shows a portion of the XPS spectra (between 164 and 172 eV binding energy) of PEDOT:PSS films before and after immersion in water. The S(2p) peak at the binding energy of ca.169 eV corresponds to the sulphur signal of PSS^-, and the doublet peaks at ca.165 eV correspond to the sulphur signal of $PEDOT^+$[122]. Interestingly, after immersion in water, the ratio between the intensities of the PSS^- and $PEDOT^+$ peaks decreases from ca. 2:1 to ca. 1.6:1, which suggests that excess PSS^- is removed from the film, thus explaining the decrease in film thickness[127]. The excess PSS^- is expected to be mostly accumulated on the surface of the films, thus its removal has negligible influence on the film conductivity[128].

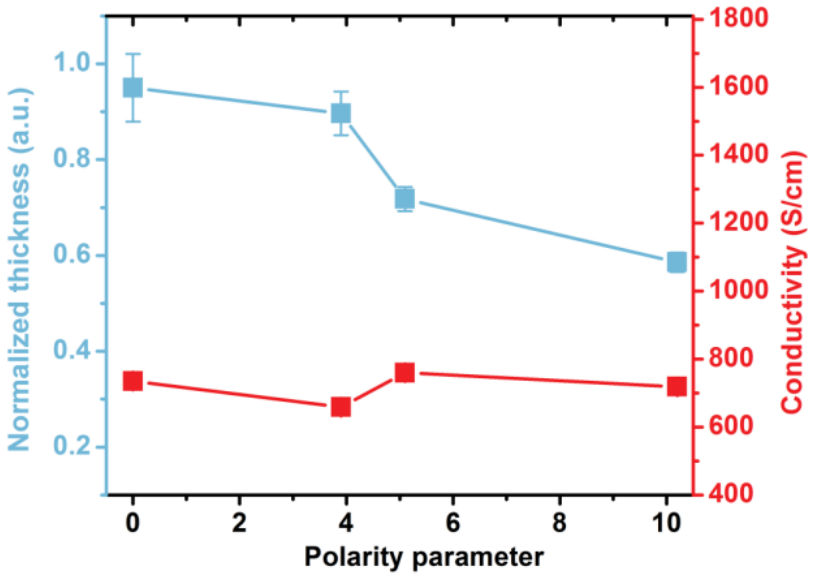

Figure 3.2. Thickness and conductivity of PEDOT:PSS films (after immersion for 10 minutes) versus polarity parameters of the solvents: isopropanol (polarity parameter 3.9), acetone (5.1), and Milli-Q deionized water (10.2). The value at polarity parameter =0 corresponds to the film thickness before immersion in the solvents. The thickness values on the left y axes are normalized with respect to the initial films thicknesses (about 150 nm). The PEDOT:PSS film is deposited from a mixture containing 94.5 v/v % of Clevios PH1000, 5 v/v % glycerol, and 0.5 v/v % DBSA.

The polarity parameters are obtained from the literature[125]. The error bars correspond to the standard deviations of three samples.

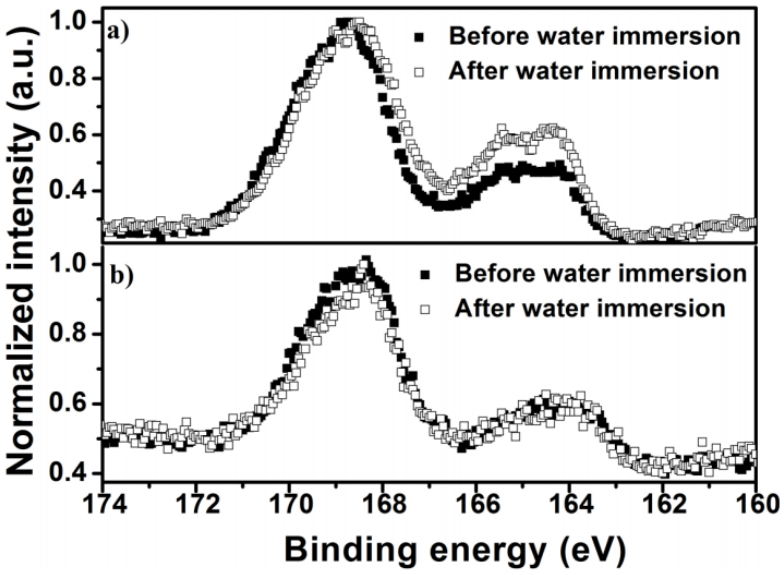

Figure 3.3. XPS S(2p) spectra of films processed from mixtures containing 94.5 v/v% of CleviosTM PH1000, 5 v/v% glycerol and 0.5 v/v% DBSA after water immersion for 10 min: (a) without GOPS; (b) with 1 v/v % GOPS.

It has been reported that the stability of PEDOT:PSS films in aqueous solutions can be improved by the addition of the cross-linker GOPS, which is expected to prevent partial dissolution or delamination of the PEDOT:PSS films when immersed into an electrolyte solution[76,77]. The detailed mechanism of the cross-linking reaction is still unclear, since several chemical reactions can take place between GOPS and the components of the mixture as well as the glass (SiO2) substrate. According to the literature, GOPS should react with glycerol via an epoxy-hydroxy (etherification) reaction, to form a network structure[129,130]. Alternative or parallel reaction paths can be the condensation of the methoxy groups with the –OH groups of glycerol[131,132] and at the glass substrate surface[133]. It is worth mentioning that we observed a thickness increase and an identical thickness before and after water immersion also for films processed from PEDOT:PSS/GOPS mixtures in the absence of glycerol. This might indicate that the GOPS is also able to react with itself or with PEDOT:PSS, as recently found for the system PEDOT/graphene oxide[134].

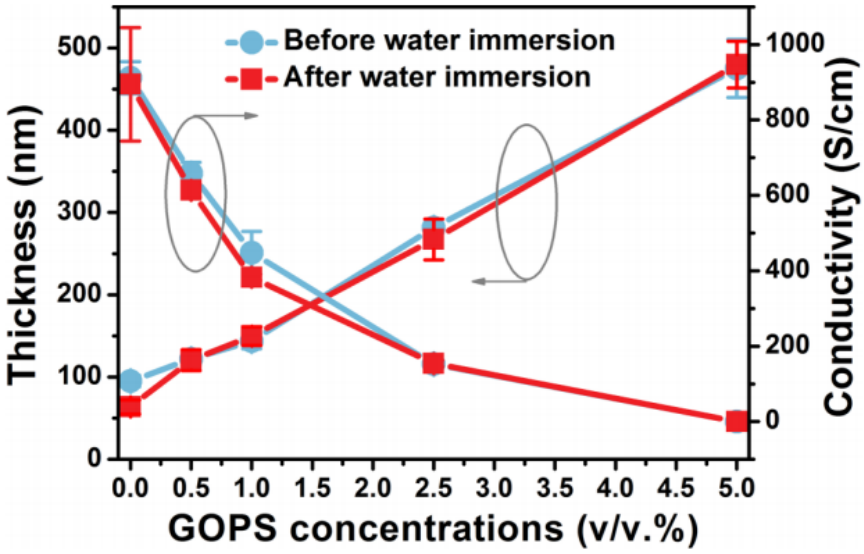

Figure 3.4. Thickness (left y scale) and conductivity (right y scale) change of films processed from mixtures containing 94.5 v/v% of CleviosTM PH1000, 5 v/v% glycerol and 0.5 v/v% DBSA with increasing GOPS concentration. The error bar stands for standard deviation of three samples.

To further clarify the role of GOPS in PEDOT:PSS film, we carried out thickness and resistivity measurements on PEDOT:PSS films with different GOPS contents. Increasing the content of GOPS in the PEDOT:PSS/DBSA/glycerol mixture causes the increase of film thickness and the decrease of film conductivity (Figure. 3.4). The film thickness increases linearly with the GOPS concentration and reaches 500 nm (i.e., ~5 times the thickness of pristine PEDOT:PSS films) when 5 v/v % GOPS is present in the mixture. This is likely due to the fact that, after the cross linking reaction takes place, a large amount of non-evaporating species (with respect to the PEDOT:PSS initial content of ~1 w/w% in the Clevios PH1000 suspension) is present in the film. To estimate the PEDOT:PSS to cross-linking network ratio, we used the elemental ratios obtained from XPS (see Figure. S2 in the supplementary material). The C/O/Si elemental ratio in the GOPS molecule ($C_9H_{20}O_5Si$) is 9/5/1. Assuming that this ratio is maintained in the film and using the Si content as a reference, we determined the amount of GOPS-related species (cross-linking network) present in the film with respect to PEDOT:PSS. For films processed from a mixture containing 1 v/v % GOPS, the amount of GOPS-related species (C, O, and Si) is ca. 52.5%, which increases to 82.5% for films processed from a mixture containing 2.5 v/v % GOPS. Such a large content of non-

evaporating and non-conducting species in the films may indicate that GOPS is able to cross-link with glycerol or other species in the films and explain the increase of thickness and the decrease of electrical conductivity.

Films containing GOPS show no thickness decrease after immersion in water and the corresponding XPS spectra did not show changes neither in PEDOT:PSS ratio (Figure. 3.3(b)) nor in C/Si ratio (Figure. S2 in the supplementary material). This result proves the effectiveness of the cross-linked network in preventing film dissolution and delamination in aqueous solutions.

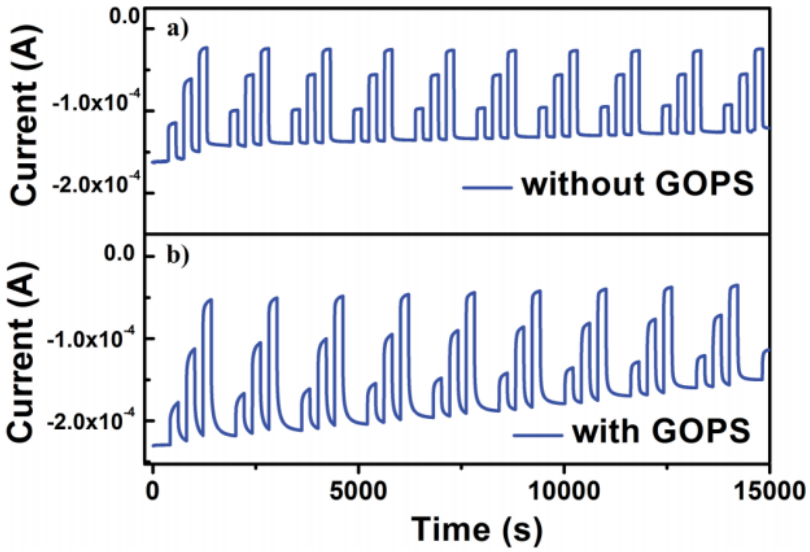

Figure 3.5. Transient electrical measurement (10 cycles) with a duration of about 15 000 s (250 min) for OECTs fabricated from PEDOT:PSS/5 v/v % glycerol/0.5 v/v % DBSA films: (a) without GOPS; (b) with 1 v/v % GOPS. The spin-coating speeds for both films are 500 rpm for 10 s followed by 1500 rpm for 45 s. The thickness of the film with and without 1 v/v % GOPS is about 350 nm and 150 nm, respectively.

As the electrical properties of PEDOT:PSS films are essential for application in OECTs, we tested the electrical stability of the PEDOT:PSS films with and without GOPS in water using a two terminal device. Before the measurements, all films were rinsed in water for 10 min to stabilize the thickness. Although the films containing GOPS show superior mechanical stability, a considerable current decrease is observed during the first 3 h of operation (see Figure. S5 in supplementary material). This phenomenon is likely related to the water absorption by the PSS^- units in the film.

The addition of GOPS yields thicker films at a given spin-coating speed. The thicker films likely contain a larger amount of PSS^- units, which are not removed by water due to the presence of the GOPS cross-linker. As a consequence, the excess of hydrophilic PSS^- would absorb larger amounts of water and cause irreversible morphological changes in the film[135], thus resulting in a decrease in conductivity. Water absorption of PSS^- likely reaches a saturation state (i.e., PSS^- is fully hydrated) within 3 h and, afterwards, the current becomes stable.

Finally, we studied the effect of GOPS on the electrochemical stability of OECTs by comparison with a device employing no GOPS (Figure. 3.5). A high surface area (1000–2000 $m^2\ g^{-1}$) activated carbon was used as the gate electrode[136]. The source-drain voltage (V_{ds}) was fixed at −0.2 V, and gate bias (V_g) was pulsed from 0 to 0.6 V with a step of 0.2 V. Each OECT was run for 10 cycles for a total time of about 250 min. As shown in Figure. 3.5, for films processed at the same spin-coating speeds, PEDOT:PSS channel containing GOPS shows a higher current (I_{ds}), which should result from the higher film thickness. OECTs with and without GOPS crosslinker show comparable electrochemical stability after 10-cycles operation. However, devices containing GOPS show a considerable negative base current shift (Figure. 3.5(b)), which is likely caused by the water absorption of PSS^- in the films, and by the presence of the non-conductive species in the cross-linked network.

3.6 Conclusion

In summary, we have investigated the variations of the properties of PEDOT:PSS films in liquids with different polarities. Increasing the solvent polarity leads to a decrease in thickness and an increase in sheet resistance, while the film electrical conductivity remains substantially unaffected. XPS analysis reveals that the thickness decrease is caused by the removal of PSS^- from the film. The thickness decrease after solvent immersion can be minimized when a GOPS crosslinker is added to the processing mixture. OECT based on PEDOT:PSS film processed with or without GOPS crosslinker shows comparable current/voltage characteristics.

3.7 Acknowledgements

The authors are grateful to Professor C. Santato and Dr. B. Liberelle for fruitful discussions and to D. Pilon, Dr. J. Lefebvre, S. Elouatik, and R. Delisle for technical support. This work is supported by a NSERC Discovery grant and by start-up funds from Polytechnique Montreal (F.C.). S.Z. is

grateful to NSERC for financial support through a Vanier Canada Graduate Scholarship. Part of this work was carried out at the Central Facilities of Polytechnique Montréal/Université de Montréal. This work is supported by CMC Microsystems through the programs MNT financial assistance and CMC Solutions.

CHAPTER 4 ARTICLE 2: WATER STABILITY AND ORTHOGONAL PATTERNING OF FLEXIBLE MICRO-ELECTROCHEMICAL TRANSISTORS ON PLASTIC

This article has been published in the journal "Journal of Materials Chemistry C" in 2016. This article reports the orthogonal patterning of PEDOT:PSS films on plastic for the fabrication of flexible micro-OECTs. The devices fabricated on plastic substrates show superior water-stability than devices on conventional glass substrates. The supporting information for this article is reprinted in Appendix B of this thesis.

4.1 Authors

Shiming Zhang[a], Elizabeth Hubis[a], Camille Girard[a], Prajwal Kumar[a], John DeFranco[b] and Fabio Cicoira*[a]

[a] Department of Chemical Engineering, Polytechnique Montréal, Montréal, Québec H3C3J7, Canada. E-mail: Fabio.cicoira@polymtl.ca

[b] Orthogonal, Inc., 1999 Lake Avenue, Rochester, NY 14650, USA.

4.2 Abstract

Water-stable, flexible and micro-scale organic electrochemical transistors (OECTs) based on poly(3,4-ethylenedioxythiophene) doped with poly(styrenesulfonate) (PEDOT:PSS) were fabricated on a plastic substrate using a new process based on a fluorinated photoresist. The PEDOT:PSS films, mixed solely with a biocompatible conductivity enhancer, show robust adhesion on plastic substrates, and exhibit unchanged electrical properties under extreme bending. This work simplifies the fabrication of high-performance OECTs and places them in a highly competitive position for flexible electronics and healthcare applications.

4.3 Introduction

Organic electronic devices present unique advantages with respect to their inorganic counterparts, such as low temperature processing, possibility to tune electronic properties via chemical synthesis, mixed electronic/ionic conduction and compatibility with printing and patterning techniques on

flexible and lightweight substrates[2,137]. In recent years, research on organic conducting polymer devices, such as organic electrochemical transistors (OECTs) and microelectrodes, has gained great momentum for applications in bioelectronics[6,10]. OECTs, being able to directly interface with aqueous electrolytes, can sense chemical and biological signals originating from redox processes[71]. OECTs based on poly(3,4-ethylenedioxythiophene) doped with poly(styrenesulfonate) (PEDOT:PSS) have already been used to detect biologically relevant species, such as glucose[77], neurotransmitters[114] and DNA[80], to monitor tissue integrity[85], and to record brain activity or local-field potentials in vivo[86,138]. Organic electronic ion pumps based on OECTs have been used as implantable devices for in vivo treatment of neuropathic pain[139].

The development of organic bioelectronics calls for viable processes to fabricate miniaturized devices on flexible substrates with long-term stability in aqueous media. Miniaturized OECT arrays are highly desired, e.g. to study the activity of individual brain cells, whose typical size ranges between 1 and 20 μm[140,141]. Flexible and conformable substrates allow to effectively place devices in contact with curvilinear and non-uniform surfaces often encountered in biomedical applications. Long-term stability (i.e. no delamination) of conducting polymer films in aqueous media is essential for bioelectronics, where applications such as implantable electrodes for chronic recording and stimulation are envisaged[142]. To date, a great deal of work has been dedicated to the development of flexible OECTs and electrodes[69,82,88]. Berggren et al. have reported lithographic patterning of commercially available PEDOT:PSS coated plastic sheets (Agfa Orgacon EL-350) with a lateral resolution above 100 μm[9]. However, the production of PEDOT:PSS coated plastic sheets has been recently discontinued by Agfa. Malliaras et al. have recently reported OECTs on ultrathin Parylene C films for measurements of in vivo brain activity[86]. However, the long-term stability of OECTs in aqueous media has not been deeply investigated so far. Moreover, high-throughput and environmentally friendly fabrication processes of miniaturized conducting polymer devices are highly demanded.

In this work we fabricated micro-scale OECTs, based on PEDOT:PSS, on flexible plastic substrates. Our PEDOT:PSS films show robust adhesion on plastic, long-term stability in aqueous media and no significant changes of their electrical properties under extreme bending. OECT patterning was achieved with a photolithographic process making use of photoresists, developers and strippers based on fluorinated materials. These materials are “orthogonal” to both polar and nonpolar solvents and, as such, are completely non-interacting with PEDOT:PSS films, which

therefore are not damaged during the patterning process[143,144]. Our OECTs can be operated at low voltage (below 1V) and exhibit stable electrical characteristics after multiple reduction/oxidation voltammetric cycles. Our studies are of paramount importance for the development of flexible and stable OECTs aiming at biological and healthcare applications.

4.4 Results and discussions

The process we employed to fabricate flexible OECTs is illustrated in Figure. 4.1 (see detailed procedure in ESI†). Pre-cleaned polyethylene terephthalate (PET) sheets (thickness of about 180 μm) were laminated on a glass wafer pre-covered with a Polydimethylsiloxane (PDMS) layer, to ensure flatness and rigidity during the lithography steps. Au source/drain contacts (40 nm thickness with 4 nm Cr as adhesion layer), with distances ranging from 100 μm to 5 μm, were patterned by conventional photolithography, metal deposition and lift-off. The Au-patterned PET substrates were treated by UV-ozone before PEDOT:PSS film deposition. PEDOT:PSS films were deposited by spin coating from mixtures containing a PEDOT:PSS aqueous suspension (Clevios™ PH1000, Haraeus), the conductivity enhancer glycerol and occasionally dodecylbenzenesulfonic (DBSA) acid and 3-glycidoxypropyltrimethoxysilane (GOPS). After spin coating, the films were dried on a hotplate at 100 °C for 20 min. PEDOT:PSS OECT channels were patterned using a subtractive process consisting of sequential film deposition, photolithography and etching. A negative-tone fluorinated photoresist (OSCoR 4000, Orthogonal, Inc.) was spin-coated on the PEDOT:PSS film, baked on a hotplate and exposed to the UV light of the mask aligner through a photomask. After a post-exposure baking, the unexposed photoresist was developed using a puddle method. The unprotected PEDOT:PSS was then etched by oxygen reactive ion etching (RIE) and the exposed photoresist remaining on the patterned PEDOT:PSS film was removed by immersing the samples in a fluorinated stripper. A further photolithography step was performed to cover the Au electrodes with photoresist in order to prevent their direct contact with the electrolyte. At the end of the fabrication process, the devices were soaked in deionized water to remove saline contaminants from the PEDOT:PSS film. This procedure yielded transistors featuring channel lengths (L) ranging from 5 μm to 100 μm and widths (W) of 80 μm and 400 μm. Finally, a glass or PDMS well was attached on the channel area to confine the electrolyte. A high surface area (1000–2000 m2 g−1) activated carbon was used as the gate electrode.

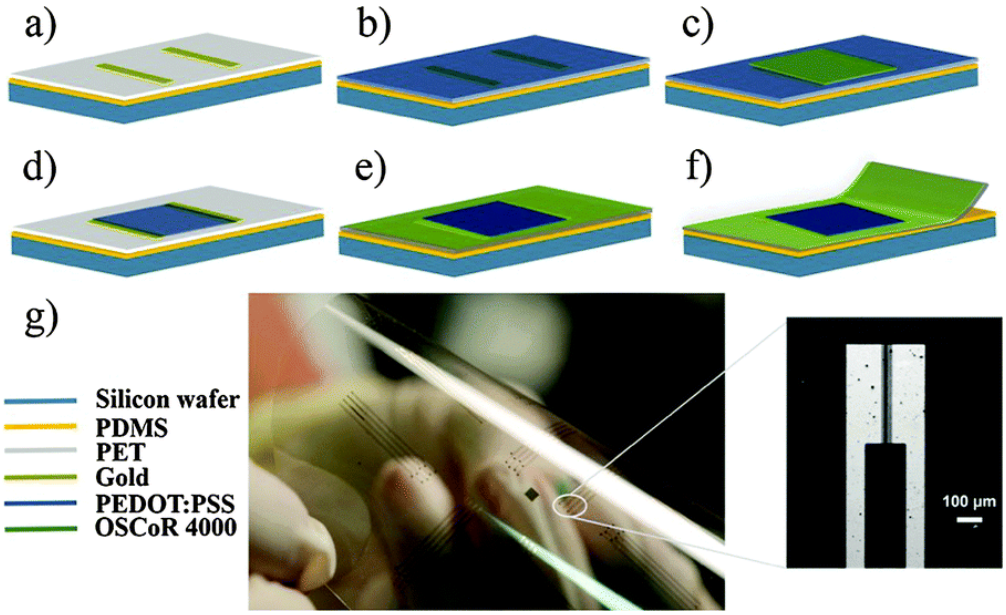

Figure 4.1. Scheme of the fabrication process of flexible OECTs: (a) photolithography patterning of gold electrodes on PET sheets laminated on PDMS/glass; (b) PEDOT:PSS spin-coating; (c) spin coating and photolithographic patterning of the fluorinated photoresist on PEDOT:PSS; (d) oxygen reactive ion etching of PEDOT:PSS and photoresist removal; (e) second photoresist pattern to protect the metal electrodes; (f) detachment of PET from PDMS/glass; (g) digital photograph of devices on a flexible PET foil and optical microscopy image showing the Au electrodes and the patterned PEDOT:PSS channel (the channel length/width is 5 µm/400 µm, the dark area between the two Au electrodes corresponds to the patterned PEDOT:PSS channel).

The long term stability of PEDOT:PSS films on PET in aqueous media was benchmarked with respect to analogous films deposited on glass. Three different formulations were used for the spin coating mixtures, i.e. PEDOT:PSS/glycerol, PEDOT:PSS/glycerol/DBSA and PEDOT:PSS/glycerol/DBSA/GOPS. While glycerol acts as a conductivity enhancer, DBSA is used to facilitate film processing and GOPS as a crosslinker to improve film stability on glass substrates[26,60,145]. The effect of additives (DBSA and GOPS) has been studies for PEDOT:PSS films deposited on glass, but it is still unknown for films deposited on plastic substrates. We found that films on glass delaminated within 1 day after water immersion unless GOPS was introduced, as previously reported[26], whereas films on plastic did not delaminate even in absence of GOPS.

Remarkably, PEDOT:PSS films on PET did not detach from the substrate even after 3 month in water (Figure. 4.2) while films on glass with GOPS showed detachment after 3 months water immersion. Similar results were achieved upon immersion into phosphate buffered saline (PBS). These results prove that the crosslinking agent GOPS is not required for PEDOT:PSS film on PET. This is an important point since GOPS has the drawback to significantly decrease the electronic and ionic conductivity of PEDOT:PSS films[26,42]. We also observed good film quality on plastic without DBSA, although it facilitates film processing and improves film conductivity on glass substrate[26]. Film obtained from mixtures containing PEDOT:PSS and glycerol showed electrical conductivities as high as ~600 S cm^{-1}, similar to those obtained on glass in the absence of GOPS[26]. Immersion of these films in aqueous media led to a thickness decrease accompanied by a sheet resistance increase (see ESI†), likely due to the removal of PSS from the film surface[26]. However these changes did not significantly affect the film conductivity. Overall, these findings point to an enhanced water stability of PEDOT:PSS on plastic substrates with respect to films on glass.

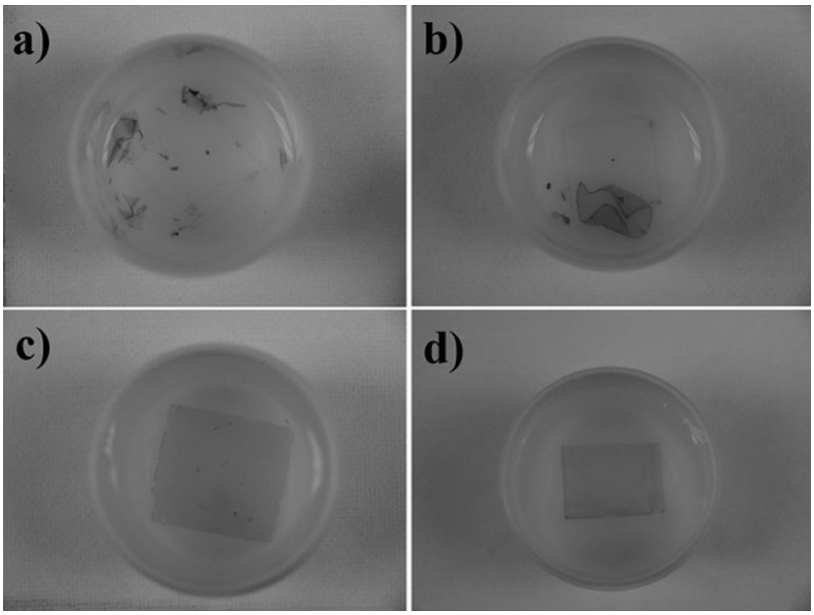

Figure 4.2. PEDOT:PSS films on glass and PET substrates after solvent immersion. (a) PEDOT:PSS/5% v/v glycerol/0.5% v/v DBSA on glass after 1 day in DI water; (b) PEDOT:PSS/5% v/v glycerol/0.5% v/v DBSA/1% v/v GOPS on glass after 3-month in DI water; (c) PEDOT:PSS/5% v/v glycerol on PET after 3-month in PBS; and (d) DI water. Films on glass that do not contain GOPS delaminate after 1 day of immersion in water, whereas those containing

GOPS delaminate after about 3-month. Films on PET containing only PEDOT:PSS and glycerol do not delaminate even after 3-month in DI water or PBS.

To gain insight into the flexibility of our PEDOT:PSS films, we measured the change of the current flowing through them upon increasing substrate bending (Figure. 4.3a). For this measurements we used ~70 nm PEDOT:PSS films deposited on PET sheets with electrodes made by copper tape covered by silver paste. The current did not show any significant decrease upon increasing substrate bending (Figure. 4.3a): a current loss of about 1% was observed when bending the film from 0 to 100% for the first 100 bending cycles (see Figure. 4.3 for the definition of bending percentage). After 500 bending cycles, the current loss was less than 4%, which demonstrates a good bendability of the films, in line with recent reports on flexible OECTs[88]. These results prove that PEDOT:PSS containing only the conductivity enhancer glycerol are excellent candidates for flexible devices on PET.

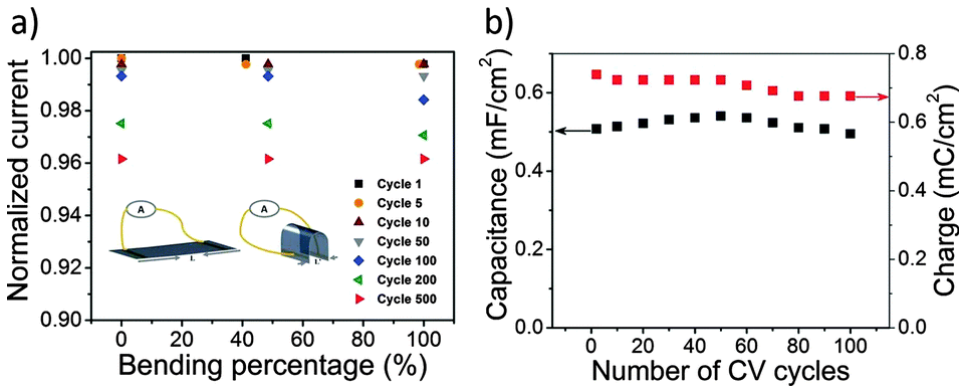

Figure 4.3. (a) Normalized current versus film bending. The inset shows the schematic of bending test methods of the PEDOT:PSS films on PET. The bending percentage is defined as [(L − L′)/L] × 100%. (b) Capacitance (left axis) and anodic charge (right axis) extracted from CV of films processed from PEDOT:PSS and 5% v/v glycerol.

We subsequently studied the redox voltammetric stability of PEDOT:PSS films (with 5% v/v glycerol) on PET using cyclic voltammetry (CV). The amount of electrical charge Q (C) accumulated in the PEDOT:PSS film during doping for each 10 cycles was calculated by integrating the anodic current over time. Similarly the pseudocapacitance was calculated from the

slope of the integrated charge (during doping) vs. electrode potential for every 10 cycles. Our results (Figure. 4.3b) show that stable charges and capacitances were maintained for up to 100 scan cycles, which indicates a good redox stability of PEDOT:PSS films on plastic.

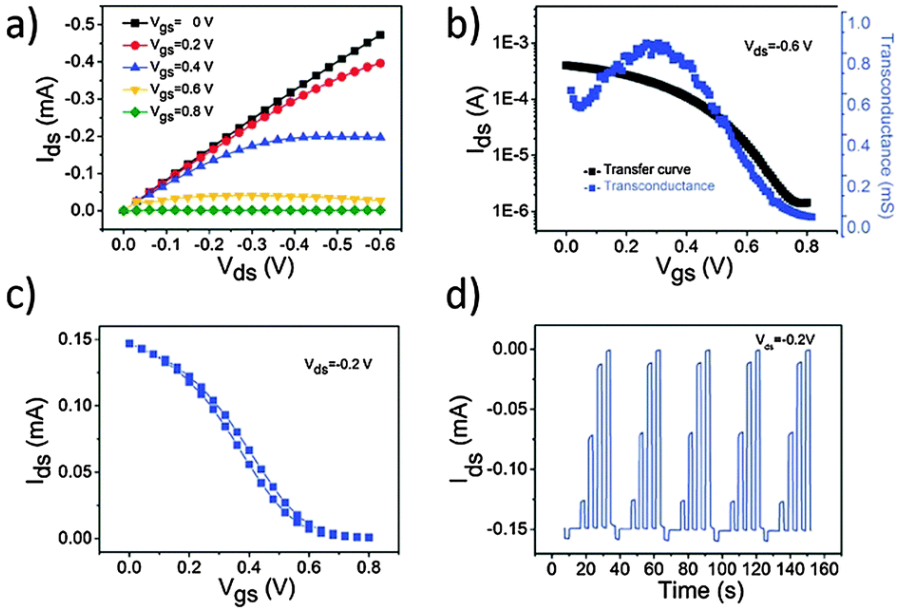

Figure 4.4. Electrical characteristics of OECT on PET. (a) Output characteristics with V_{ds} swept from 0 V to −0.6 V and V_{gs} varying from 0 (top curve) to 0.8 V (bottom curve) with a step of 0.2 V. (b) Transfer curve for V_{ds} = −0.6 V and V_{gs} sweeping from 0 to 0.8 V and the associated transconductance. (c) Hysteresis curve for V_{gs} varying from 0 to 0.8 V at V_{ds} = −0.2 V with sweeping rate of 200 mV s−1. (d) Transient characteristics (I_{ds} versus time) measured at a fixed drain-source voltage (V_{ds}) while pulsing for 2 seconds the gate-source voltage (V_{gs}) from −0.2 to 0.8 V in 0.2 V steps.

Finally, we characterized micro-OECTs on PET (channel width 80 µm and channel length 5 µm) employing a 0.01M aqueous NaCl solution as the electrolyte and a high surface area activated carbon (AC) as the gate electrode. AC gate electrodes lead to large current modulations and do not require any additional reference electrode to monitor the channel potential due to their high double-layer capacitance[146]. Figure. 4.4(a) and (b) show the output and transfer characteristics of the OECTs. The transistor shows linear output curves at V_{gs} = 0, in agreement with the high conductivity of PEDOT:PSS. Saturation behaviour appears at a gate bias ranging from 0.2 V to 0.8

V. An ON/OFF ratio of about 300 and a maximum transconductance of about 0.8 mS is extracted for the device with 5 μm length and 80 μm width at V_{ds} = −0.6 V from the transfer plot in Figure. 4.4b. The transconductance is comparable with results (∼0.1–1 mS) obtained on glass substrates[68,69]. This transconductance can be further improved by increasing the film thickness since a higher film thickness leads to higher transconductance[68]. In addition, our devices show minor hysteresis (Figure. 4.4c) between 0 V and 0.8 V gate voltage, similarly to our recent studies on glass substrates[147]. These results indicate a relatively fast dedoping/doping of the PEDOT:PSS films on PET substrates by electrolyte ions due to the small film volume. Figure. 4.4d shows that for transient OECT measurements the current at gate voltages ranging from −0.2 V to 0.8 V remains stable for successive cyclic measurements. We also measured the mobility of our patterned PEDOT:PSS film on PET, and extracted a value of ca. 10^{-1} cm^2 V^{-1} s^{-1} (see ESI†), which is similar to results on glass substrates.

4.5 Conclusion

In summary, we have demonstrated stable OECTs based on PEDOT:PSS on plastic substrates. PEDOT:PSS films, processed from a mixture containing only PEDOT:PSS and glycerol, remain stable even after 3 months of immersion in water and PBS, which demonstrates a robust film adhesion on plastic. Bending tests show that the films can undergo extreme bending with negligible effect on the current. Flexible OECTs arrays with channel lengths as short as 5 μm were achieved by directly patterning PEDOT:PSS films on PET with a fluorinated photoresist. OECT characterization further proves that the devices have good performance on plastic. Our results contribute to overcome some of the challenges faced when developing large-scale processing of flexible and stable devices.

4.6 Materials and Methods

Polyethylene terephthalate (PET) sheets were purchased from Policrom Inc (Bensalem, PA, USA). The PEDOT:PSS aqueous suspension (Clevios™ PH1000) was purchased from Heraeus Electronic Materials GmbH (Leverkusen, Germany). Glycerol (99.5+% purity) was purchased from Caledon Laboratories Ltd (Georgetown, ON). Dodecylbenzenesulfonic acid (DBSA, 95+% purity) and anhydrous 3-glycidoxypropyltrimethoxysilane (GOPS, 98+% purity) were obtained from Sigma-Aldrich Canada Ltd. (Oakville, ON). The Fluorinated photoresist kit, including a negative-tone

chemically amplified photoresist (OSCoR 4000), a developer and a stripper, was supplied by Orthogonal Inc. (Rochester, NY, USA). A Karl Suss MA-6/BA-6 mask aligner (wavelength 365 nm, intensity of ~8 mW cm^{-2}) was used for photolithography. Reactive ion etching was performed with an ENI OEM-6 apparatus. Cyclic voltammetry measured was performed with BioLogic Science Instruments VSP-300. Transistor characterization and electrical measurements under bending were performed using an Agilent B2902A source-measure unit controlled by Labview software. The film thickness was measured with a profilometer (Dektak 150) and the sheet resistance was obtained by four point probe measurements.

4.7 Acknowledgements

The authors are grateful to Clara Santato and Gaia Tomasello for fruitful discussions and Daniel Pilon for technical support. This work is supported by grants Discovery (NSERC) and Établissement de Nouveau Chercheur (FRQNT) awarded to F. C. S. Z. is grateful to NSERC for financial support through a Vanier Canada Graduate Scholarship. C. G. is grateful to NSERC for financial support through an Undergraduate Student Research Award. The authors are grateful to CMC Microsystems for financial support through the programs MNT financial assistance and CMC Solutions. We have also benefited from the support of FRQNT and its Regroupement stratégique program through a grant awarded to RQMP.

CHAPTER 5 ARTICLE 3: PATTERNING OF STRETCHABLE ORGANIC ELECTROCHEMICAL TRANSISTORS

This article has been published in the journal "Chemistry of Materials" in 2017. This article reports a new transfer patterning method to fabricate high-resolution metal microelectrodes on elastomer and its application for the development of stretchable electronic devices such as organic electrochemical transistors. The supporting information for this article is reprinted in Appendix C of this thesis.

5.1 Authors

Shiming Zhang, Elizabeth Hubis, Gaia Tomasello, Guido Soliveri, Prajwal Kumar, and Fabio Cicoira*

Department of Chemical Engineering, Polytechnique Montreal, Montreal, Quebec H3C 3A7, Canada.

Email: fabio.cicoira@polymtl.ca.

5.2 Abstract

The fabrication of stretchable electronic devices is presently rather challenging on account of both the limited number of materials showing the desired combination of mechanical and electrical properties and the lack of techniques to process and pattern them. Here we report on a fast and reliable transfer patterning process to fabricate high-resolution metal microelectrodes on polydimethylsiloxane (PDMS) by using ultrathin Parylene films (2 μm thick). By combining transfer patterning of metal electrodes with orthogonal patterning of the conducting polymer poly(3,4-ethylenedioxythiophene) doped with polystyrenesulfonate (PEDOT:PSS) on a prestretched PDMS substrate and a biocompatible "cut and paste" hydrogel, we demonstrated a fully stretchable organic electrochemical transistor, relevant for wearable electronics, biosensors, and surface electrodes to monitor body conditions.

5.3 Introduction

Stretchable electronic devices, based on materials combining high electrical conductivity with mechanical elasticity, are of great interest for applications in wearable electronics and bioelectronics. They can be placed on textiles, three-dimensional objects, and soft biological tissues such as skin, heart, brain, and muscles to monitor electrical and mechanical signals as well as body conditions[93]. Significant progress in the development of stretchable electronic devices has been achieved in recent years. Devices showing attachable[100], implantable[148], self-healing[149], and dissolvable features[150] have been used for several in vitro or in vivo applications. Rogers and co-workers developed high-performance stretchable integrated circuits by buckling ultrathin inorganic films[99,151]. Bao and co-workers explored stretchable electronic skin[152], capacitive pressure sensors[105], and solar cells[153] based on conducting polymers and carbon nanotubes. Lacour and co-workers proposed a strategy to increase the stretchability of metal films and electronic interconnects on elastomer surfaces[154,155]. Someya and co-workers reported stretchable ultralightweight transistors[104] and stretchable displays[102]. Other groups also reported stretchable devices based on nanomaterials, such as carbon nanotubes[156], graphene[157], ionic conductors[158], and liquid metals[159].

The large majority of stretchable electronic devices are currently fabricated on the organosilicon compound polydimethylsiloxane (PDMS)[91]. PDMS offers a number of unique and attractive features, such as optical transparency, biocompatibility, ease of process, and a moderate elastic modulus, which permits conformable surface coverage of a wide variety of surfaces[160]. The key steps for the fabrication of high-resolution stretchable electronic devices (e.g., transistors) on PDMS are the patterning of the metallic contacts and the electroactive material. In principle, several techniques can be used for these processes, such as shadow masking, elastomer stamp, printing, and photolithography. Shadow masking, although very simple, presents several drawbacks, such as limited lateral resolutions (tens of microns), diffusion of material below the mask features, mask clogging after a few uses (especially for small features) and contact with substrate leading to materials damage. Besides that, this technique is unsuitable for alignment of multilayer patterning. The use of elastomer stamps requires critical control of the adhesion between the carrier stamp and donor/acceptor substrates, which sometimes produces low yield due to variation of the contact area[161]. As a result, transferred patterned metallic electrodes onto soft substrates using this method

have minimum feature sizes of tens of micrometers[162]. Printing techniques (e.g., inkjet or screen printing), although very promising to produce large-scale patterns on PDMS, still have limited lateral resolution (typically above 20 μm)[163,164]. In addition, ink formulation and alignment of multilayer patterns remain very challenging. Photolithography, on the other hand, yields high resolution on multilayer patterns with high throughput, without contact with the substrate. However, on PDMS and other elastomers, the use of photolithography results in low yield, due to poor adhesion of the photoresist on elastomer surfaces[165], swelling of the elastomer induced by organic solvents, and when chemical etching is used, diffusion of corrosive chemicals into the porous PDMS matrix, an undesirable effect for bioelectronics devices to be interfaced with living systems[10,166-168]. Therefore, an alternative high-fidelity process to pattern high-resolution features on stretchable substrates is highly desirable.

In this work, we propose high-fidelity processes to pattern both metal electrodes and organic electroactive materials on PDMS with high resolution. Metal electrodes, with a channel length as short as 5 μm, were realized using Parylene transfer patterning, whereas the organic electroactive material was patterned by unconventional orthogonal photolithography. By taking advantage of those two patterning techniques and of a "cut and paste" hydrogel as stretchable electrolyte, we demonstrated a fully stretchable organic electrochemical transistors (OECTs). The biocompatibility of all device components make our technology viable for in vivo bioelectronics.

5.4 Results and discussion

We fabricated organic electrochemical transistors (OECT) on PDMS by using a combination of Parylene pattern transfer and orthogonal photolithography. We demonstrated both microscale devices, with channel lengths as low as 5 μm, and fully stretchable devices, featuring larger dimensions to facilitate probing.

Thin films of the chemically stable and biocompatible polymer Parylene (ca. 2 μm thickness, comparable to photoresist thickness) can be used as seamless sacrificial masks to pattern microbioelectronic devices, such as organic neural pixels[169] and OECTs[53,60,138], used for in vivo recording of brain activity[86] or treatment of neuropathic pain[139]. However, Parylene patterning on PDMS is challenging due to the strong adhesion between these two materials, which makes difficult the removal (lift-off) of the Parylene mask after material deposition[170]. To circumvent this

problem and pattern the metallic electrodes on PDMS, we first deposited a thin Parylene film (2 µm) on a flexible polyethylene terephthalate (PET) sheet attached to a glass substrate to ensure its flatness during the photolithography process (Figure 5.1 and experimental part). We created patterns corresponding to the desired microelectrode geometry on the Parylene layer by photolithography and reactive ion etching. Successively, we detached the PET sheet carrying the patterned Parylene from the glass support (Figure 5.1a) and gently attached it to freshly prepared PDMS (Figure 5.1b). Because of the higher adhesion force of Parylene onto PDMS with respect to the surfactant-treated PET (Figure 5.1c), detaching of the PET sheet leads to the transfer of the patterned Parylene film to the PDMS, thus creating a seamless mask for metal deposition. After Au deposition (Figure 5.1d), we mechanically peeled off the patterned Parylene from the PDMS (Figure 5.1e), leaving the desired Au pattern on the PDMS (Figure 5.1f). Notably, the Parylene film is not damaged by this process and can therefore be reused (see Figure S1). We would like to stress that this fabrication process permitted us to pattern electrodes with distances as short as 5 µm (Figure 5.1g and Figure 5.1h) with a yield close to 100% (see Video S1). Moreover, the process is totally dry and is carried out at room temperature, thus being viable for large-scale, roll-to-roll production of devices on elastomers.

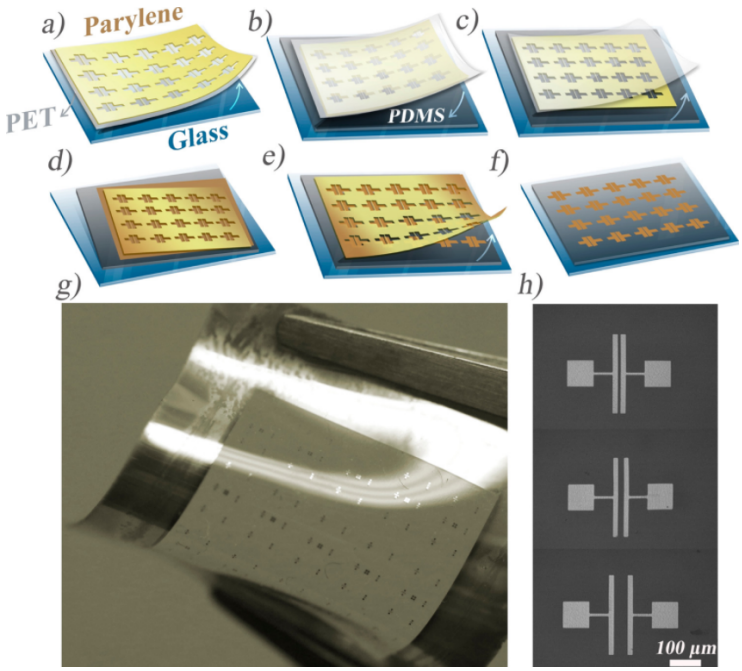

Figure 5.1. Parylene transfer process used to fabricate microelectrode arrays on PDMS. (a) Detaching PET (CTAB-treated)-carried Parylene patterns from glass; (b) laminating of the

PET/Parylene onto freshly prepared PDMS; (c) detaching PET, leaving Parylene patterns on PDMS; (d) metal deposition; (e) lift-off of the Parylene film; (f) electrode arrays on PDMS; (g) PDMS patterned with Au electrodes with substrate dimension of 15 mm × 15 mm; and (h) Au microelectrodes with channel lengths of 5, 20, and 50 μm.

After patterning of the contacts, we performed patterning of the organic active material, in our case the conducting polymer, poly(3,4-ethylenedioxythiophene) polystyrenesulfonate (PEDOT:PSS). Conventional photolithography is not suitable for this purpose because exposure to photoresists, solvents, and developers leads to chemical deterioration of organic electronic materials[53]. Here, we patterned the PEDOT:PSS film on PDMS via orthogonal photolithography, which is based on fluorinated photoresists, developers, and strippers that are totally inert to organic materials[38,61,143,171,172], by adapting a process we recently developed for PET flexible substrates[38]. Combining Parylene pattern transfer and orthogonal lithography, we fabricated the first microscale OECTs on PDMS, featuring channel lengths as small as 5 μm (inset of Figure 5.2b). The OECT fabrication was completed by exposing the PEDOT:PSS channel to a 0.01 M aqueous solution of CTAB (confined within a PDMS or glass well), with a high surface area activated carbon (AC) gate electrode immersed in it. As shown in our previous work, the combination of AC gate and CTAB electrolyte leads to high current modulation in OECTs[146]. Our devices show the typical behavior of PEDOT:PSS OECTs working in depletion mode (Figure 5.2a). The device performance remained stable for successive cyclic transient measurements (Figure S2). From the transfer curves (Figure 5.2b), we extracted a maximum transconductance (i.e., I_{ds} sensitivity to V_{gs} variations) of about 0.6 mS (at V_{gs} = 0.1 V), a value comparable to those typically measured for devices on more conventional glass[69] or plastic substrates[38]. Micro-OECTs on PDMS with relatively high transconductance are promising as conformal devices for in vivo (bio) sensing applications[86,140] and for detection of electrically active single cells, whose dimensions are in the range 1–10 μm[140].

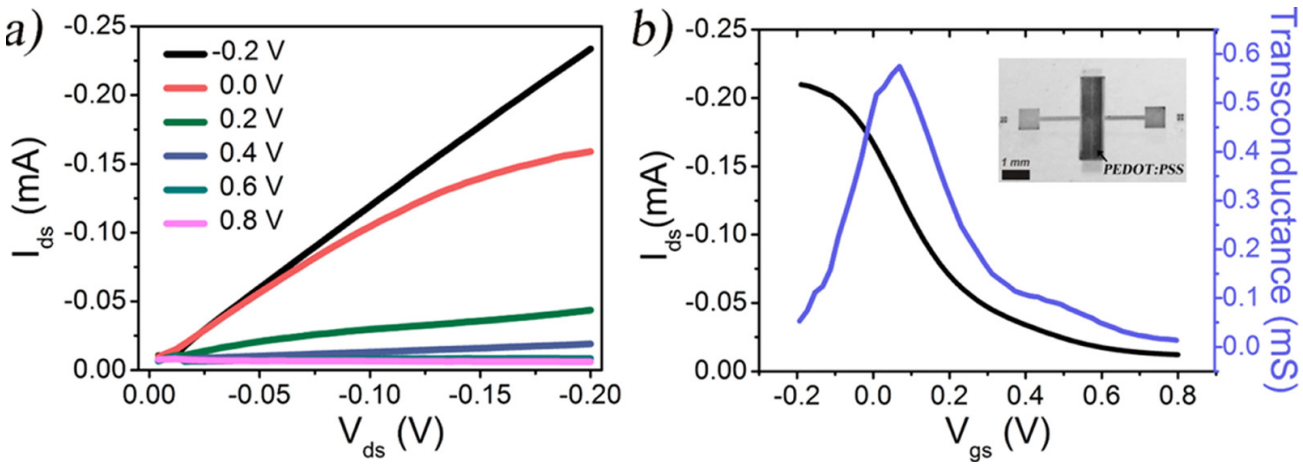

Figure 5.2. Electrical characteristics of PEDOT:PSS micro-OECTs on PDMS. (a) Output (V_{gs} varying from −0.2 to 0.8 V) and (b) transfer characteristics (V_{ds} = −0.2 V) with associated transconductance. Optical micrograph of the patterned OECT with channel width of 4000 µm, channel length of 10 µm, and channel thickness of about 400 nm (inset). The dark region corresponds to the patterned PEDOT:PSS film.

Although the ON/OFF ratio can be increased by increasing the PEDOT:PSS film thickness (Figure S3), it remains lower than that obtained on glass or PET substrates[38,146], indicating a more difficult doping/dedoping of PEDOT:PSS, likely due to a higher concentration of impurities at the PEDOT:PSS/PDMS interface[173].

Patterning of OECTs on stretchable PDMS substrates can be exploited to obtain fully stretchable OECTs (i.e., devices with stretchable electrodes, channel, and electrolyte). Stretchable transistors based on organic semiconductors, such as pentacene[102] and poly(3-hexylthiophene) (P3HT)[97], have been recently reported. However, these materials cannot compete with PEDOT:PSS for in vivo bioelectronics due to their lower sensitivity (transconductance) and instability in air and water. A possible strategy to achieve stretchable devices is to use intrinsically stretchable materials for all the device components. However, although intrinsic stretchability can be achieved for PEDOT:PSS (via blending with soft polymers[46] or plasticizers[45]), the same is not possible for evaporated metallic electrodes. An advantageous approach to achieve stretchable devices is the buckling method. As first shown by Whitesides et al.[96], deposition of high-modulus thin films on expanded (prestretched) PDMS substrates leads to the formation of buckled (wavy) films upon relaxation. The buckled structure permits all the components on PDMS to be stretched up to the value of the

prestrain, without considerable degradation of the active components. To verify the effect of the prestretching, we measured the variation of the current flowing in buckled PEDOT:PSS films upon stretching the PDMS substrate along the longitudinal direction of the film (current versus strain, Figure 5.3c). Our data demonstrates that PEDOT:PSS films show an unchanged current flow up to applied strain percentages close to the initial prestretching (i.e., films deposited on 30% prestretched substrates show an unchanged current flow up to about 30% applied strain). We therefore carried out device patterning on a PDMS substrate prestretched by 30% of initial length (the maximum strain human skin can undergo[174]), which resulted in buckled OECTs upon releasing the prestrain (Figure 5.3a–c). In agreement with previous literature[45], optical microscopy images show that the application of larger strains (i.e., 45% and 60%) leads to the formation of cracks in PEDOT:PSS films (Figure S4), in turn resulting in a current decrease. Imaging of the bucked Au contacts shows that no cracks are formed in the films within 30% strain, and microcracks appear at larger strains[155] (Figure S5). To permit the measurement of the strain-dependent behavior of our buckled OECTs on PDMS, we employed devices using a planar PEDOT:PSS gate, parallel to the PEDOT:PSS channel. A polyacrylamide-based stretchable hydrogel containing sodium chloride (NaCl) was used as the electrolyte (see experimental part and Video S2)[175,176]. The channel and electrode dimensions were increased from micrometer to millimeter scale, to facilitate hydrogel assembling onto the device electrical and electrical probing during device stretching[97,177]. The strain-dependent OECT electrical characteristics were measured in the following order: no strain applied, application of 15% strain and, finally, application of 30% strain. As shown in Figure 5.3d, the devices operate at low voltage range (0–1.2 V), demonstrating that the stretchable hydrogel can efficiently induce reversible PEDOT:PSS doping/dedoping. Significantly, the OECT shows identical transfer (Figure 5.3d) and transconductance (Figure S6) characteristics under 0%, 15%, and 30% applied strains. These results demonstrate the potential of our stretchable OECTs toward in vivo conformable sensing applications. For larger applied strains (50% and 65%), the transistor performance deteriorates (Figure S7), in line with morphological changes observed by optical microscopy (Figure S4). The long-term cyclic stability test shows a decrease in the source-drain current after multiple cycles (Figure S8), which could be related to changes in PEDOT:PSS morphology and the viscoelastic properties of the PDMS substrate, in agreement with previous findings for P3HT on PDMS[97].

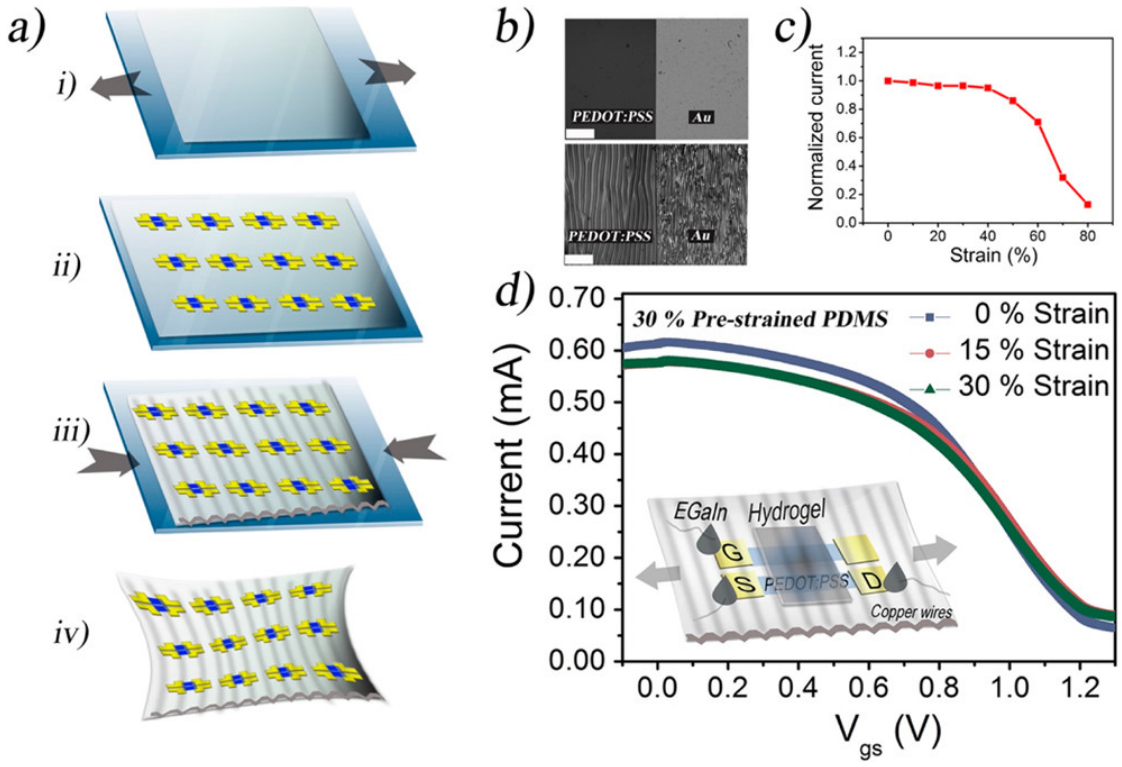

Figure 5.3. (a) Fabrication of stretchable OECT, using Parylene transfer and orthogonal patterning, carried out on 30% prestrained PDMS: (i) Prestretching PDMS substrate; (ii) Au patterning via Parylene transfer and PEDOT:PSS patterning via orthogonal photolithography; (iii) stretchable OECTs obtained upon PDMS relaxation; (iv) detachment of PDMS from glass substrate; (b) optical images of PEDOT:PSS and Au film surface morphology showing a transition from smooth to buckled morphology after release of prestretched PDMS; (c) prestretching effect on the stain-current profile of the PEDOT:PSS channel on PDMS; PEDOT:PSS films (with 5 % (v/v) glycerol and 1 % (v/v) Capstone FS-30) deposited on 30% prestretched substrate; d) transfer characteristics (V_{ds} = −0.5 V) of stretchable OECTs at 0%, 15%, and 30% strains. The inset shows the schematic representation of our OECT configuration. The distance between the PEDOT:PSS gate and channel is 200 μm. The channel and the gate electrode are both 8 mm long and 2 mm wide.

5.5 Conclusion

We have developed a new process to pattern metal microelectrodes on PDMS substrate based on Parylene transfer pattern. This process permits the high fidelity transfer of microscale patterns, with a totally dry process, from flexible substrates onto stretchable substrates such as PDMS, which are challenging to pattern by conventional lithography. Parylene pattern transfer of metal contacts

together with conducting polymer patterning with orthogonal photolithography have been used to fabricate microscale OECTs on PDMS. Fully stretchable OECTs were developed by employing these pattern processes on a prestretched PDMS substrates and by using a cut-and paste stretchable acrylamide-based hydrogel as the electrolyte.

These results pave the way to the development of new technologies for conformal/implantable healthcare devices for in vivo bioelectronic studies, electronic skins, or wearable sensors, and they help to overcome some of the challenges associated with fabrication of stretchable devices, especially those requiring both high resolution and biocompatibility. In addition, the high fidelity and scalability of the Parylene transfer pattern makes it a reliable way to fabricate thin film electrodes or driving circuits on elastomers, with possible applications in next generation large-area stretchable displays and wearable electronics. Further high-impact applications of our technology can be achieved by integrating stretchable OECTs with flexible/stretchable light sources (e.g., OLEDs) for the fabrication of tactile sensors and interfacing stretchable electrodes to the human body to detect electromyography or electrocardiography signals.

5.6 Experimental section

Materials:

Polydimethylsiloxane (PDMS, Sylgard 184 silicone elastomer kit) was purchased from Dow Corning. Polyethylene terephthalate (PET) sheets were purchased from Policrom Inc. (Bensalem, PA, U.S.A.). Parylene (Parylene C) was purchased from SCS coating. The PEDOT:PSS aqueous suspension (Clevios PH1000) was purchased from Heraeus Electronic Materials GmbH (Leverkusen, Germany). Glycerol (99.5+ % purity) was purchased from Caledon Laboratories Ltd. (Georgetown, ON). Capstone FS-30 was purchased from Alfa Chemicals. The fluorinated photoresist kit, including a negative tone chemically amplified photoresist (OSCoR 4000), a developer (Orthogonal developer 700), and a stripper (Stripper 103), was supplied by Orthogonal Inc. (Rochester, NY, U.S.A.). Hexadecyltrimethylammonium bromide (or cetyltrimethylammonium bromide, CTAB), sodium chloride, the liquid metal alloy EGaIn and acrylamide used for hydrogel synthesis were purchased from Sigma-Aldrich Canada Ltd. (Oakville, ON). CTAB solutions were prepared by dissolving CTAB salt in deionized water.

Parylene Patterning

PET sheets were cleaned by sequential sonication in acetone, isopropanol, and deionized (DI) water (10 min for each step), dried using nitrogen flow and laminated on glass slides precoated with a PDMS adhesion layer, to ensure PET flatness and rigidity during the following lithography steps. To facilitate Parylene peel-off at the end of the process, a CTAB solution (0.005 M) was spin coated on the PET substrate prior to Parylene coating. Within 30 min after CTAB spin coating, 2 μm of Parylene (Parylene C, SCS coating) was deposited. The photoresist SPR 220.3 (Micro Chemicals Ltd.) was spin coated on the Parylene layer, and then the samples were exposed to the UV light of a mask aligner (Karl Suss MA6) and developed in the developer AZ-726 (Micro Chemicals Ltd.). Next, the unprotected Parylene was etched with an oxygen plasma in a RIE chamber (ENI OEM-6 apparatus). After the etching process, the remaining photoresist was stripped using PG 1165 (Micro Chemicals Ltd.) and the PET with the patterned Parylene layer on top was detached from the PDMS. A similar procedure was used to pattern Parylene film on glass and silicon.

Preparation of PDMS Substrates

Glass slides were cleaned using acetone, isopropyl alcohol, and DI-water and dusted off using a nitrogen gun. They were then spin coated with CTAB solution (0.005 M) acting as an antiadhesive for the PDMS peel-off at the end of the process. Next, the premixed PDMS (base:curing agent ratio of 10:1) was spin coated on the glass substrates at 500 rpm for 30s. Afterward, the samples were cured at 85 °C for 40 min in an oven. Finally, the PDMS substrates (thickness of about 300 μm) were detached from the glass slides using tweezers.

PEDOT:PSS Processing, Patterning, and Device Fabrication

OECTs were fabricated by first defining Parylene patterns on PDMS. After the Parylene film transfer onto PDMS (see main text), 4 nm of Cr and 40 nm Au were deposited using E-beam evaporation. After metal deposition, the patterned Parylene film was manually peeled from PDMS, leaving the microelectrode arrays on PDMS.

PEDOT:PSS aqueous suspensions (PH 1000) were first stirred for 3 min and then mixed with glycerol (5 v/v%) and Capstone FS-30 (1 v/v%) in a centrifugal mixer (Thinky M310) at 2000 rpm for 5 min. Glycerol is used to enhance film a conductivity and 1 Capstone FS-30 to enable the wetting on PDMS. The detailed effects of the Capstone FS-30 on PEDOT:PSS film conductivity, chemical composition, and morphology are shown in Figures S9–S11.

The resulting suspension was then spin coated on PDMS substrates pretreated with UV/O3 for 20 min. After drying of the PEDOT:PSS film on a hot plate at 100 °C for 30 min, the negative-tone OSCoR 4000 fluorinated photoresist was spin coated (1000 rpm, 30s) on the PEDOT:PSS film and baked on a hot plate (90 °C, 1 min). The samples were then exposed to the UV light of the mask aligner (Karl Suss MA-6/BA-6) through a photomask for 5 s. After postexposure baking (85 °C, 1 min), the unexposed photoresist was developed using a "puddle" method: the developer (Orthogonal 103) was dropped on the samples for 25 s, and then the spin coater was started. The unprotected PEDOT:PSS film was then etched by an oxygen reactive-ion etching (RIE). The exposed photoresist remaining on the patterned PEDOT:PSS film was removed by a 3 min stripping process (using Orthogonal 700 stripper). For the micro-OECT, a PDMS well was placed on the micro-OECT to confine the electrolyte (a 10–3 M CTAB aqueous solution), and a high-surface-area (1000–2000 m2g–1) activated carbon was used as the gate electrode. For the stretchable OECT, an acrylamide-based hydrogel (i.e., pasted on the channel and gate) was used as the stretchable electrolyte, and a PEDOT:PSS film was used as the planar gate electrode. Devices operated at 50% and 65% applied strain used gallium indium (EGaIn, liquid metal) electrodes and a 0.01 M NaCl solution as the electrolyte.

Hydrogel Synthesis

To prepare our stretchable hydrogel, we adapted to our application a procedure reported in the literature. We prepared a mixture of acrylamide 2.2 M (3.1 g) and NaCl 0.1 M (0.12 g) in 20 mL of Milli-Q water. After dissolution of the monomer and of the salt, which took approximately 15 min, the solution was cooled in an ice bath, and then the cross-linking agent (N,N′-methylenebis(acrylamide): 6 mg), the thermo-initiator (ammonium persulfate: 19 mg), and the accelerator of polymerization (N,N,N′,N′-tetramethyl ethylene diamine: 6 μL) were added while stirring. The transparent solution was then drop-casted onto a glass substrate. The samples were then gelled on a hot plate at 80 °C for 10 min. The hydrogel thin film obtained in this way is transparent and stretchable, and subsequently, it could be cut into the desired shapes with a razor blade and then pasted onto the PDMS substrates.

Characterization of PEDOT:PSS Films and Devices

Film thickness measurements were performed with a Dektak 150 profilometer. The sheet resistance of PEDOT:PSS films was measured by Jandel four-point probe equipment with a Keithley 2400

voltage–current source measure unit. The prestretching effect was evaluated by measuring the current flowing in PEDOT:PSS films between two eutectic gallium indium (EGaIn, liquid metal) electrodes, as a function of the applied tensile strain percentage for PEDOT:PSS films on PDMS. The films are 10 mm wide, 35 mm long, and about 400 nm thick. The applied strain percentage is defined as $[(L' - L)/L] \times 100\%$ where L and L' denote, respectively, the relaxed and stretched lengths of the PDMS substrate. The current is normalized with respect to the value measured for unstretched films. The transistor electrical characteristics were measured with Agilent B2900A, controlled with Quick IV Measurement software, and the strain was either applied in situ with an Instron E-3000 tensile tester or with a LabVIEW software-controlled tensile tester. The OECT electrical measurements (output, transfer, transient) were performed using an Agilent B2902A source-measure unit controlled by LabVIEW software.

5.7 Acknowledgement

The authors are grateful to Clara Santato for fruitful discussions and Daniel Pilon, Christophe Clement, and Alireza H. Mesgar for technical support. This work is supported by grants Discovery (NSERC), Établissement de Nouveau Chercheur (FRQNT) and PSR-SIIRI 810 and 956 (Québec MESI) awarded to F.C. S.Z. is grateful to NSERC for financial support through a Vanier Canada Graduate Scholarship, and to Qian Li from Youxinpai Inc., China, for the schematic drawing. The authors are grateful to CMC Microsystems for financial support through the programs MNT financial assistance and CMC Solutions. We have also benefited from the support of FRQNT and its Regroupement stratégique program through a grant awarded to RQMP.

CHAPTER 6 ARTICLE 4: WATER-ENABLED HEALING OF CONDUCTING POLYMER FILMS

This article has been published in the journal "Advanced Materials" in 2017. This article reports the observation of electrical healing of PEDOT:PSS films upon exposure to water. The healing property was utilized to demonstrate self-healing organic transistors and ultrasensitive flexible water detectors. The supporting information for this article is reprinted in Appendix D of this thesis.

6.1 Authors

Shiming Zhang and Fabio Cicoira*

Department of Chemical Engineering, Polytechnique Montréal, Montréal, Québec, Canada

E-mail: fabio.cicoira@polymtl.ca

6.2 Abstract

The conducting polymer polyethylenedioxythiophene doped with polystyrene sulfonate (PEDOT:PSS) has become one of the most successful organic conductive materials due to its high air stability, high electrical conductivity, and biocompatibility. In recent years, a great deal of attention has been paid to its fundamental physicochemical properties, but its healability has not been explored in depth. This communication reports the first observation of mechanical and electrical healability of PEDOT:PSS thin films. Upon reaching a certain thickness (about 1 μm), PEDOT:PSS thin films damaged with a sharp blade can be electrically healed by simply wetting the damaged area with water. The process is rapid, with a response time on the order of 150 ms. Significantly, after being wetted the films are transformed into autonomic self-healing materials without the need of external stimulation. This work reveals a new property of PEDOT:PSS and enables its immediate use in flexible and biocompatible electronics, such as electronic skin and bioimplanted electronics, placing conducting polymers on the front line for healing applications in electronics.

6.3 Introduction

Materials able to heal damage caused by external agents are highly desirable for applications in the electronics, biomedical, automotive, and aerospace fields[178]. The healing can be autonomic or nonautonomic, depending on whether or not an external stimulation is required. In particular, self-healing electronic materials can find applications in wearable, stretchable, and bendable electronics, as well as in artificial electronic skin[179]. The major challenges for self-healing electronic materials is to combine fast and reproducible healing characteristics, high conductivity, facile processing and, in the case of applications for electronic skin, biocompatibility[91,179]. In this context, Bao and co-workers reported the first example of an intrinsic self-healing conductive composite that heals at room temperature[149]. This composite, consisting of nanostructured nickel microparticles (μ Ni particles) embedded in a hydrogen-bonded polymer matrix, showed a conductivity of 40 S cm^{-1}. The conductivity of this material was restored within 15 s after damage by applying pressure to the separated slices. The same group recently reported a stretchable and healable semiconducting polymer, where cracks could be healed by post-treatment consisting of heating (150 °C for 30 min) and solvent annealing (CHCl3 vapor), which are able to promote polymer chain movement[52]. Sun and co-workers obtained a self-healing conductor by coating conductive Ag nanowires on nonconductive healable polyelectrolyte films[180]. The film conductivity was similar to that of indium thin oxide (ITO), while the response time required for healing after damage was more than 2 min. White Moore and co-workers developed a self-healing conductor using micrometer-sized polymeric urea-formaldehyde capsules containing conductive gallium–indium eutectic (EGaIn)[181]. Upon mechanical damage, the microcapsules broke and the encapsulated EGaIn leaked and diffused to the damaged area, resulting in a fast healing process. More recently, Shi et al. reported an electrically self-healable hybrid gel based on a self-assembled supramolecular gel and nanostructured polypyrrole[182]. This material showed a conductivity of 12 S cm^{-1} and a healing time of more than 1 min. Despite progress in the field, however, a material that can synchronously combine electrical healability with a fast healing time and biocompatibility for practical bioapplications is still highly required.

Conducting polymers have been the object of intense research since Shirakawa et al. demonstrated a high electrical conductivity in iodine-doped polyacetylene[1]. In the late 1980s, Bayer AG research laboratories developed a large-scale synthesis of the conducting polymer

polyethylenedioxythiophene doped with polystyrene sulfonate (PEDOT:PSS)[20], which has become commercially available since then. Despite that, PEDOT:PSS has encountered enormous success due to its remarkable properties such as ease of processing, high conductivity, and high stability in air[19]; however its healability has not been explored in depth. A healable material in the form of a dough has been obtained from a blend containing 20 wt% PEDOT:PSS and 80 wt% of the surfactant Triton X-100[47]. However, no self-healing was observed after decreasing the surfactant percentage to 70 wt%, thus proving that the healing properties were mostly due to the surfactant rather than to PEDOT:PSS itself. Besides that, the dough had a conductivity of about 60 S cm^{-1} due to the presence nonconductive surfactant, and a fairly high thickness of 50 μm was required for the healing.

In this communication, we report the first observation of healable PEDOT:PSS thin film (as thin as 1 μm) with an electrical conductivity as high as 500 S cm^{-1}. We observed instantaneous electrical healing of pure PEDOT:PSS film after damage by simply covering the damaged area of the films with a droplet of water. The healing process takes place within an extremely short time (about 150 ms) and enables complete restoration of the initial film conductivity, even after multiple damages. Significantly, PEDOT:PSS films wet with water behave as autonomic self-healing conductors: the current flow in the film is totally insensitive to external damage. This is the first observation in conducting polymers of such self-healing properties, which are generally found only in liquid or gel conductors. We show how the healing can be further controlled by humidity. The rapid electrical healing, combined with high conductivity and biocompatibility, places PEDOT:PSS in a highly competitive position among electrically healable materials for applications in large-area self-healable electronics and electronic skin.

6.4 Results and discussion

PEDOT:PSS films were obtained by drop-casting a Clevios PEDOT:PSS PH 1000 suspension (with or without conductivity enhancers) on glass, then baking them on a hot plate with the temperature gradually increased (refer to the Experimental Section for details). To perform the healing experiments, we biased the film at a constant voltage of 0.2 V using EGaIn contacts, which resulted in a current of 10−5 A (or higher for films containing conductivity enhancers). The film was then cut with a razor blade, which created a gap in the film, thus interrupting the current flow across it (Figure 6.1). Surprisingly, covering the damaged area with a drop of DI water leads to the

recovery of the current, up to 100% of its initial value, within a remarkably short time of ≈150 ms (Figure 6.1, inset). This effect is observed after repeated damage and repair in different regions of the same film (Figure 6.1), without significant variation of the recovered current and the response time. These results demonstrate the high reproducibility and reliability of the process. We would like to emphasize here that such a rapid healing time is among the fastest reported so far for materials that are both electrically and mechanically healable[52,149,179,180,183], and is the fastest for a conducting polymer thin film[52]. Remarkably, the current remained stable even after baking (140 °C, 1 h) the healed film, thus proving that the presence of water is not required to ensure conduction in the film. The water-induced healing behavior was also observed for PEDOT:PSS films processed with additives, such as conductivity enhancers (glycerol) and plasticizers (Capstone FS-30) on several kinds of substrates, such as flexible polyethylene terephthalate (PET) and polyimide, confirming that the substrate does not play an important role in the healing process.

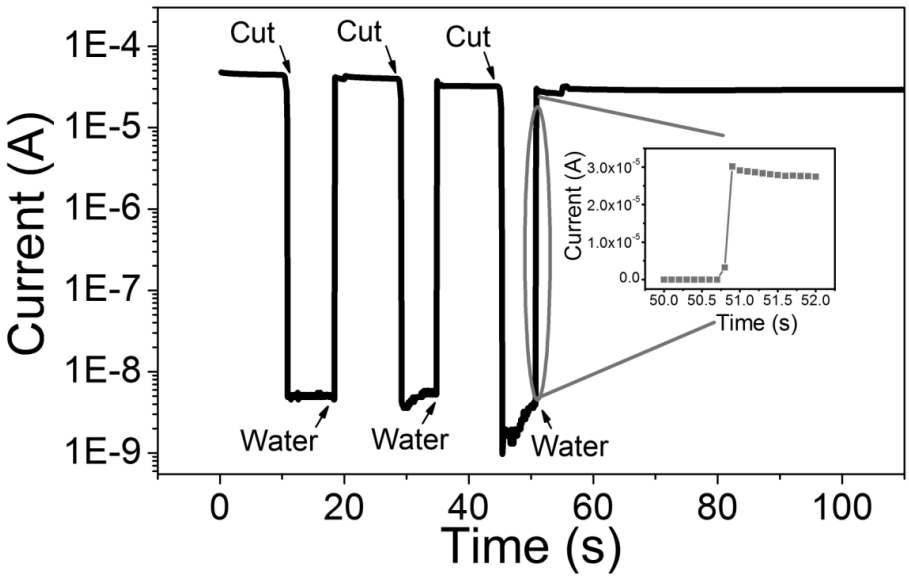

Figure 6.1. Current versus time measurements (applied voltage 0.2 V) for PEDOT:PSS film (thickness: 10 μm; width: 4 mm; length: 20 mm) showing the effect of damage (cutting with a razor blade) and healing (covering the damaged area with a drop of water). The damage/healing process was repeated three times on different regions of the film. The inset shows the magnified image of the current response time to highlight the rapidity of the healing process.

To gain insight into the healing process, we carried out a scanning electron microscopy (SEM) investigation of the damaged area before and after its exposure to water (Figure 6.2). A gap in the film, with a width of about 40 µm is clearly visible after film cutting (Figure 6.2a). Strikingly, the gap is mechanically healed after adding water (Figure 6.2b) and the healing remains after baking above 100 °C. A schematic representation of the water-enabled healing process is illustrated in Figure 6.2c.

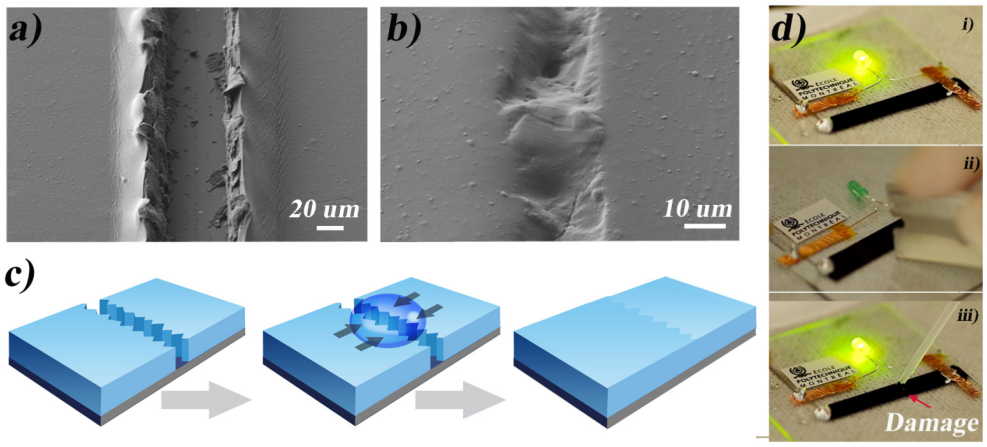

Figure 6.2. SEM images of the damaged area of a PEDOT:PSS film (obtained adding 5 v/v.% glycerol to Clevios PH1000) before (a) and after (b) healing with a 10 µL drop of deionized water; c) schematic representation of water-induced mechanical and electrical healing of a PEDOT:PSS film (thickness: 10 µm; width: 4 mm; length: 20 mm); d) demonstration of the damage and healing effect on a PEDOT:PSS film connected in a circuit with a LED bulb at a constant voltage of 3 V: i) as-prepared intact film; ii) film damaged with a cut; iii) film healed by dropping DI water on the cut, which enables an immediate repair of the circuit (within 150 ms).

We investigated the healing effect for PEDOT:PSS films of variable thickness and we found that a thickness greater than 1 µm is needed to trigger a fast electrical healing (≈150 ms) of the 40 µm gap (Figure S1, Supporting Information). For film thicknesses ranging from 1 to 10 µm, the healing time does not significantly depend on the thickness (see Figure S1, Supporting Information).

We demonstrated the healing properties of PEDOT:PSS films by damaging and repairing a film connected in a simple circuit to a commercial light-emitting diode (LED) bulb (Figure 6.2d; and Video S1, Supporting Information). The LED switched off after the film was cut and switched on

immediately after it was healed with water. The process could be observed for repeated cuts (Video S1, Supporting Information).

The properties of water healable PEDOT:PSS films can be exploited for water-activated components in integrated logic circuits (Figure S2, Supporting Information), such as inverters and water-erasable read-only memory[184]; water-controlled switches for inflatable life jackets, water-controlled LEDs, and wireless transmitters for maritime search and rescue (Figure S3, Supporting Information), and disposable water detectors for food packaging. Here, we demonstrate a commercial potential ultrasensitive water leak sensor by combining our healable PEDOT:PSS films with a radio frequency wireless device based on low power long range (LoRa) technology (with communication range of over 15 km)[185]. Wireless water sensors based on our water-healable PEDOT:PSS films allow a custom-design dimension and an arbitrary shape. They can be used on rigid (Video S2, Supporting Information), as well as on flexible and soft substrates such as human skin (Videos S3 and S4, Supporting Information), which makes them attractive for wearable and biocompatible applications.

Inspired by the above observations, we investigated the healing properties of wet PEDOT:PSS films, i.e., after soaking them into DI water for 5 s (the water remaining on the film surface after immersion was removed using a lint-free paper and a nitrogen gun). Figure 6.3 shows the current versus time characteristics of the wet film upon application of a voltage of 0.2 V. Surprisingly, we observed that the current was totally unresponsive to repeated cuts in different regions of the film and maintained the initial value of $\approx$10 mA. In other words, wet PEDOT:PSS films show autonomic self-healing. The autonomic self-healing of wet PEDOT:PSS films can be again demonstrated by using them as part of a circuit connected to a LED. This time (as shown in Video S5, Supporting Information) the LED stays in the on state despite the several cuts. This is the first observation on conducting polymer thin films (>1 μm) with such a self-healing property.

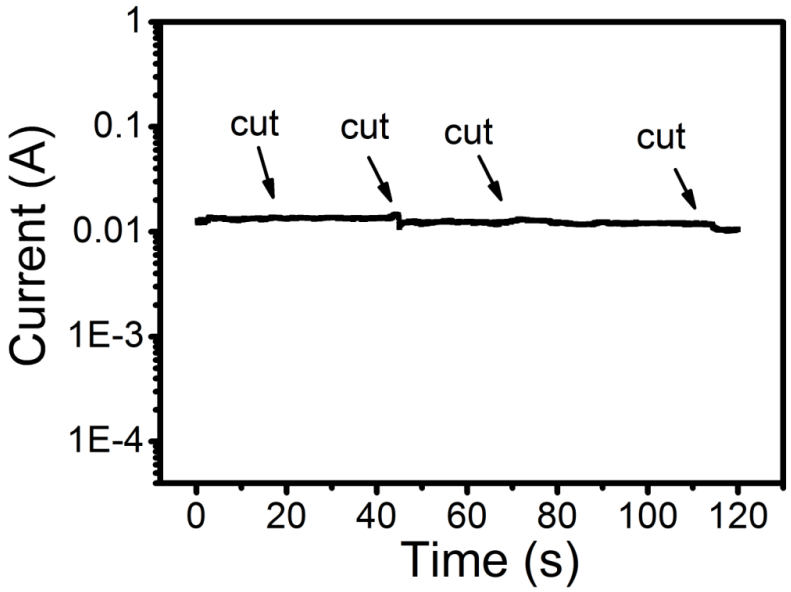

Figure 6.3. Current versus time profile of wetted PEDOT:PSS film containing the conductivity enhancer glycerol (thickness: 10 μm; width: 4 mm; length: 20 mm) after several cuts in different areas of the film. The applied voltage was 0.2 V. The higher current with respect to Figure 6.1 is due to the presence of a conductivity enhancer.

The ultrafast electrical self-healing of wet PEDOT:PSS films, together with their other remarkable properties such as mechanical flexibility, ease of processing, and biocompatibility, makes them attractive for in vivo self-healing applications, such as electronic skin[91], autonomic self-healable interconnects for neurodetectors[86], and epidermal electronics[100]. The PEDOT:PSS film thickness only shows a decrease after the first time water immersion (1 h) due to the polymer (PSS^-) dissolution in water[26]. No loss in thickness or conductivity observable during the subsequent water immersions (Figure S4, Supporting Information).

As a further potential application, we exploited wet PEDOT:PSS as channel material for a self-healable organic electrochemical transistor (OECT). These devices typically work in aqueous solution, and thus water is always in contact with the PEDOT:PSS channel. OECTs based on PEDOT:PSS has been widely used for in vivo bioelectronics studies[10,86]. The transfer curves of OECT based on our water-healable PEDOT:PSS film are shown in Figure S5 (Supporting Information). Strikingly, we observed the OECT shows identical transfer curves before and after in situ damage, thus behaving as a self-healable device. We would like to stress that this is the first

report of self-healing PEDOT:PSS OECTs. This remarkable observation is of great importance since it improves the device lifetime, especially in conditions where frequent replacements need to be avoided (i.e., in vivo applications).

The healing effect can even be achieved by exposure to water vapor, as shown by damage/healing experiments carried out in a humidity chamber (Figure 6.4). After damage at an initial relative humidity (RH) of 50%, the current dropped to the noise level and did not show any significant recovery even after about 30 min at RH between 50% and 70%. A considerable current recovery started when the RH was increased to 80%. The current gradually increased by about two orders of magnitude in about 5 min and then reached a plateau. A further increase of the RH to 90% brought the current back to its initial value. Overall, the healing process in water vapor is slower than in liquid. However, at high RH (80–90%) the current recovered to its initial value within a few minutes. The humidity-induced healing can be exploited when the direct exposure of the damaged area to liquid water is not desirable, for instance in a self-healable large-scale integrated circuit[181], to heal simultaneous multiple cuts without the need to precisely identify their locations in the circuit.

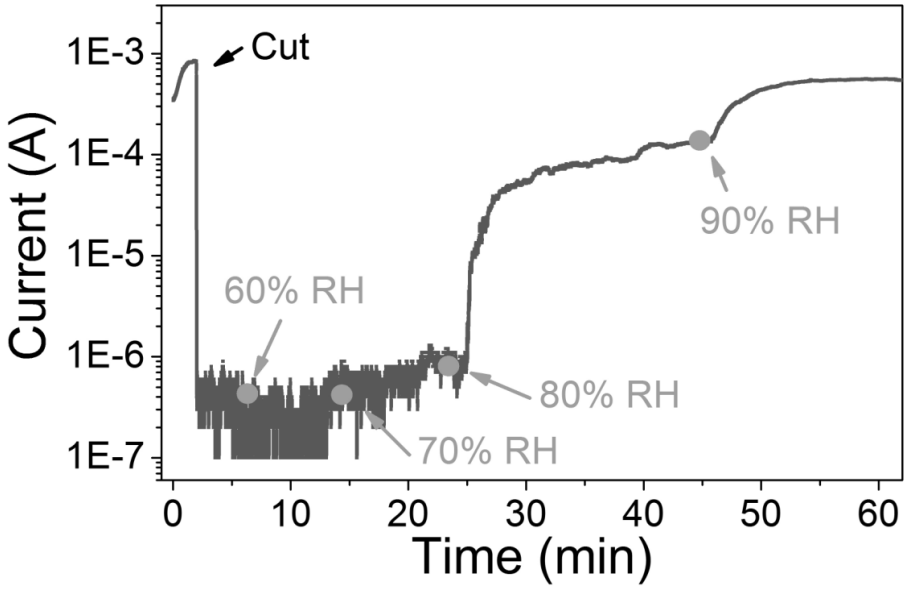

Figure 6.4. Current versus time plot of PEDOT:PSS film containing the conductivity enhancer glycerol (thickness: 10 μm; width: 4 mm; length: 20 mm) measured in a humidity chamber with RH varying from 60% to 90%, at a constant voltage of 0.2 V. A complete current recovery was observed within 5 min after increasing the humidity to 80% RH and 90% RH.

The details of the mechanism of water healing on PEDOT:PSS films are currently under investigation. We tentatively attribute the healing effect to the swelling of PSS^- chains upon water exposure, leading to an increase of viscoelasticity and softness of the film. The conductive $PEDOT^+$ chains, after drying, are hydrophobic and insoluble in water, while the PSS^- chains are hydrophilic and, as such, can be swelled or dissolved by water[19]. The PEDOT/PSS weight ratio in the commercial suspension Clevios PH 1000 is 1/2.5[29], therefore an excess of PSS^- is present. We previously reported that a thickness decrease of 30–40% occurs for 100 nm thick PEDOT:PSS films after water immersion and subsequent drying, due to partial dissolution of excess PSS^-[26]. In this work, for films with thicknesses of about 10 μm, we observed only 10–20% (1–2 μm) thickness decrease after water immersion (Figure S6, Supporting Information), indicating that, in percentage, more PSS^- remains in the thick film as compared to the thinner ones. In accordance with previous works[135], PEDOT:PSS films gain 25% of mass in a moisturized atmosphere due to the water-uptake by PSS^-. Therefore, when water is added to the damaged area of a PEDOT:PSS film, the PSS^- chains quickly uptake water, increase volume (swelling), and propagate toward the damaged site. The swelling of PSS^- simultaneously enables the $PEDOT^+$ chains (where $PEDOT^+$ indicates the oxidized form) to shift, since $PEDOT^+$ and PSS^- are entangled in the film[186], thus allowing formation of $PEDOT^+$-$PEDOT^+$ conducting paths across the damage, finally restoring the film electrical conductivity (see Figure S7, Supporting Information). This assumption is supported by time-of-flight secondary-ion mass spectrometry (TOF-SIMS) analyses, where there are no noticeable significant differences between the film composition in the healed gap and in the original film (Figure S8, Supporting Information). The fast response is expected to benefit from the rapid PSS^- water uptake, which can also increase ionic conduction. In the wet films, the water uptake of the PSS^- chains causes a significant increase in film softness and a decrease in tensile strength (Figure S9, Supporting Information). Thus, once the film is cut and the material is pushed aside by the razor blade, it instantly flows back to the damaged area, due to increased viscoelasticity, thus explaining the current's insensitivity to damage. The slower current recovery upon exposure to water vapor is due to the lower water absorption rate. The fast healing may also benefit from a water-induced reversible hydrogen bond breaking and restoring. It is a consensus that PEDOT:PSS film is composed of grains with core–shell structure ($PEDOT^+$ core and PSS^- shell)[186,187]. The $PEDOT^+$ and PSS^- chains interact via electrostatic (Coulomb) forces, while the individual grains

are held together by hydrogen bonds formed between the sulfonate groups ($R\text{-}SO_3^-$) of PSS^- (Figure S7, Supporting Information). These hydrogen bonds, as reported by Dauskardt and co-workers may break after exposure to water[186]. This will cause decohesion among the grains with consequent increase of their mobility in water, which, in turn, accelerates the separation and propagation of PSS^- (and thus $PEDOT^+$) grains to the damaged area. The broken hydrogen bonds, after water evaporates, will reform, and hence the cohesion between grains will be restored. The nature of healing in this way would be a dynamic hydrogen bond controlled by water.

According to the tentative healing mechanism described above, solvents with a low chemical affinity with PSS^- should not be able to heal the film. To verify this assumption, we used as the healing agent a fluorinated solvent (Orthogonal 700), which has a similar viscosity to water but is totally inert toward PSS^-. In line with our expectations, the fluorinated solvent neither electrically restores the current nor mechanically heals the film (see Figure S10, Supporting Information). A similar result was obtained with glycerol and with the ionic liquid 1-Ethyl-3-methylimidazolium bis(trifluoromethylsulfonyl)imide (EMIM-TFSI), indicating these materials are not able to efficiently swell PSS− or break the hydrogen bonding between PSS^- chains. These experiments further point to a chemical nature of the healing process (PSS^- swelling) and exclude the possibility that the current recovery results from mechanical movements of the film or by the transport of conducting debris, created during the cut, to the damaged area.

We would like to stress here that although the water healable films require a thickness greater than 1 μm, they maintain a high conductivity ($\approx$500 S cm^{-1} for 1 μm film). This high conductivity, together with the rapid healing time, makes PEDOT:PSS films much superior to other electrically healable materials reported so far. In addition, the fact that the films maintain their healability after additives are introduced is also of great importance since it allows property modification (such as hydrophobicity, stability, and elasticity) of the PEDOT:PSS films by using cosolvents, thus extending their applications[26,188].

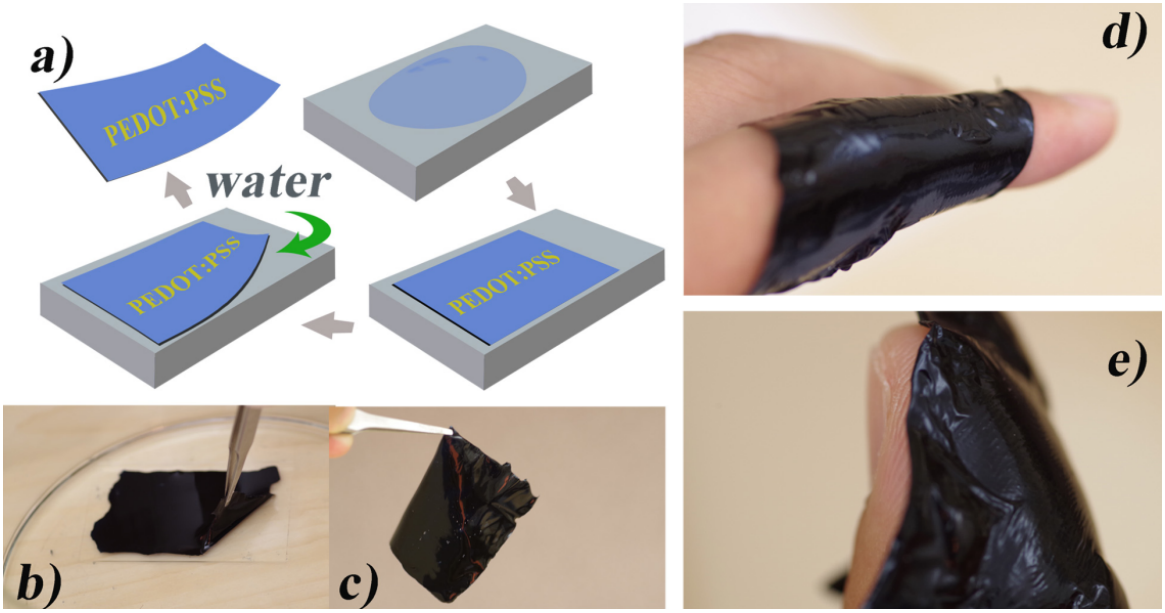

Figure 6.5. a) Illustration of the water-assisted wedging method used to obtain free-standing PEDOT:PSS films, b) the film is detached from the glass substrate with tweezers, and c) does not deteriorate during the process. d) Excellent film conformability of PEDOT:PSS free-standing films (10 μm thickness) on finger and e) on fingertip. The fingerprint details are clearly visible in (e).

To fully take advantage of the healability of these films, it is important to obtain them in a free-standing form, to enable transfer onto various substrates. We obtained free-standing films with a high yield by using water-assisted delamination from glass substrates (Figure 6.5a)[38]. We immersed the thick films on glass in DI water and, after 1 h of gentle stirring, we were able to detach them from the substrate with tweezers without any rupture (Figure 6.5b,c). These free-standing films maintain their high conductivity after drying. The detached wet free-standing films can be easily shaped with scissors and plastered on objects with irregular shapes, such as fingers and even fingertips (Figure 6.5d,e), hence they have potential applications as conformable and healable electrodes or electrical patches. For instance, they show high conformability to fingers and are even able to reflect fingerprint details on their surface (Figure 6.5e). The wet films can be further used for erasable imprinting (Figure S11, Supporting Information) or shape-memory materials[189] because the shaped films can recover their smoothness after absorbing water (Video S6, Supporting Information). They can also be developed as a healable conductive patch to repair a damaged Au connection on an elastomer substrate by simply pasting it on top of the damaged

region (Figure S12, Supporting Information). The free-standing patch showed perfect conformability to the elastomer surface and led to a current recovery of 100% of its initial value, which remained stable even after crumpling the polydimethylsiloxane (PDMS). In comparison, when a copper conductive tape was used for the same repair, a much lower current was achieved after repair, due to the poor conformability of the tape to the PDMS surface.

In summary, we have demonstrated healability of PEDOT:PSS films. After increasing the thickness to a threshold of about 1 μm, the films are electrically healed within ≈150 ms upon the addition of a water droplet. The healed damage can be more than 40 times larger than the film thickness and the healing ability remains after multiple damages. Significantly, a wet film became an autonomic self-healing conductor. Moreover, instead of a water droplet, we showed the current healing can be further controlled by humidity, suggesting potential applications in self-healable large-scale electronics. We also introduced an easy and reliable way to obtain free-standing films by using a water-assisted wedging method, and demonstrated their excellent conformability on various surfaces and efficient use as electronic welding patches.

The electrically healable PEDOT:PSS films we presented possess the following outstanding advantages: i) ease of to process from commercially available suspensions; ii) electrical conductivity (500 S cm^{-1}) among the highest reported for electrically healable materials; iii) healing achievable at room temperature and ambient air simply by using water; iv) long-term stability in air and water; v) the films are free-standing, without the need for substrate support, and therefore can be directly laminated on either regular or irregular objects; iv) biocompatibility that can be exploited for biological applications, such as in vivo studies or electronic skin.

As the most successful conducting polymer, PEDOT:PSS is now expanding its importance to the field of self-healable electronics. We believe it will greatly further research in electronic skin, self-healing circuits, water-enabled sensors, and wearable electronics.

6.5 Experimental section

The PEDOT:PSS aqueous suspension (Clevios PH1000) was purchased from Heraeus Electronic Materials GmbH (Leverkusen, Germany). Glycerol (99.5+% purity) was purchased from Caledon Laboratories Ltd. (Georgetown, ON). Capstone FS-30 was purchased from Alfa Chemicals. The liquid metal gallium–indium eutectic (EGaIn 495425) was purchased from Sigma-Aldrich. The

fluorinated stripper Orthogonal 700 solution (part of a photoresist kit) was supplied by Orthogonal Inc. Glass slides were purchased from Corning. PET sheets were purchased from Policrom Inc. (Bensalem, PA, USA). PDMS (Sylgard 184 silicone elastomer kit) was purchased from Dow Corning. The wireless transmitter and receiver were further designed based on the Demo ZM470SX (supplied by Guangzhou Zhiyuan Electronics co., ltd.). ZM470SX is a LoRa based low power wide area network specification intended for wireless (up to 15 km) battery operated things in a regional, national, or global network.

The films were processed by directly drop-casting the PEDOT:PSS suspension onto glass substrates. The thickness was controlled by spreading different volumes of the suspension on glass. After drop-casting, the films were baked on a hot plate with the following sequence: 80 °C for 1 h, 110 °C for 1 h, and finally 140 °C for 4 h. The gradual temperature increase permitted us to obtain continuous films without bubbles.

Film electrical characterization was performed using a National Instruments NI PXIe-1062Q source-measure unit controlled by Labview software. Electrical contacts were made via two tungsten probes immersed into EGaIn contacts at two sides of the film. The film thickness was measured with a profilometer (Dektak 150) using a 12.5 μm stylus tip with a 10 mg stylus force. The sheet resistance was measured by a Jandel four-point probe with an Agilent B2902A voltage–current source measure unit.

The cuts were performed manually with a standard razor blade. Deionized water (18.2 MΩ cm at 25 °C, Millipore), Orthogonal 700 stripper, the ionic liquid EMIM-TFSI and glycerol were used as healing agents. Electrical measurements at relative humidity between 50% and 90% were performed in a Cole-Parmer humidity-controlled chamber (03323-14).

SEM measurements were performed with a JEOL JSM-7600TFE Field Emission Scanning Electron Microscope with a voltage of 5.0 KV (LEI) under a vacuum of 10−4 Pa. The strain–stress characterization was performed with an Instron E-3000 tensile tester. The TOF-SIMS was performed with an IONTOF TOF-SIMS IV. The optical images were obtained with a Carl Zeiss AX10 (10x magnification) microscope. For the repair test on Au contacts, 4 nm Ti and 40 nm Au were deposited by E-beam evaporation on 300-μm-thick PDMS substrates at 1 Å s^{-1}.

6.6 Acknowledgments

The authors are grateful to Prof. Clara Santato and Dr. Gaia Tomasello for fruitful discussions, Qian Li of Youxin Pai Inc. for schematic image drawing, and Bo Zhang of Zhiyuan Electronics Co., Ltd. for discussion on the wireless communications. This work was supported by grants Discovery (NSERC), Établissement de Nouveau Chercheur (FRQNT), PSR-SIIRI 810 and 956 (Quebec Ministry of Economy, Science and Innovation), and John Evans Research Fund (CFI), awarded to F.C. S.Z. is grateful to NSERC for financial support through a Vanier Canada Graduate Scholarship and to CMC Microsystems through the program MNT financial assistance. The authors have also benefited from the support of FRQNT and its Regroupement stratégique program through a grant awarded to RQMP.

CHAPTER 7 GENERAL DISCUSSION

In the following, the results of Chapter 3 to 6 are discussed as a whole with reference to the literature presented in Chapter 2. A detailed study of the fundamental properties of PEDOT:PSS is presented in this thesis, and many insights have been gained in terms of processing, electrical properties, water stability, mechanical flexibility/stretchability and self-healing ability. We develop advanced patterning methods for both PEDOT:PSS and metallic electrodes on soft substrates. We demonstrate for the first time self-healing PEDOT:PSS films as well as stretchable and self-healing OECTs.

Article 1 deals with conducting polymer processing. We process PEDOT:PSS films by spin coating with the addition of different additives to modify their conductivity. We identify glycerol as a conductivity enhancer in our subsequent research, considering the higher conductivity obtained as well as its excellent biocompatibility with respect to other additives. The surfactant DBSA is shown to not only increase the films' processability, but also to increase their conductivity. Although DBSA is necessary to obtain a uniform film quality on a glass substrate, we prove in Article 2 that uniform films on plastic substrates can be obtained without the need for DBSA. The reason that conductivity increase after adding conductivity enhancers is because they cause a re-arrangement in the morphology of the PEDOT:PSS films upon drying. The re-arrangement results in larger and straighter $PEDOT^+$ grains and increased phase separation between the conducting $PEDOT^+$ and the insulating PSS^-, leading to a better $PEDOT^+$-$PEDOT^+$ connecting network in the film and the removal of insulating PSS components. In addition, in Article 1 we show that the introduction of the crosslinker GOPS is mandatory to avoid film delamination and dissolution in water. We analyze the films' composition after baking, and confirmed that most of the conductivity enhancers evaporate during baking, while the crosslinker remains in the films. The fundamental understanding of PEDOT:PSS, gained in Article 1, is essential for the work carried out in Articles 2, 3 and 4, where critical PEDOT:PSS processing is required for film conductivity, stability and stretchability.

In Article 2, we focus on the patterning of PEDOT:PSS on PET to develop flexible micro-OECTs on plastic. We reveal that PEDOT:PSS films on plastic show more robust adhesion than films on glass, and no crosslinkers are needed to prevent film delamination or dissolution in water. We explore and optimize microfabrication conditions for reliable patterning of metallic electrodes as

well as orthogonal patterning of PEDOT:PSS films on PET. The same PEDOT:PSS patterning method is further performed on an stretchable PDMS substrate (Article 3). Patterning PEDOT:PSS on soft substrates is of high importance for the research community because the chemicals used in standard photolithography (photoresists, developers, strippers) may dissolve or contaminate conducting polymers. Taking advantage of the orthogonal patterned PEDOT:PSS films, in Article 2, we demonstrate high performance flexible OECTs, with high cyclic bending stability and water stability.

After making flexible devices, in Article 3 we step into the area of stretchable electronics and demonstrated the first stretchable OECTs. We develop a novel parylene-based method for metallic patterning of electrodes on PDMS, with higher resolution and fidelity compared to other patterning techniques reported for similar substrates. In the same article we engineer a wrinkled device structure by the "bulking method", which ensures OECTs' stretchability while maintaining identical electrical properties under strains. With the orthogonal patterning methods developed in Article 2, the use of an ionic conductive hydrogel as the electrolyte, and optimized PEDOT:PSS processing following methodology in Article 1, we demonstrate a fully stretchable solid-state OECT in Article 3. In Article 4, we demonstrate self-sealing properties of PEDOT:PSS films. Upon controlling the film thickness, we obtain rapid self-healing PEDOT:PSS films. We find that PEDOT:PSS films (>1 μm) show instantaneous electronic healing after wetting the damaged area with water. The healing process of the films is not affected by repeated damage to the films and occurred within 150 ms of wetting, making PEDOT:PSS thin films promising for use in self-healing circuits. It is also demonstrated that healing occurs after exposure to water vapor. We tentatively suggest that the healing process can be attributed to the swelling of PSS^- chains upon exposure to water and the increased ionic conductivity due to PSS^- dissolution. The swollen PSS^- chains swell towards the damage site, causing the $PEDOT^+$ chains to shift and form conducting paths across the damage. Detailed mechanism is still under investigation. Despite the films regain the conductivity after healing, their mechanical property become weaker and may easily break upon delamination from the substrate. We further demonstrate the potential of PEDOT:PSS films as ultrasensitive flexible water leak sensors and as channel materials for self-healing OECTs. Film processing with additives (Article 1) doesn't affect the healing properties. The healing of PEDOT:PSS films endues conducting polymers with a new property.

We believe the fabrication technologies we develop in Article 2 (flexible) and Article 3 (stretchable), as well as the self-healing properties observed in Article 4, will pave the way to self-healing wearable electronics in the areas of interconnects, surface coatings, biomedical sensors, energy storage devices, as well as logic circuits. The current technology ensures its application as biosensors for in vitro organ-on-chip study. Despite there are still limitations for the devices towards in vivo applications (discussed in chapter 8), this thesis contributes to the advancement of technology in organic bioelectronics and we believe a significant improvement can be realized in the near future to meet the requirements for commercial applications.

CHAPTER 8 CONCLUSION AND RECOMMENDATIONS

This PhD thesis explored the use of conducting polymer PEDOT:PSS for application in flexible, stretchable and self-healing electronic devices.

Our first step was to gain insight into the fundamental properties of PEDOT:PSS. We have shown that additives play an essential role in determining film conductivity, thickness, wettability, water-stability and stretchability. We revealed how conductivity enhancers, surfactants and crosslinkers react with PEDOT:PSS and modify its corresponding properties. We found that the PEDOT:PSS film thickness decreases upon immersion in polar solvents, while the electrical conductivity remains unchanged. The thickness decrease can be prevented by adding a cross-linking agent to the mixture before coating.

Miniaturized OECT arrays on flexible substrate are highly desirable to effectively place devices in contact with the curvilinear surfaces often encountered in biomedical applications. We therefore developed micro-scale OECTs on flexible PET substrates, taking advantage of high resolution patterning of PEDOT:PSS with fluorinated photoresists. The flexible OECTs operate at low voltage (below 1V), exhibit high performance, and show stable electrical characteristics after extreme bending. We noted, compared to films on glass, PEDOT:PSS on PET show more robust and long-term stability in aqueous media.

Development of stretchable OECTs could further their potential as conformal/implantable healthcare devices, and ease the integration with other wearable electronic systems. To attain this goal, we first identified a combination of additives, containing a biocompatible conductivity enhancer (glycerol) and a stretchability enhancer (Zonyl-FS300), for PEDOT:PSS processing. Combining orthogonal patterning of PEDOT:PSS with parylene transfer patterning of metallic electrodes, and using ionic hydrogel as electrolyte, we fabricated solid-state stretchable OECTs. And finally, self-healing PEDOT:PSS films were realized by engineering the film thickness and controlling the water content in the film.

We have developed technologies in the area of conducting-polymer research of potential interest for both academia and industry, e.g., for wearable electronics and healthcare. The innovative patterning methods for flexible and stretchable electronics, as well as the ground-breaking

observation of self-healable conducting polymers, will be of permanent importance for future research.

Despite the fact that stretchable PEDOT:PSS films with robust performance in water were finally obtained in this project for use in stretchable OECT, in-depth study of the mechanism needs to be further addressed. Clarifying the mechanism requires the synergistic efforts of various disciplines of polymer science (molecular level), mechanical engineering (strain, stress, cracks), and electrical engineering. Further investigation of molecular and mechanical dynamics will be of great importance in finding a general rule to predict the stretchability of a certain material and to develop materials with better stretchability.

The stretchable OECTs we developed still suffer a low ON/OFF ratio and more work is needed to clarify the reasons for it (impurities at the porous interface which prevent the doping/dedoping process). Stretchable PEDOT:PSS films can be immediately introduced to explore stretchable OEIP, ionic transistors, neuron-electrodes and neuromorphic devices. Introduction of high arrays of stretchable PEDOT:PSS-based bioelectronic devices directly in in-vivo will be necessary to verify their commercial potential.

Our observation of healing behavior represents one of the significant results of this thesis. It will inspire researchers to investigate the healing properties of other conducting polymers and conducting polyelectrolytes by interfacing them with water or other liquids, or during chemical synthesis. We tentatively attribute the healing to the swelling of PSS^- and to increased ionic conduction. More experimental results are needed to verify this conclusion. An in-situ close recording of the healing process (scanning probe, microscope and fluorescent staining) might provide deeper insight into the mechanism. More healable PEDOT:PSS-based devices, such as batteries, capacitors and memories, can be engineered and developed following this work. Integration of the self-healing behavior simultaneously with stretchable functions will be another interesting topic for further research.

Investigation of conducting polyelectrolytes or other polyelectrolytes in addition to PEDOT:PSS for soft OECTs could be another research topic since PSS is acidic and might deteriorate a device's long-term stability. Modifying ionic side groups of conducting polyelectrolyte can balance electronic and ionic conductivity in the polyelectrolyte, and might also help obtain highly stretchable films. Further developing new conducting polyelectrolytes that allow OECTs to work

in accumulation mode will make it possible to realize complementary OECT logics, thus promoting OECT applications.

BIBLIOGRAPHY

1 Shirakawa, H., Louis, E. J., MacDiarmid, A. G., Chiang, C. K. & Heeger, A. J. Synthesis of electrically conducting organic polymers: halogen derivatives of polyacetylene,(CH) x. *Journal of the Chemical Society, Chemical Communications*, 578-580 (1977).

2 Cicoira, F. & Santato, C. *Organic electronics: emerging concepts and technologies*. (John Wiley & Sons, 2013).

3 Reineke, S. *et al.* White organic light-emitting diodes with fluorescent tube efficiency. *MRS Online Proceedings Library Archive* **1212** (2009).

4 Tang, C. W. & VanSlyke, S. A. Organic electroluminescent diodes. *Applied physics letters* **51**, 913-915 (1987).

5 Rivnay, J., Owens, R. M. & Malliaras, G. G. The Rise of Organic Bioelectronics. *Chemistry of Materials* **26**, 679-685, doi:10.1021/cm4022003 (2014).

6 Berggren, M. & Richter‐Dahlfors, A. Organic bioelectronics. *Advanced Materials* **19**, 3201-3213 (2007).

7 Tarabella, G. *et al.* New opportunities for organic electronics and bioelectronics: ions in action. *Chemical Science* **4**, 1395-1409 (2013).

8 White, H. S., Kittlesen, G. P. & Wrighton, M. S. Chemical derivatization of an array of three gold microelectrodes with polypyrrole: fabrication of a molecule-based transistor. *Journal of the American Chemical Society* **106**, 5375-5377 (1984).

9 Nilsson, D. *et al.* Bi-stable and dynamic current modulation in electrochemical organic transistors. *Advanced Materials* **14**, 51-54 (2002).

10 Rivnay, J., Owens, R. M. & Malliaras, G. G. The rise of organic bioelectronics. *Chemistry of Materials* **26**, 679-685 (2013).

11 Neamen, D. *Semiconductor physics and devices*. (McGraw-Hill, Inc., 2002).

12 Klauk, H. *Organic electronics: materials, manufacturing, and applications*. (John Wiley & Sons, 2006).

13 Shirakawa, H., McDiarmid, A. & Heeger, A. Twenty-five years of conducting polymers. *Chemical Communications* **2003**, 1-4 (2003).

14 Burroughes, J. *et al.* Light-emitting diodes based on conjugated polymers. *nature* **347**, 539-541 (1990).

15 Skotheim, T. A. *Handbook of conducting polymers*. (CRC press, 1997).

16 https://www.iapp.de.

17 Balint, R., Cassidy, N. J. & Cartmell, S. H. Conductive polymers: towards a smart biomaterial for tissue engineering. *Acta biomaterialia* **10**, 2341-2353 (2014).

18 Heywang, G. & Jonas, F. Poly (alkylenedioxythiophene) s—new, very stable conducting polymers. *Advanced Materials* **4**, 116-118 (1992).

19 Groenendaal, L., Jonas, F., Freitag, D., Pielartzik, H. & Reynolds, J. R. poly (3, 4‐ethylenedioxythiophene) and its derivatives: past, present, and future. *Advanced Materials* **12**, 481-494 (2000).

20 Jonas, F., Krafft, W. & Muys, B. in *Macromolecular Symposia.* 169-173 (Wiley Online Library).

21 Rivnay, J. *et al.* Structural control of mixed ionic and electronic transport in conducting polymers. *Nature communications* **7** (2016).

22 Isaksson, J. *et al.* Electronic control of Ca2+ signalling in neuronal cells using an organic electronic ion pump. *Nature materials* **6**, 673-679 (2007).

23 https://www.heraeus.com.

24 Elschner, A., Kirchmeyer, S., Lovenich, W., Merker, U. & Reuter, K. *PEDOT: principles and applications of an intrinsically conductive polymer*. (CRC Press, 2010).

25 Kim, N. *et al.* Highly Conductive PEDOT: PSS Nanofibrils Induced by Solution‐Processed Crystallization. *Advanced materials* **26**, 2268-2272 (2014).

26 Zhang, S. *et al.* Solvent-induced changes in PEDOT: PSS films for organic electrochemical transistors. *APL materials* **3**, 014911 (2015).

27 Li, C. & Imae, T. Electrochemical and optical properties of the poly (3, 4-ethylenedioxythiophene) film electropolymerized in an aqueous sodium dodecyl sulfate and lithium tetrafluoroborate medium. *Macromolecules* **37**, 2411-2416 (2004).

28 Meskers, S. C., van Duren, J. K., Janssen, R. A., Louwet, F. & Groenendaal, L. Infrared Detectors with Poly (3, 4‐ethylenedioxy thiophene)/Poly (styrene sulfonic acid)(PEDOT/PSS) as the Active Material. *Advanced Materials* **15**, 613-616 (2003).

29 Vosgueritchian, M., Lipomi, D. J. & Bao, Z. Highly conductive and transparent PEDOT: PSS films with a fluorosurfactant for stretchable and flexible transparent electrodes. *Advanced functional materials* **22**, 421-428 (2012).

30 Wang, Y. *et al.* A highly stretchable, transparent, and conductive polymer. *Science Advances* **3**, e1602076 (2017).

31 Kim, J., Jung, J., Lee, D. & Joo, J. Enhancement of electrical conductivity of poly (3, 4-ethylenedioxythiophene)/poly (4-styrenesulfonate) by a change of solvents. *Synthetic Metals* **126**, 311-316 (2002).

32 Ouyang, J., Chu, C. W., Chen, F. C., Xu, Q. & Yang, Y. High‐conductivity poly (3, 4‐ethylenedioxythiophene): poly (styrene sulfonate) film and its application in polymer optoelectronic devices. *Advanced Functional Materials* **15**, 203-208 (2005).

33 Xia, Y., Sun, K. & Ouyang, J. Solution‐processed metallic conducting polymer films as transparent electrode of optoelectronic devices. *Advanced Materials* **24**, 2436-2440 (2012).

34 Kim, N. *et al.* Highly Conductive All‐Plastic Electrodes Fabricated Using a Novel Chemically Controlled Transfer‐Printing Method. *Advanced Materials* **27**, 2317-2323 (2015).

35 Li, Z. *et al.* Free‐Standing Conducting Polymer Films for High‐Performance Energy Devices. *Angewandte Chemie International Edition* **55**, 979-982 (2016).

36 Zhou, J. *et al.* The temperature-dependent microstructure of PEDOT/PSS films: insights from morphological, mechanical and electrical analyses. *Journal of Materials Chemistry C* **2**, 9903-9910 (2014).

37 Lim, F. J., Ananthanarayanan, K., Luther, J. & Ho, G. W. Influence of a novel fluorosurfactant modified PEDOT: PSS hole transport layer on the performance of inverted organic solar cells. *Journal of Materials Chemistry* **22**, 25057-25064 (2012).

38 Zhang, S. *et al.* Water stability and orthogonal patterning of flexible micro-electrochemical transistors on plastic. *Journal of Materials Chemistry C* **4**, 1382-1385 (2016).

39 Lee, J. Y. Indium blocking in polymer light emitting diodes with a crosslinked poly (3, 4-ethylenedioxythiophene)/silane hole transport layer. *Synthetic metals* **156**, 537-540 (2006).

40 Berezhetska, O., Liberelle, B., De Crescenzo, G. & Cicoira, F. A simple approach for protein covalent grafting on conducting polymer films. *Journal of Materials Chemistry B* **3**, 5087-5094 (2015).

41 Håkansson, A. *et al.* Effect of (3‐glycidyloxypropyl) trimethoxysilane (GOPS) on the electrical properties of PEDOT: PSS films. *Journal of Polymer Science Part B: Polymer Physics* **55**, 814-820 (2017).

42 Stavrinidou, E. *et al.* Direct measurement of ion mobility in a conducting polymer. *Advanced Materials* **25**, 4488-4493 (2013).

43 Mantione, D. *et al.* Low temperature cross-linking of PEDOT: PSS films using divinylsulfone. *ACS Applied Materials & Interfaces* (2017).

44 Lipomi, D. J. *et al.* Electronic properties of transparent conductive films of PEDOT: PSS on stretchable substrates. *Chemistry of Materials* **24**, 373-382 (2012).

45 Savagatrup, S. *et al.* Plasticization of PEDOT: PSS by Common Additives for Mechanically Robust Organic Solar Cells and Wearable Sensors. *Advanced Functional Materials* **25**, 427-436 (2015).

46 Li, P., Sun, K. & Ouyang, J. Stretchable and Conductive Polymer Films Prepared by Solution Blending. *ACS Applied Materials & Interfaces* **7**, 18415-18423 (2015).

47 Oh, J. Y., Kim, S., Baik, H. K. & Jeong, U. Conducting polymer dough for deformable electronics. *Advanced Materials* **28**, 4455-4461 (2016).

48 Hansen, T. S., West, K., Hassager, O. & Larsen, N. B. Highly stretchable and conductive polymer material made from poly (3, 4‐ethylenedioxythiophene) and polyurethane elastomers. *Advanced functional materials* **17**, 3069-3073 (2007).

49 Lee, Y. Y. *et al.* A Strain‐Insensitive Stretchable Electronic Conductor: PEDOT: PSS/Acrylamide Organogels. *Advanced Materials* **28**, 1636-1643 (2016).

50 Seyedin, M. Z., Razal, J. M., Innis, P. C. & Wallace, G. G. Strain‐Responsive Polyurethane/PEDOT: PSS Elastomeric Composite Fibers with High Electrical Conductivity. *Advanced Functional Materials* **24**, 2957-2966 (2014).

51 Huynh, T. P. & Haick, H. Self‐Healing, Fully Functional, and Multiparametric Flexible Sensing Platform. *Advanced Materials* **28**, 138-143 (2016).

52 Oh, J. Y. *et al.* Intrinsically stretchable and healable semiconducting polymer for organic transistors. *Nature* **539**, 411-415 (2016).

53 DeFranco, J. A., Schmidt, B. S., Lipson, M. & Malliaras, G. G. Photolithographic patterning of organic electronic materials. *Organic Electronics* **7**, 22-28 (2006).

54 Taylor, P. G. *et al.* Orthogonal patterning of PEDOT: PSS for organic electronics using hydrofluoroether solvents. *Advanced Materials* **21**, 2314-2317 (2009).

55 DeFranco, J. Patterning And Processing Of Organic Electronic Devices Using Photolithography. (2011).

56 Taylor, P. Lithographic Patterning Processes For Organic Electronics And Biomaterials. (2011).

57 Xia, Y. & Whitesides, G. M. Soft lithography. *Annual review of materials science* **28**, 153-184 (1998).

58 Meitl, M. A. *et al.* Transfer printing by kinetic control of adhesion to an elastomeric stamp. *Nature materials* **5**, 33 (2006).

59 Qin, D., Xia, Y. & Whitesides, G. M. Soft lithography for micro-and nanoscale patterning. *Nature protocols* **5**, 491 (2010).

60 Sessolo, M. *et al.* Easy‐to‐Fabricate Conducting Polymer Microelectrode Arrays. *Advanced Materials* **25**, 2135-2139 (2013).

61 Zakhidov, A. A. *et al.* Orthogonal processing: A new strategy for organic electronics. *Chemical Science* **2**, 1178-1182 (2011).

62 Sze, S. M. & Ng, K. K. *Physics of semiconductor devices*. (John wiley & sons, 2006).

63 Niccolai, J. Intel pushes 10nm chip-making process to 2017, slowing Moore's Law. *InfoWorld* (2015).

64 Carnie, S. L. & Torrie, G. M. The statistical mechanics of the electrical double layer. *Advances in Chemical Physics, Volume 56*, 141-253 (2007).

65 Brett, C., Brett, M. O., Brett, A. M. C. M. & Brett, A. M. O. *Electrochemistry: principles, methods, and applications*. (1993).

66 Bard, A. J., Faulkner, L. R., Leddy, J. & Zoski, C. G. *Electrochemical methods: fundamentals and applications*. Vol. 2 (wiley New York, 1980).

67 Simon, D. T., Gabrielsson, E. O., Tybrandt, K. & Berggren, M. Organic bioelectronics: bridging the signaling gap between biology and technology. *Chem. Rev* **116**, 13009-13041 (2016).

68 Rivnay, J. *et al.* Organic electrochemical transistors with maximum transconductance at zero gate bias. *Advanced Materials* **25**, 7010-7014 (2013).

69 Khodagholy, D. *et al.* High transconductance organic electrochemical transistors. *Nature communications* **4** (2013).

70 Rivnay, J. *et al.* High-performance transistors for bioelectronics through tuning of channel thickness. *Science advances* **1**, e1400251 (2015).

71 Bernards, D. A. & Malliaras, G. G. Steady‐state and transient behavior of organic electrochemical transistors. *Advanced Functional Materials* **17**, 3538-3544 (2007).

72 Robinson, N. D., Svensson, P.-O., Nilsson, D. & Berggren, M. On the current saturation observed in electrochemical polymer transistors. *Journal of the Electrochemical Society* **153**, H39-H44 (2006).

73 Nilsson, D., Kugler, T., Svensson, P.-O. & Berggren, M. An all-organic sensor–transistor based on a novel electrochemical transducer concept printed electrochemical sensors on paper. *Sensors and Actuators B: Chemical* **86**, 193-197 (2002).

74 Tarabella, G. *et al.* Organic electrochemical transistors monitoring micelle formation. *Chemical Science* **3**, 3432-3435 (2012).

75 Bernards, D. A. *et al.* Enzymatic sensing with organic electrochemical transistors. *Journal of Materials Chemistry* **18**, 116-120 (2008).

76 Kergoat, L. *et al.* Detection of glutamate and acetylcholine with organic electrochemical transistors based on conducting polymer/platinum nanoparticle composites. *Advanced Materials* **26**, 5658-5664 (2014).

77 Yang, S. Y. *et al.* Electrochemical transistors with ionic liquids for enzymatic sensing. *Chemical Communications* **46**, 7972-7974 (2010).

78 Xiong, C. *et al.* Highly sensitive detection of gallic acid based on organic electrochemical transistors with poly (diallyldimethylammonium chloride) and carbon nanomaterials nanocomposites functionalized gate electrodes. *Sensors and Actuators B: Chemical* **246**, 235-242 (2017).

79 Tang, H., Yan, F., Lin, P., Xu, J. & Chan, H. L. Highly sensitive glucose biosensors based on organic electrochemical transistors using platinum gate electrodes modified with enzyme and nanomaterials. *Advanced Functional Materials* **21**, 2264-2272 (2011).

80 Lin, P., Luo, X., Hsing, I. & Yan, F. Organic electrochemical transistors integrated in flexible microfluidic systems and used for label‐free DNA sensing. *Advanced Materials* **23**, 4035-4040 (2011).

81 Zhang, M. *et al.* High‐Performance Dopamine Sensors Based on Whole‐Graphene Solution‐Gated Transistors. *Advanced Functional Materials* **24**, 978-985 (2014).

82 Liao, C., Mak, C., Zhang, M., Chan, H. L. & Yan, F. Flexible organic electrochemical transistors for highly selective enzyme biosensors and used for saliva testing. *Advanced Materials* **27**, 676-681 (2015).

83 Bolin, M. H. *et al.* Active Control of Epithelial Cell‐Density Gradients Grown Along the Channel of an Organic Electrochemical Transistor. *Advanced Materials* **21**, 4379-4382 (2009).

84 Lin, P., Yan, F., Yu, J., Chan, H. L. & Yang, M. The application of organic electrochemical transistors in cell‐based biosensors. *Advanced Materials* **22**, 3655-3660 (2010).

85 Jimison, L. H. *et al.* Measurement of barrier tissue integrity with an organic electrochemical transistor. *Advanced Materials* **24**, 5919-5923 (2012).

86 Khodagholy, D. *et al.* In vivo recordings of brain activity using organic transistors. *Nature communications* **4**, 1575 (2013).

87 Ramuz, M. *et al.* Combined optical and electronic sensing of epithelial cells using planar organic transistors. *Advanced Materials* **26**, 7083-7090 (2014).

88 Campana, A., Cramer, T., Simon, D. T., Berggren, M. & Biscarini, F. Electrocardiographic recording with conformable organic electrochemical transistor fabricated on resorbable bioscaffold. *Advanced Materials* **26**, 3874-3878 (2014).

89 Stavrinidou, E. *et al.* Electronic plants. *Science advances* **1**, e1501136 (2015).

90 Braendlein, M. *et al.* Lactate Detection in Tumor Cell Cultures Using Organic Transistor Circuits. *Advanced Materials* **29** (2017).

91 Hammock, M. L., Chortos, A., Tee, B. C. K., Tok, J. B. H. & Bao, Z. 25th anniversary article: the evolution of electronic skin (e‐skin): a brief history, design considerations, and recent progress. *Advanced Materials* **25**, 5997-6038 (2013).

92 Cheng, T., Zhang, Y., Lai, W. Y. & Huang, W. Stretchable Thin‐Film Electrodes for Flexible Electronics with High Deformability and Stretchability. *Advanced Materials* **27**, 3349-3376 (2015).

93 Rogers, J. A., Someya, T. & Huang, Y. Materials and mechanics for stretchable electronics. *Science* **327**, 1603-1607 (2010).

94 Qian, Y. *et al.* Stretchable organic semiconductor devices. *Advanced Materials* **28**, 9243-9265 (2016).

95 Trung, T. Q. & Lee, N. E. Recent progress on stretchable electronic devices with intrinsically stretchable components. *Advanced Materials* **29** (2017).

96 Bowden, N., Brittain, S., Evans, A. G., Hutchinson, J. W. & Whitesides, G. M. Spontaneous formation of ordered structures in thin films of metals supported on an elastomeric polymer. *Nature* **393**, 146-149 (1998).

97 Chortos, A. *et al.* Highly stretchable transistors using a microcracked organic semiconductor. *Advanced Materials* **26**, 4253-4259 (2014).

98 Khang, D.-Y., Jiang, H., Huang, Y. & Rogers, J. A. A stretchable form of single-crystal silicon for high-performance electronics on rubber substrates. *Science* **311**, 208-212 (2006).

99 Ko, H. C. *et al.* A hemispherical electronic eye camera based on compressible silicon optoelectronics. *Nature* **454**, 748 (2008).

100 Kim, D.-H. *et al.* Epidermal electronics. *science* **333**, 838-843 (2011).

101 Zhang, Y. *et al.* A mechanically driven form of Kirigami as a route to 3D mesostructures in micro/nanomembranes. *Proceedings of the National Academy of Sciences* **112**, 11757-11764 (2015).

102 Sekitani, T. *et al.* Stretchable active-matrix organic light-emitting diode display using printable elastic conductors. *Nature materials* **8**, 494-499 (2009).

103 Sekitani, T. *et al.* A rubberlike stretchable active matrix using elastic conductors. *Science* **321**, 1468-1472 (2008).

104 Kaltenbrunner, M. *et al.* An ultra-lightweight design for imperceptible plastic electronics. *Nature* **499**, 458 (2013).

105 Lipomi, D. J. *et al.* Skin-like pressure and strain sensors based on transparent elastic films of carbon nanotubes. *Nature nanotechnology* **6**, 788-792 (2011).

106 Xu, F. & Zhu, Y. Highly conductive and stretchable silver nanowire conductors. *Advanced materials* **24**, 5117-5122 (2012).

107 Boubée de Gramont, F. *et al.* Highly stretchable electrospun conducting polymer nanofibers. *Applied Physics Letters* **111**, 093701 (2017).

108 Malliaras, G. & Friend, R. An organic electronics primer. *Physics Today* **58**, 53-58 (2005).

109 Tang, C. W. Two‐layer organic photovoltaic cell. *Applied Physics Letters* **48**, 183-185 (1986).

110 Horowitz, G. Organic field-effect transistors. *Advanced Materials* **10**, 365-377 (1998).

111 Tarabella, G. *et al.* Effect of the gate electrode on the response of organic electrochemical transistors. *Applied Physics Letters* **97**, 205 (2010).

112 Lin, P., Yan, F. & Chan, H. L. Ion-sensitive properties of organic electrochemical transistors. *ACS applied materials & interfaces* **2**, 1637-1641 (2010).

113 Cicoira, F. *et al.* Influence of device geometry on sensor characteristics of planar organic electrochemical transistors. *Advanced Materials* **22**, 1012-1016 (2010).

114 Tang, H., Lin, P., Chan, H. L. & Yan, F. Highly sensitive dopamine biosensors based on organic electrochemical transistors. *Biosensors and Bioelectronics* **26**, 4559-4563 (2011).

115 Yang, S. Y. *et al.* Integration of a surface-directed microfluidic system with an organic electrochemical transistor array for multi-analyte biosensors. *Lab on a Chip* **9**, 704-708 (2009).

116 Tybrandt, K., Forchheimer, R. & Berggren, M. Logic gates based on ion transistors. *Nature communications* **3**, 871 (2012).

117 Ouyang, J. *et al.* On the mechanism of conductivity enhancement in poly (3, 4-ethylenedioxythiophene): poly (styrene sulfonate) film through solvent treatment. *Polymer* **45**, 8443-8450 (2004).

118 Martin, B. D. *et al.* Hydroxylated secondary dopants for surface resistance enhancement in transparent poly (3, 4-ethylenedioxythiophene)–poly (styrenesulfonate) thin films. *Synthetic metals* **142**, 187-193 (2004).

119 Elschner, A. & Lövenich, W. Solution-deposited PEDOT for transparent conductive applications. *MRS bulletin* **36**, 794-798 (2011).

120 Smits, F. Measurement of sheet resistivities with the four‐point probe. *Bell Labs Technical Journal* **37**, 711-718 (1958).

121 Zhang, F., Nyberg, T. & Inganäs, O. Conducting polymer nanowires and nanodots made with soft lithography. *Nano Letters* **2**, 1373-1377 (2002).

122 Kim, Y. H. *et al.* Highly conductive PEDOT: PSS electrode with optimized solvent and thermal post‐treatment for ITO‐free organic solar cells. *Advanced Functional Materials* **21**, 1076-1081 (2011).

123 Jönsson, S. *et al.* The effects of solvents on the morphology and sheet resistance in poly (3, 4-ethylenedioxythiophene)–polystyrenesulfonic acid (PEDOT–PSS) films. *Synthetic Metals* **139**, 1-10 (2003).

124 Oliveira, M., Teles, A., Queimada, A. & Coutinho, J. Phase equilibria of glycerol containing systems and their description with the Cubic-Plus-Association (CPA) Equation of State. *Fluid Phase Equilibria* **280**, 22-29 (2009).

125 Sadek, P. C. *HPLC solvent guide*. (Wiley-Interscience, 2002).

126 Snyder, L. R. Classification of the solvent properties of common liquids. *Journal of Chromatography A* **92**, 223-230 (1974).

127 Mengistie, D. A., Ibrahem, M. A., Wang, P.-C. & Chu, C.-W. Highly conductive PEDOT: PSS treated with formic acid for ITO-free polymer solar cells. *ACS applied materials & interfaces* **6**, 2292-2299 (2014).

128 Greczynski, G., Kugler, T. & Salaneck, W. Characterization of the PEDOT-PSS system by means of X-ray and ultraviolet photoelectron spectroscopy. *Thin Solid Films* **354**, 129-135 (1999).

129 Doszlop, S., Vargha, V. & Horkay, F. Reactions of epoxy with other functional groups and the arising sec-hydroxyl groups. *Periodica Polytechnica. Chemical Engineering* **22**, 253 (1978).

130 Pascault, J.-P. & Williams, R. J. *Epoxy polymers: new materials and innovations*. (John Wiley & Sons, 2009).

131 Noll, W. *Chemistry and technology of silicones*. (Elsevier, 2012).

132 Brook, M. A. *et al.* Proteins entrapped in silica monoliths prepared from glyceroxysilanes. *Journal of sol-gel science and technology* **31**, 343-348 (2004).

133 Wong, A. K. & Krull, U. J. Surface characterization of 3-glycidoxypropyltrimethoxysilane films on silicon-based substrates. *Analytical and bioanalytical chemistry* **383**, 187-200 (2005).

134 Tung, V. C., Kim, J., Cote, L. J. & Huang, J. Sticky interconnect for solution-processed tandem solar cells. *Journal of the American Chemical Society* **133**, 9262-9265 (2011).

135 Nardes, A. M. *et al.* Conductivity, work function, and environmental stability of PEDOT: PSS thin films treated with sorbitol. *Organic Electronics* **9**, 727-734 (2008).

136 Sayago, J., Soavi, F., Sivalingam, Y., Cicoira, F. & Santato, C. Low voltage electrolyte-gated organic transistors making use of high surface area activated carbon gate electrodes. *Journal of Materials Chemistry C* **2**, 5690-5694 (2014).

137 Forrest, S. R. The path to ubiquitous and low-cost organic electronic appliances on plastic. *Nature* **428**, 911-918 (2004).

138 Khodagholy, D. *et al.* NeuroGrid: recording action potentials from the surface of the brain. *Nature neuroscience* **18**, 310-315 (2015).

139 Jonsson, A. *et al.* Therapy using implanted organic bioelectronics. *Science Advances* **1**, e1500039 (2015).

140 Khodagholy, D. *et al.* High speed and high density organic electrochemical transistor arrays. *Applied Physics Letters* **99**, 163304 (2011).

141 Fromherz, P. Three levels of neuroelectronic interfacing. *Annals of the New York Academy of Sciences* **1093**, 143-160 (2006).

142 Lin, P. & Yan, F. Organic Thin‐Film Transistors for Chemical and Biological Sensing. *Advanced materials* **24**, 34-51 (2012).

143 Taylor, P. G. *et al.* Orthogonal patterning of PEDOT: PSS for organic electronics using hydrofluoroether solvents. *Adv. Mater* **21**, 2314-2317 (2009).

144 Ouyang, S. *et al.* Photolithographic patterning of highly conductive PEDOT: PSS and its application in organic light‐emitting diodes. *Journal of Polymer Science Part B: Polymer Physics* **52**, 1221-1226 (2014).

145 Williamson, A. *et al.* Localized neuron stimulation with organic electrochemical transistors on delaminating depth probes. *Advanced Materials* **27**, 4405-4410 (2015).

146 Tang, H. *et al.* Conducting polymer transistors making use of activated carbon gate electrodes. *ACS applied materials & interfaces* **7**, 969-973 (2014).

147 Kumar, P. *et al.* Effect of channel thickness, electrolyte ions, and dissolved oxygen on the performance of organic electrochemical transistors. *Applied Physics Letters* **107**, 77_71 (2015).

148 Kim, D.-H. *et al.* Dissolvable films of silk fibroin for ultrathin, conformal bio-integrated electronics. *Nature materials* **9**, 511 (2010).

149 Tee, B. C., Wang, C., Allen, R. & Bao, Z. An electrically and mechanically self-healing composite with pressure-and flexion-sensitive properties for electronic skin applications. *Nature nanotechnology* **7**, 825-832 (2012).

150 Kang, S.-K. *et al.* Bioresorbable silicon electronic sensors for the brain. *Nature* **530**, 71-76 (2016).

151 Kim, D.-H. *et al.* Stretchable and foldable silicon integrated circuits. *Science* **320**, 507-511 (2008).

152 Mannsfeld, S. C. *et al.* Highly sensitive flexible pressure sensors with microstructured rubber dielectric layers. *Nature materials* **9**, 859 (2010).

153 Lipomi, D. J., Tee, B. C. K., Vosgueritchian, M. & Bao, Z. Stretchable organic solar cells. *Advanced Materials* **23**, 1771-1775 (2011).

154 Lacour, S. P., Jones, J., Wagner, S., Li, T. & Suo, Z. Stretchable interconnects for elastic electronic surfaces. *Proceedings of the IEEE* **93**, 1459-1467 (2005).

155 Lacour, S. P., Chan, D., Wagner, S., Li, T. & Suo, Z. Mechanisms of reversible stretchability of thin metal films on elastomeric substrates. *Applied Physics Letters* **88**, 204103 (2006).

156 Xu, F. *et al.* Highly stretchable carbon nanotube transistors with ion gel gate dielectrics. *Nano letters* **14**, 682-686 (2014).

157 Lee, S.-K. *et al.* Stretchable graphene transistors with printed dielectrics and gate electrodes. *Nano letters* **11**, 4642-4646 (2011).

158 Wang, J. *et al.* Extremely stretchable electroluminescent devices with ionic conductors. *Advanced Materials* **28**, 4490-4496 (2016).

159 Matsuzaki, R. & Tabayashi, K. Highly stretchable, global, and distributed local strain sensing line using GaInSn electrodes for wearable electronics. *Advanced Functional Materials* **25**, 3806-3813 (2015).

160 Qin, D., Xia, Y. & Whitesides, G. M. Soft lithography for micro-and nanoscale patterning. *Nature protocols* **5**, 491-502 (2010).

161 Kim, T.-H. *et al.* Kinetically controlled, adhesiveless transfer printing using microstructured stamps. *Applied Physics Letters* **94**, 113502 (2009).

162 Moon, G. D. *et al.* Highly stretchable patterned gold electrodes made of Au nanosheets. *Advanced Materials* **25**, 2707-2712 (2013).

163 Hyun, W. J. *et al.* Screen printing of highly loaded silver inks on plastic substrates using silicon stencils. *ACS applied materials & interfaces* **7**, 12619-12624 (2015).

164 Jiang, J. *et al.* Fabrication of transparent multilayer circuits by inkjet printing. *Advanced Materials* **28**, 1420-1426 (2016).

165 Chen, W., Lam, R. H. & Fu, J. Photolithographic surface micromachining of polydimethylsiloxane (PDMS). *Lab on a Chip* **12**, 391-395 (2012).

166 Lee, J. N., Park, C. & Whitesides, G. M. Solvent compatibility of poly (dimethylsiloxane)-based microfluidic devices. *Analytical chemistry* **75**, 6544-6554 (2003).

167 Toepke, M. W. & Beebe, D. J. PDMS absorption of small molecules and consequences in microfluidic applications. *Lab on a Chip* **6**, 1484-1486 (2006).

168 Mukhopadhyay, R. (ACS Publications, 2007).

169 Jonsson, A. *et al.* Bioelectronic neural pixel: Chemical stimulation and electrical sensing at the same site. *Proceedings of the National Academy of Sciences* **113**, 9440-9445 (2016).

170 Lei, Y., Liu, Y., Wang, W., Wu, W. & Li, Z. Studies on Parylene C-caulked PDMS (pcPDMS) for low permeability required microfluidics applications. *Lab on a Chip* **11**, 1385-1388 (2011).

171 Zakhidov, A. A. *et al.* Hydrofluoroethers as orthogonal solvents for the chemical processing of organic electronic materials. *Advanced Materials* **20**, 3481-3484 (2008).

172 Fong, H. H. *et al.* Orthogonal Processing and Patterning Enabled by Highly Fluorinated Light‐Emitting Polymers. *Advanced Materials* **23**, 735-739 (2011).

173 Schwartz, G. *et al.* Flexible polymer transistors with high pressure sensitivity for application in electronic skin and health monitoring. *Nature communications* **4**, 1859 (2013).

174 Chortos, A. & Bao, Z. Skin-inspired electronic devices. *Materials Today* **17**, 321-331 (2014).

175 Chen, B. *et al.* Stretchable and transparent hydrogels as soft conductors for dielectric elastomer actuators. *Journal of Polymer Science Part B: Polymer Physics* **52**, 1055-1060 (2014).

176 Karadağ, E., Saraydin, D., Çetinkaya, S. & Güven, O. In vitro swelling studies and preliminary biocompatibility evaluation of acrylamide-based hydrogels. *Biomaterials* **17**, 67-70 (1996).

177 Sun, Y., Kumar, V., Adesida, I. & Rogers, J. A. Buckled and Wavy Ribbons of GaAs for High‐Performance Electronics on Elastomeric Substrates. *Advanced Materials* **18**, 2857-2862 (2006).

178 Hager, M. D., Greil, P., Leyens, C., van der Zwaag, S. & Schubert, U. S. Self‐healing materials. *Advanced Materials* **22**, 5424-5430 (2010).

179 Benight, S. J., Wang, C., Tok, J. B. & Bao, Z. Stretchable and self-healing polymers and devices for electronic skin. *Progress in Polymer Science* **38**, 1961-1977 (2013).

180 Li, Y., Chen, S., Wu, M. & Sun, J. Polyelectrolyte multilayers impart healability to highly electrically conductive films. *Advanced Materials* **24**, 4578-4582 (2012).

181 Blaiszik, B. J. *et al.* Autonomic restoration of electrical conductivity. *Advanced Materials* **24**, 398-401 (2012).

182 Shi, Y. *et al.* A conductive self-healing hybrid gel enabled by metal–ligand supramolecule and nanostructured conductive polymer. *Nano letters* **15**, 6276-6281 (2015).

183 Oh, J. Y., Kim, S., Baik, H.-K. & Jeong, U. Conducting Polymer Dough for Deformable Electronics. *Advanced Materials* **28**, 4455-4461, doi:10.1002/adma.201502947 (2016).

184 Ling, Q.-D. *et al.* Polymer electronic memories: Materials, devices and mechanisms. *Progress in Polymer Science* **33**, 917-978 (2008).

185 Petajajarvi, J., Mikhaylov, K., Roivainen, A., Hanninen, T. & Pettissalo, M. in *ITS Telecommunications (ITST), 2015 14th International Conference on.* 55-59 (IEEE).

186 Dupont, S. R., Novoa, F., Voroshazi, E. & Dauskardt, R. H. Decohesion kinetics of PEDOT: PSS conducting polymer films. *Advanced Functional Materials* **24**, 1325-1332 (2014).

187 Lee, I., Kim, G. W., Yang, M. & Kim, T.-S. Simultaneously enhancing the cohesion and electrical conductivity of PEDOT: PSS conductive polymer films using DMSO additives. *ACS applied materials & interfaces* **8**, 302-310 (2015).

188 Zhang, S. *et al.* Patterning of Stretchable Organic Electrochemical Transistors. *Chemistry of Materials* **29**, 3126-3132 (2017).

189 Liu, C., Qin, H. & Mather, P. Review of progress in shape-memory polymers. *Journal of Materials Chemistry* **17**, 1543-1558 (2007).

APPENDIX A – SUPPORTING INFORMATION OF ARTICLE SOLVENT-INDUCED CHANCES IN PEDOT:PSS FILMS FOR ORGANIC ELECTROCHEMICAL TRANSISTORS

Shiming Zhang, Prajwal Kumar, Amel Sarah Nouas, Laurie Fontaine, Hao Tang and Fabio Cicoira

Department of Chemical Engineering, Polytechnique de Montreal, Montreal, Québec, H3C3J7, Canada

Preparation of PEDOT:PSS films.

PEDOT:PSS films were prepared by spin coating from mixture containing a PEDOT:PSS aqueous dispersion (CleviosTM PH1000, Haraeus Electronic Materials), one high boiling point co-solvent among glycerol, sorbitol, ethylene glycol (EG) and dimethyl sulfoxide (DMSO), dodecyl benzene sulfonic acid (DBSA) and 3-glycidoxypropyltrimethoxysilane (GOPS), when applicable. Different amount of co-solvents where employed, as shown in FIG.1 and FIG.S1. In particular, for preparation of PEDOT:PSS films with glycerol as co-solvent, 20 ml of aqueous dispersion were mixed with 1 ml of glycerol, 100 μL of dodecyl benzene sulfonic acid (DBSA), and 200 μL of 3-glycidoxypropyltrimethoxysilane (GOPS) if applicable. The spin speed and spin time for PEDOT:PSS were fixed at 500 rpm for 15s and 1500 rpm for 45s unless otherwise specified. Film preparation was completed by an annealing on a hot plate at 140 °C for 60 min.

Sheet resistance and thickness measurements

Films were immersed in deionized water (Milli-Q Millipore, 18.2 MΩ cm at 25 °C). The sheet resistance was measured by a Jandel four-point probe equipment with a Keithley 2400 voltage–current source measure unit. Film thickness measurements were performed with a Dektak 150 profilometer.

X-ray photoelectron spectroscopy

X-ray photoelectron spectroscopy (XPS) was performed using a VG ESCALAB 3 MKII system with Mg-Ka X-ray source in ultra-high vacuum.

Fourier-transform infrared spectroscopy

To further investigate the effect of the water immersion on film chemical composition, we performed Fourier transform infrared (FTIR) spectroscopy (FIG. S4) of PEDOT:PSS films obtained from mixtures of Clevios^{TM} PH1000, DBSA and glycerol, without and with GOPS, before and after water exposure.

The spectra were acquired using a FTIR, Digilab FTS7000 FTIR spectrometer coupled to a UMA600 infrared microscope with a MCT detector.

For films without GOPS, a change in the spectra after water immersion was observed, suggesting a composition change of the film (e.g., loss of PSS, film delamination) after water exposure. The spectra of films containing GOPS are identical before and after water immersion, which confirms that the films are not affected by water immersion.

Analytical balance weighing experiment

To determine the conductivity enhancement agent to PEDOT:PSS ratio we performed a weighing experiment with a 5-digit analytical balance (Sartorius 1712). As a first step, we measured the densities of the processing mixtures in order to know the weight of the amount of solution used for spin coating. Density measurements were performed with an Anton Paar density meter (DMA 4500 M). Each measurement was performed three times (the values are shown in Table. S2). The total weight of suspensions used for spin-coating is about 0.25 g for all films (as shown in Table S2). The films were weighted right after spin coating (wet films) and after a thermal treatment of 30 minutes at 140 °C (dry films). Wet film processed from all the solutions show similar weights (FIG. S3). Mixing Clevios^{TM} PH1000 with 5 v/v% of glycerol or with 1 v/v% GOPS does not significantly affect the film weight. After baking, the weight is reduced by about a factor of two for all films. Among the dry films, the one processed from a mixture containing both GOPS and glycerol experiences the smallest weight loss. These results indicate that, when both GOPS and glycerol are present in the mixture, part of the components of the mixture remains in the film after baking. However, care should be taken in interpreting these results, as the film weight is close to the detection limit of the balance.

OECT Fabrication and characterization

OECTs were fabricated on hexamethyldisilazane primer treated glass wafers. Ti (5 nm)/Au (40 nm) contact pads were patterned with photolithography (AZ 5214-E photoresist and MF 319 developer). PEDOT:PSS channels with a width of 2 mm and a length of 8 mm were patterned with a parylene lift-off technique.

The electrolyte (0.01 M NaCl) regions were defined by glass tubes attached to the substrate with polydimethylsiloxane (PDMS). The transistor characteristics were evaluated using an Agilent B2900 A source measure unit controlled by Labview software. OECTs were characterized by measuring source–drain current (I_{ds}) versus time at a constant drain voltage (V_{ds}) while pulsing the gate voltage (V_{gs}).

Figures

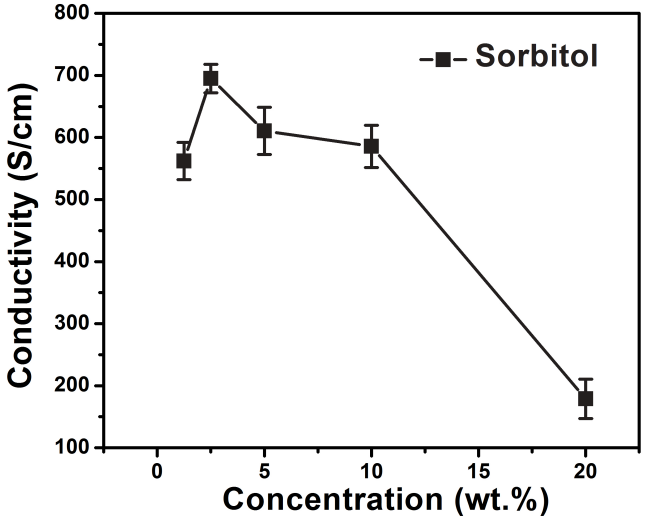

FIGURE. S1. Conductivity of the PEDOT:PSS films with 0.5 v/v% DBSA and different concentrations of sorbitol. The error bar stands for standard deviation of three samples.

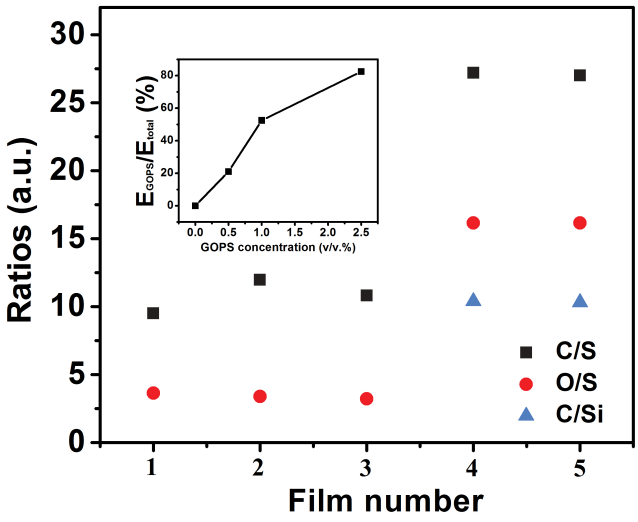

FIGURE. S2. C/S, O/S and C/Si ratios calculated from XPS measurements for films of 1: PEDOT:PSS; 2: PEDOT:PSS/Glycerol (5 v/v%); 3: PEDOT:PSS/Glycerol (5 v/v%) after water immersion; 4: PEDOT:PSS/Glycerol (5 v/v%): GOPS (2 v/v%); 5: PEDOT/PSS/Glycerol (5 v/v%)/GOPS (2 v/v%) after water immersion. The inset shows the calculated element signal (sum of C, O and Si) from GOPS (E_{GOPS}) with respect to the total element signal obtained from the XPS measurement (E_{total}) for mixtures of PEDOT:PSS/glycerol (5 v/v%) with different GOPS concentrations.

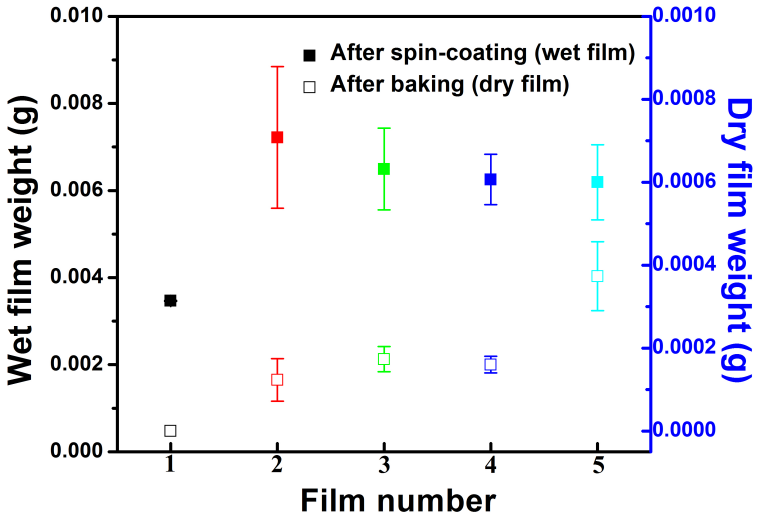

FIGURE. S3. 5-digit balance measurements for films obtained from 1: DI water; 2: PEDOT:PSS; 3: PEDOT:PSS/DBSA (0.5 v/v%); 4: PEDOT:PSS/DBSA (0.5 v/v%):Glycerol (5 v/v%); 5: PEDOT:PSS/DBSA (0.5 v/v%)/Glycerol (5 v/v%)/GOPS (1 v/v%). The solid squares indicate the wet film weight (left) measured immediately after spin-coating. The open squares indicate the dry film weight (right) measured after a thermal treatment of 30 minutes at 140 °C. The error bar stands for standard deviation of three samples.

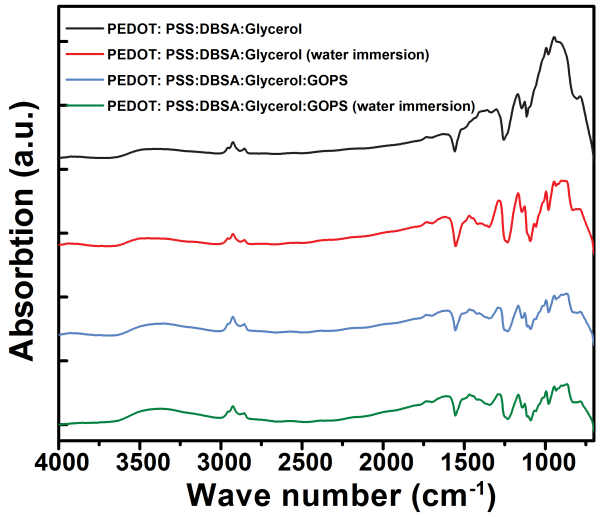

FIGURE. S4. FTIR spectra of films processed from from PEDOT:PSS/DBSA (0.5 v/v%):Glycerol (5 v/v%), and PEDOT:PSS/DBSA (0.5 v/v%)/Glycerol (5 v/v%)/GOPS (1 v/v%) mixtures before and after water immersion.

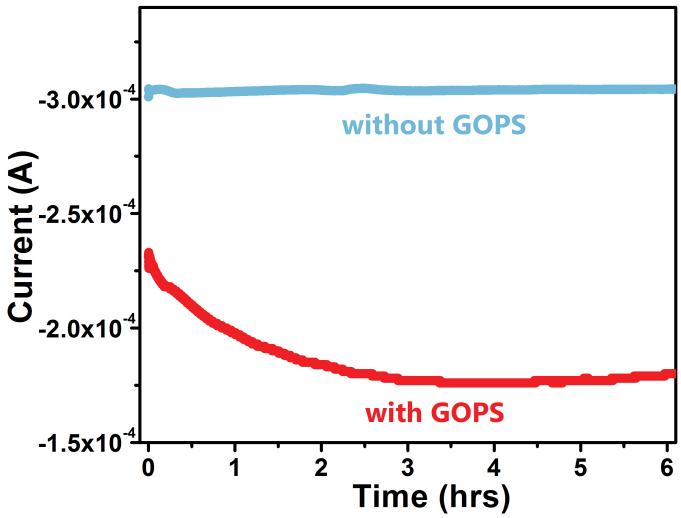

FIGURE. S5. Two-terminal (source-drain) electrical measurements of patterned PEDOT:PSS films (channel width of 2 mm and length of 8 mm) with and without 1 v/v% GOPS. The thickness of the film with and without 1 v/v% GOPS is about 350 nm and 150 nm, respectively. The spin-coating speeds for both films are 500 rpm for 10s and 1500 rpm for 45s.

TABLE. S1. Sheet resistance of PEDOT:PSS films treated with 0.5 v/v% DBSA and different secondary dopants at the optimal concentration shown in FIG. 1/FIG. S1, and thickness decrease ratio for thin and thick PEDOT:PSS films.

	Sheet resistance[1] (ohm sq^{-1})	Sheet resistance[2] (ohm sq^{-1})	Decrease ratio[3a]	Decrease ratio[3b]
Sorbitol	99.6	135.9	0.44 ± 0.02	0.57 ± 0.02
EG	122.3	158.5	0.56 ± 0.07	0.52 ± 0.04
DMSO	113.2	131.7	0.63 ± 0.07	0.60 ± 0.02
Glycerol	104.2	131.3	0.40 ± 0.06	0.41 ± 0.01

1: before water immersion; 2: after water immersion for 10 min;

3: Decrease ratio = thickness after 10 min water immersion/initial thickness:

a) for ca.150 nm thin films spin-coated at 500 rpm for 10s and 1500 rpm for 45s;

b) for ca.400 nm thick films spin-coated at 500 rpm for 20s.

TABLE. S2. Density of PEDOT:PSS dispersion mixed with different co-solvents, and volume/total weight/weight loss (of the solutions during spin-coating). The concentration of DBSA, glycerol and GOPS is 0.5 v/v%, 5 v/v%, and 1 v/v%, respectively.

Mixtures	PEDOT:PSS	PEDOT:PSS: DBSA	PEDOT:PSS: DBSA: Glycerol	PEDOT:PSS: DBSA: Glycerol: GOPS
Density (g/ml)	1.00249 ± 3.8E-5	1.00272 ± 1.3E-5	1.01835 ± 1.0E-5	1.04510 ± 1.1E-2
Volume (ml)	0.25	0.25	0.25	0.25
Total weight (g)	0.25062	0.25068	0.25459	0.26128
Weight Loss (g)	0.24340	0.24419	0.24834	0.25509

APPENDIX B –SUPPORTING INFORMATION OF ARTICLE WATER STABILITY AND ORTHOGONAL PATTERNING OF FLEXIBLE MICRO-ELECTROCHEMICAL TRANSISTORS ON PLASTIC

Shiming Zhang[a], Elizabeth Hubis[a], Camille Girard[a], Prajwal Kumar[a], John DeFranco[b] and Fabio Cicoira*[a]

[a] Department of Chemical Engineering, Polytechnique Montréal, Montréal, Québec H3C3J7, Canada. E-mail: Fabio.cicoira@polymtl.ca

[b] Orthogonal, Inc., 1999 Lake Avenue, Rochester, NY 14650, USA.

Experimental details:

Polyethylene terephthalate (PET) substrates were cleaned by sequential sonication in acetone, and isopropanol, and de-ionized (DI) water (10 min for each step), dried using nitrogen flow and laminated on a cleaned glass wafer pre covered with a 300 μm polydimethylsiloxane (PDMS) layer (spin-coated at 500 rpm for 40 s), which served as an adhesive layer to ensure flatness and rigidity during the successive patterning steps. Au source/drain contacts (40 nm thickness with 4 nm Cr/Ti as adhesion layer), with distances ranging from 100 μm to 5 μm, were patterned by photolithography, metal deposition and lift-off using SPR 220.3 (MicroChem) as the photoresist (ca. 2.5 um), AZ-726 (Micro Chemicals) as the developer (4 min immersion) and PG 1165 (MicroChem) as the stripper. PEDOT:PSS OECT channels were patterned using a subtractive process consisting of film deposition, photolithography, etching and lift off. PEDOT:PSS films were first deposited on the Au-patterned PET substrates after a 10 min UV-ozone treatment of the substrate. The films were spin coating for a mixture containing filtered Clevios PH1000 (previously filtered through a 0.45 um cellulose syringe filter), the conductivity enhancer glycerol (5 v/v.%) and occasionally dodecylbenzenesulfonic acid (DBSA, 0.5 v/v.%) and 3-glycidoxypropyltrimethoxysilane (GOPS, 1 v/v.%). Prior to spin coating the mixtures were homogenized in a planetary Thinky Mixer (ARM-310) for 5 min at 2000 rpm. After spin coating, the films were immediately dried on a hotplate at 100 °C for 20 min. The negative-tone OSCoR 4000 fluorinated photoresist (Orthogonal, Inc.) was then spin-coated on the PEDOT:PSS film (1000 rpm for 30 seconds), baked on a hotplate (90 °C, 1 min) and exposed to the UV light of the

mask aligner (for ca. 1 second) through a photomask. After a post-exposure baking (85 °C, 1 min), the unexposed photoresist was developed using a double-puddle method (30 seconds etch): the developer (Developer 103, Orthogonal, Inc.) was dropped on the sample covered with the photoresist and left on it for 25 s to react, then the spin-coating was started to remove the developer. This process was repeated two times. The unprotected PEDOT:PSS was then etched by an oxygen reactive ion etching (RIE) plasma for 1 min (150W, 125 mTorr and 10 standard cubic centimeters per minute, sccm) and the exposed photoresist remaining on the patterned PEDOT:PSS film was removed by a three minutes stripping process (Stripper 700, Orthogonal, Inc.). Subsequently, a further photolithography step (same procedure as mentioned above) was used to cover the Au electrodes with photoresist in order to prevent direct contact between Au and the electrolyte. At the end of the fabrication process, the devices were soaked in DI water for 10 min to remove water soluble contaminants from the PEDOT:PSS films. This procedure yielded transistors featuring channel lengths ranging from 5 µm to 100 µm and channel with of 80 µm and 400 µm. Finally, the PET foil is peeled-off PET from PDMS/glass substrates. For device characterizations, a glass well was attached on the channel area using PDMS layer to confine the electrolytes and then the samples were placed in an oven at 80 °C for 20 min to solidify the PDMS. The OECTs were characterized by recording source–drain current (I_{ds}) versus time (t), versus drain voltage (V_{ds}) or gate voltage (V_g). A high surface area (1000~2000 m^2g^{-1}) activated carbon was used as the gate electrode. Before depositing PEDOT:PSS films on glass (CORNING) substrates, the glasses were pre-cleaned with Acetone, IPA and DI water in sonication bath for 10-min each, followed by a UV treatment for 10-min. For the CV measurements, we used a three electrode configuration where a PEDOT:PSS film on plastic acted as the working electrode, Pt foil as the counter electrode and aq. Ag/AgCl as the reference electrode. The scan rate was 100 mV/s.

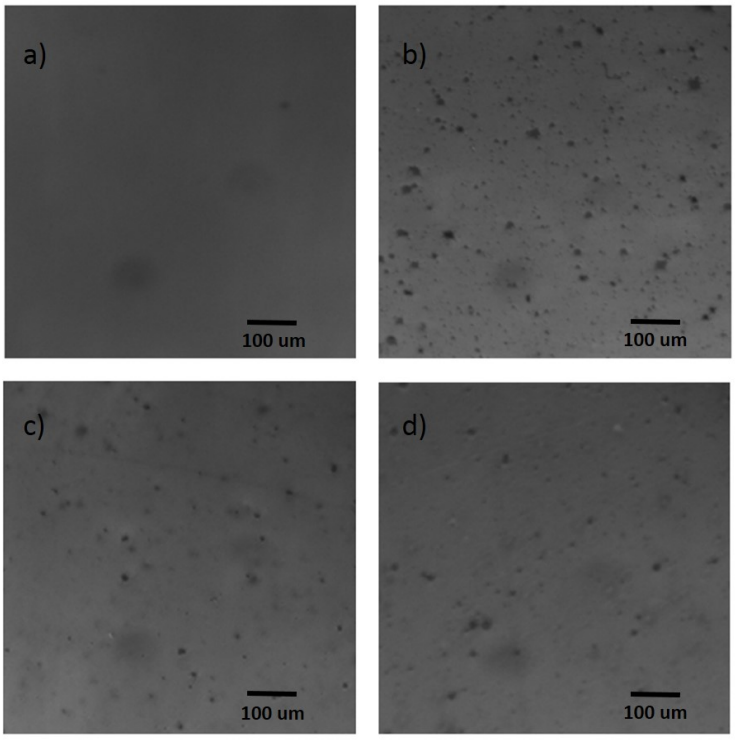

Figure. S1. Film morphologies of a) PEDOT:PSS: 5 v/v.% glycerol on glass substrate; b) pure PET substrate; c) PEDOT:PSS: 5 v/v.% glycerol on PET substrate; and d) PEDOT:PSS: 5 v/v.% glycerol on PET substrate after 1 day water immersion. PEDOT:PSS: 5 v/v.% glycerol film on glass is not shown since it delaminated after 1 day water immersion.

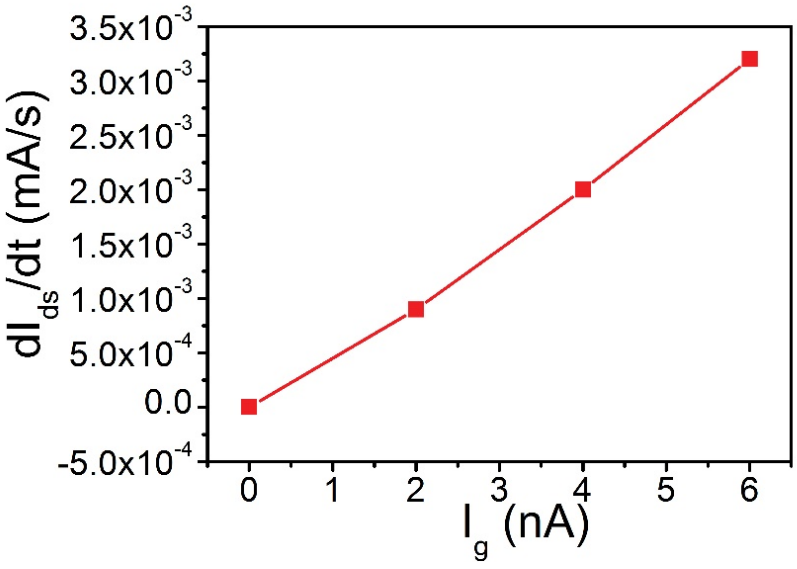

Figure. S2. Derivative of I_{ds} with respect to time as a function of I_g. The line is a fit to Eq. (1).[1] The data are from the OECT with channel length (L) of 100 um and a channel width of 400 μm. The V_{ds} was -0.2 V. Hole mobility of PEDOT:PSS on plastic can be obtained via Eq. (2) and (3). The extracted mobility is 0.25 $cm^2V^{-1}S^{-1}$.

$$I_{ds}(t, I_g)=I_{ds0}-I_g(f+\frac{t}{\tau_e}) \quad (1)$$

$$dI_{ds}/dt=-\frac{Ig}{\tau_e} \quad (2)$$

$$\tau_e=L^2/\mathbf{u}V_{ds} \quad (3)$$

where t is the time, I_{ds0} is the source-drain current prior to application of a gate current (I_g), f is a proportionality constant to account for the spatial non-uniformity of the de-doping process, τ_e is the electronic transit time, L is the channel length of OECT and V_{ds} is the source-drain voltage. u denotes the hole mobility of PEDOT:PSS film.

Table.S1. Changes in thickness, sheet resistance and conductivity of PEDOT:PSS films on plastic after water immersion. The PEDOT:PSS films were deposited by spin-coating a mixture containing 20 ml Clevios PH1000 and 1 ml glycerol at 500 rpm for 10s and 1500 rpm for 40s.

Films on plastic	Before water immersion	After 1 day water immersion
Thickness (nm)	142±8	118±11
Sheet resistance (ohm/sr)	115±3	150±12
Conductivity (S/cm)	614±20	567±22

APPENDIX C – SUPPORTING INFORMATION OF ARTICLE PATTERNING OF STRETCHABLE ORGANIC ELECTROCHEMICAL TRANSISTORS

Shiming Zhang, Elizabeth Hubis, Gaia Tomasello, Guido Soliveri, Prajwal Kumar, and Fabio Cicoira*

Department of Chemical Engineering, Polytechnique Montreal, Montreal, Quebec H3C 3A7, Canada.

Email: fabio.cicoira@polymtl.ca

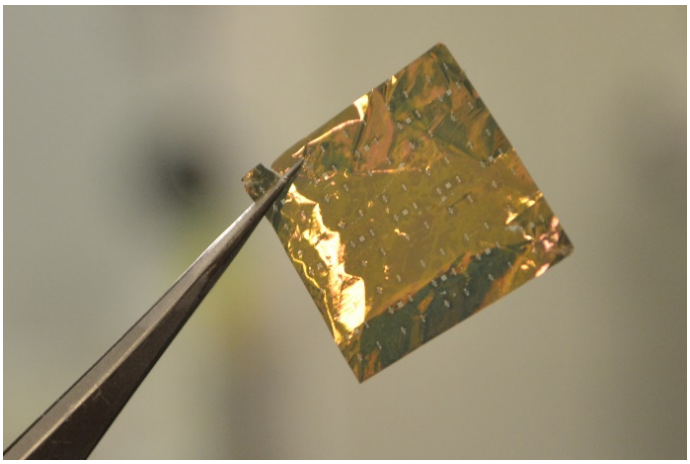

Figure S1. Optical image of a delaminated Parylene film (2 um) after Au deposition on PDMS.

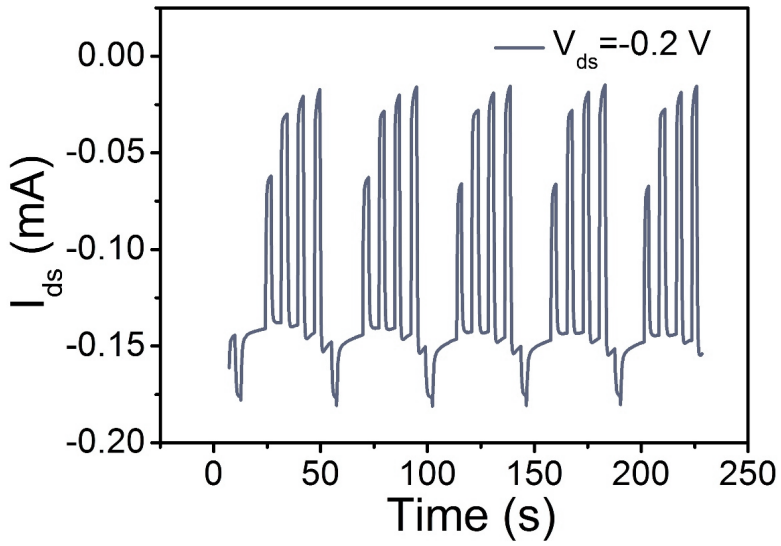

Figure S2. Transient behavior of micro-OECTs on PDMS while pulsing the V_{gs} from -0.2 to 0.8 V in 0.2 V steps. The pulsing time is 2.5 seconds and the rest time is 5 seconds for each period. The data are from micro-OECT with a channel length of 10 um and a channel width of 4000 μm. The V_{ds} is fixed at -0.2 V. The PEDOT:PSS film is processed from 5 v/v.% glycerol and 1 v/v.% Capstone FS-30. The film thickness is about 400 nm.

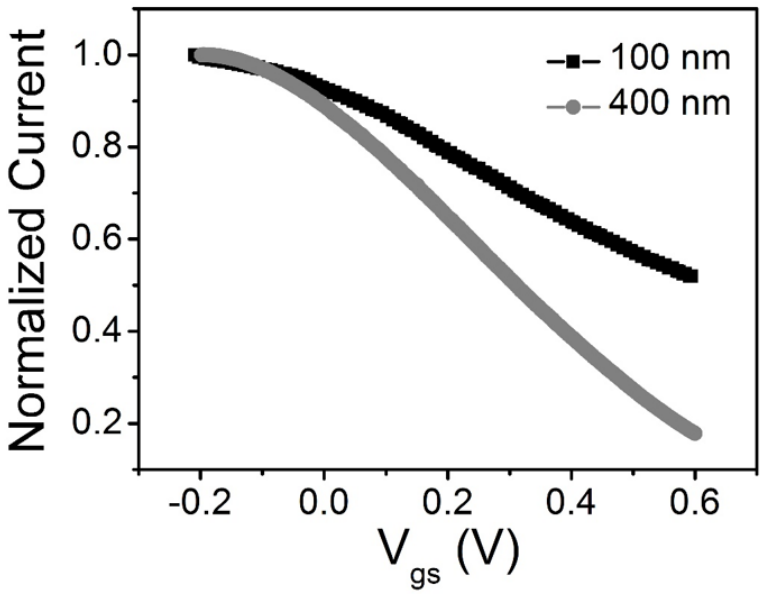

Figure S3. Transfer curves of OECTs using 100 nm and 400 nm thick PEDOT:PSS films as channels. The channel length is 0.8 mm and channel width is 0.2 mm. The ON/OFF ratio is about 2 for 100 nm thick films, and about 400 nm thick film shows ON/OFF ratio of 10. Increasing the channel thickness leads to an increase in ON/OFF ratio, attributable to the increase of the ON current.

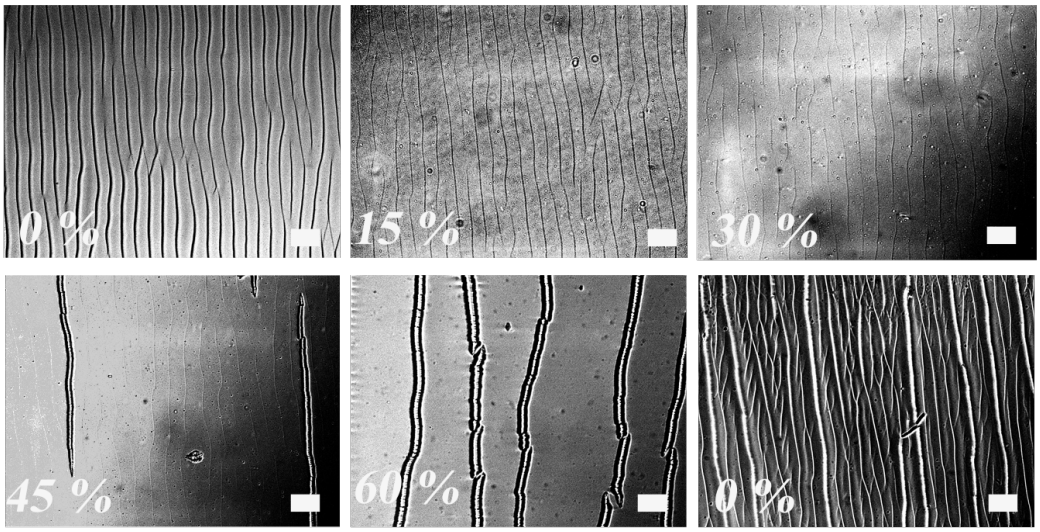

Figure S4. Optical images of 150 nm PEDOT: PSS film (PEDOT:PSS with 5 v/v.% glycerol and 1 v/v.% Capstone FS-30) at different strains. The PEDOT:PSS film was spin-coated on a 30% pre-stretched PDMS substrate with a thickness of 300 um.

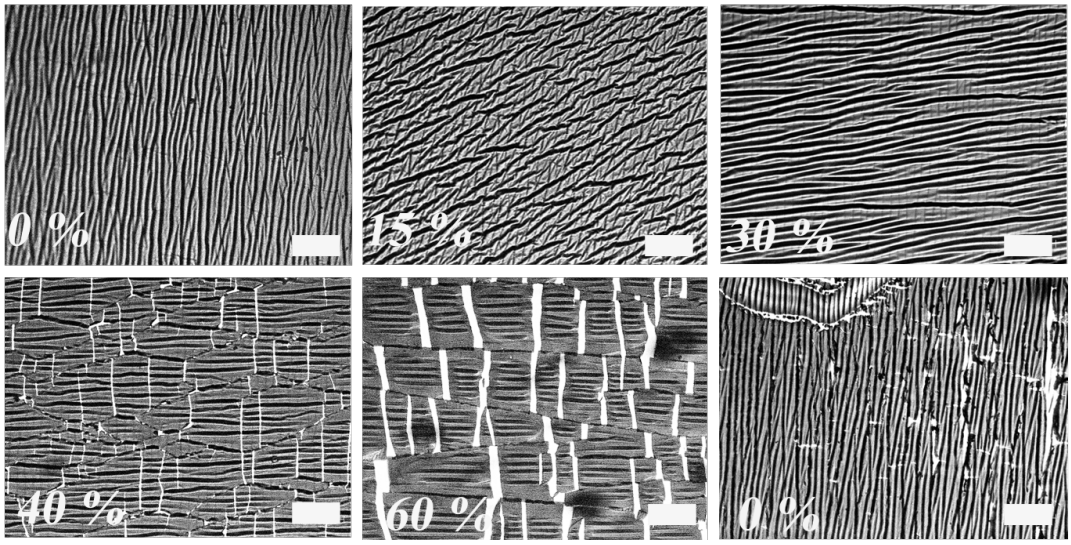

Figure S5. Optical images of 4 nm Ti/ 40 nm Au film at different strains. The Ti/Au film was E-beam deposited on 30% pre-stretched PDMS substrate with a thickness of 300 um.

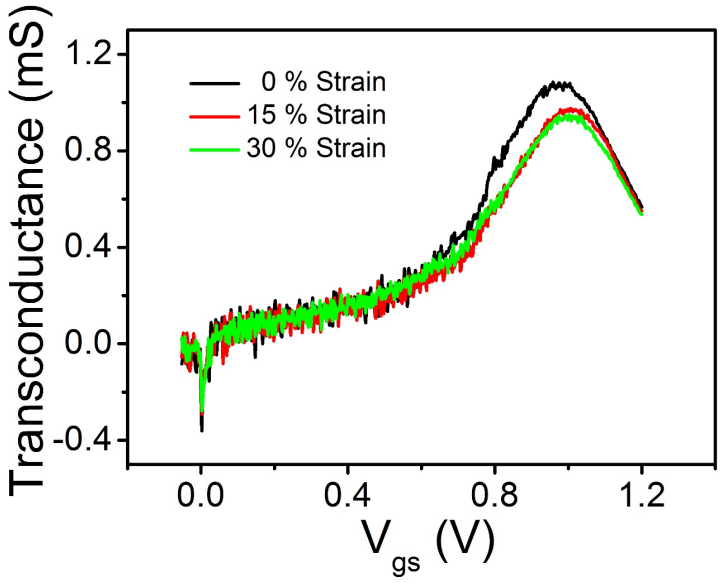

Figure S6. Transconductance changes of OECTs obtained on a 30% prestretched PDMS when stretched from 0 to 30% strain.

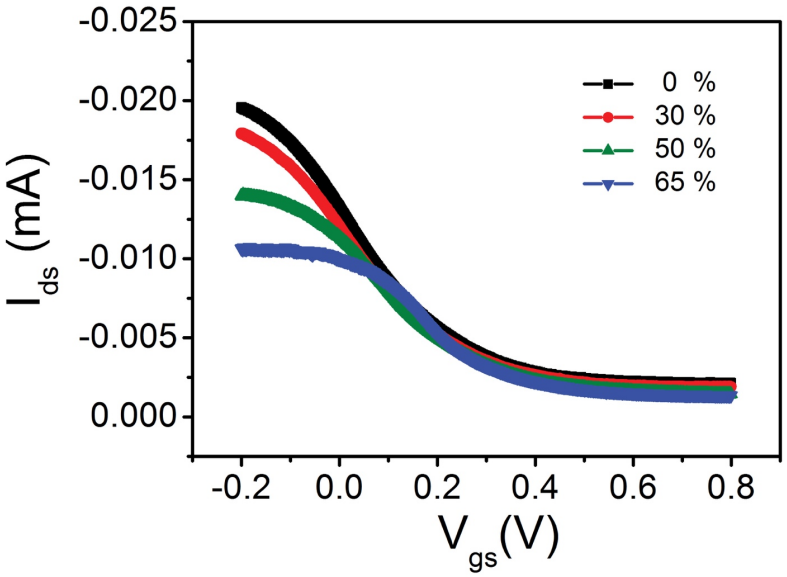

Figure S7: Transfer curves of stretchable OECT at different strains. NaCl (0.01M) solution was used as electrolyte, EGaIn was drop-casted on source and drain electrodes to ease the probing. The channel length is 8 mm by 2 mm.

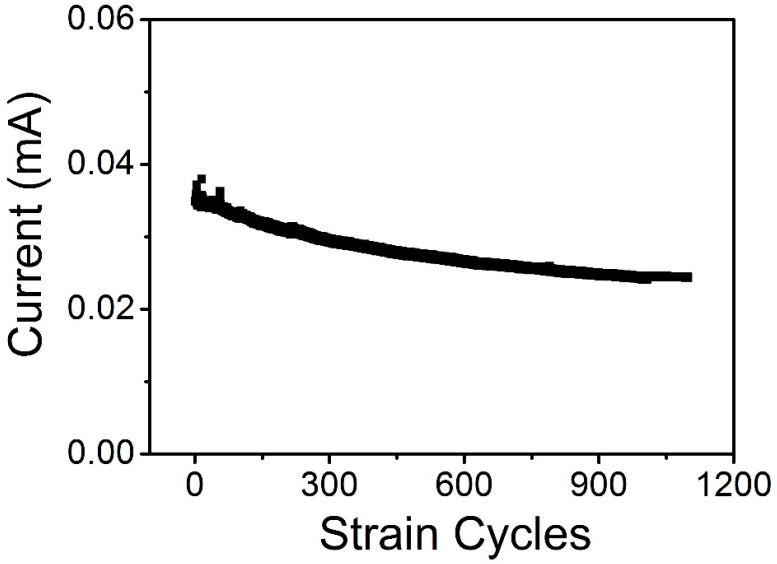

Figure S8. Current change versus number of strain cycles for PEDOT:PSS films from 0 to 30% strain, for 1000 cycles. The PEDOT:PSS film was obtained on 30% pre-strained PDMS. Within the first 500 strain cycles, the film lost 25% of the initial current, which successively remained stable for the subsequent 500 cycles (with 8% of current loss).

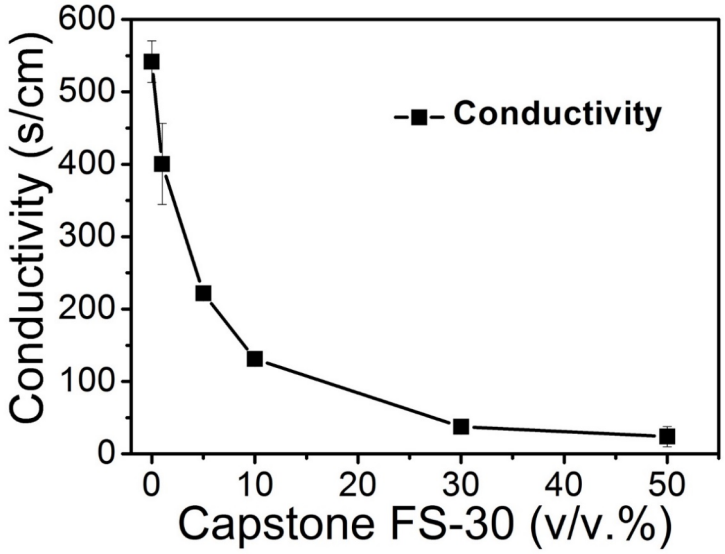

Figure S9. Conductivity change of PEDOT:PSS films processed with different Capstone FS-30 concentrations. 5 v/v% glycerol was added as conductivity enhancer. The resistivity is extracted with a four-point probe by using the following equation: $\rho/d = 4.5324 \times V/I$ where ρ is the resistivity of the film, d is the film thickness, I is the current and V is the voltage. The conductivity σ can then be extracted using the relation of $\sigma = 1/\rho$.

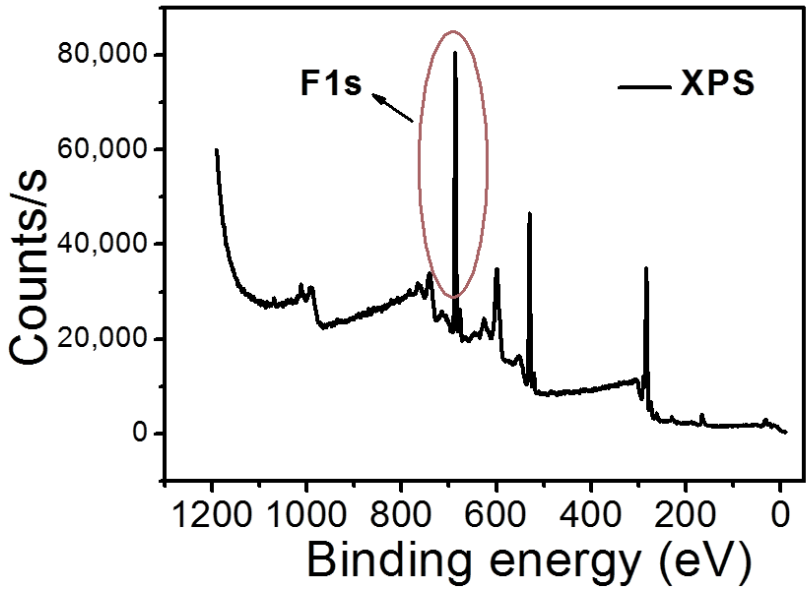

Figure S10. XPS spectra of PEDOT:PSS film processed with Capstone FS-30 (10 v/v%) on glass substrates after baking at 140℃ for 30 mins. The F1s peak is from the fluorine species of the Capstone FS-30, which indicates its presence in the film after baking. XPS of PEDOT:PSS films was performed using a VG ESCALAB 3 MKII system with Mg-Ka X-ray source in an ultra-high vacuum.

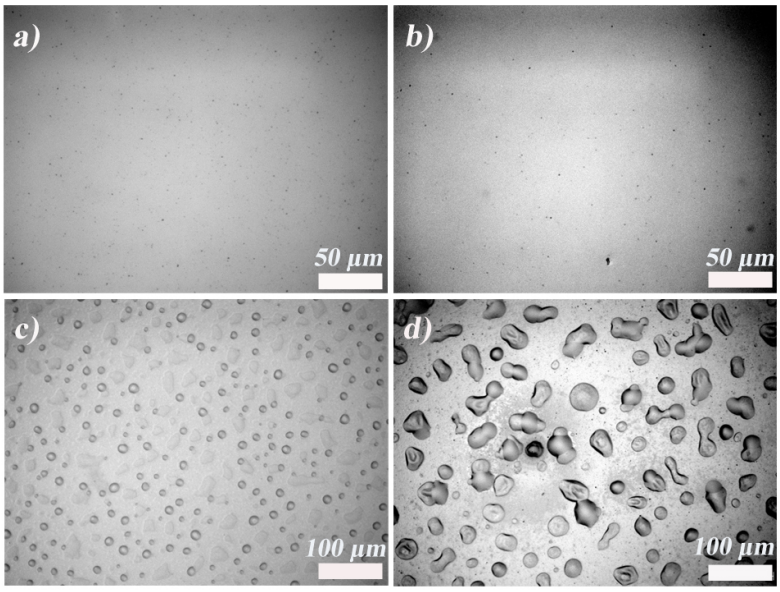

Figure S11. Optical images of PEDOT:PSS films with different Capstone FS-30 concentrations on glass substrates. a) 1 v/v%; b) 5 v/v%; c) 10 v/v% and d) 50 v/v%. 5 v/v% glycerol was added as a conductivity enhancer.

APPENDIX D – SUPPORTING INFORMATION OF ARTICLE WATER-ENABLED HEALING OF CONDUCTING POLYMER FILMS

Shiming Zhang and Fabio Cicoira*

Department of Chemical Engineering, Polytechnique Montreal, Montreal, Quebec H3C 3A7, Canada.

Email: fabio.cicoira@polymtl.ca

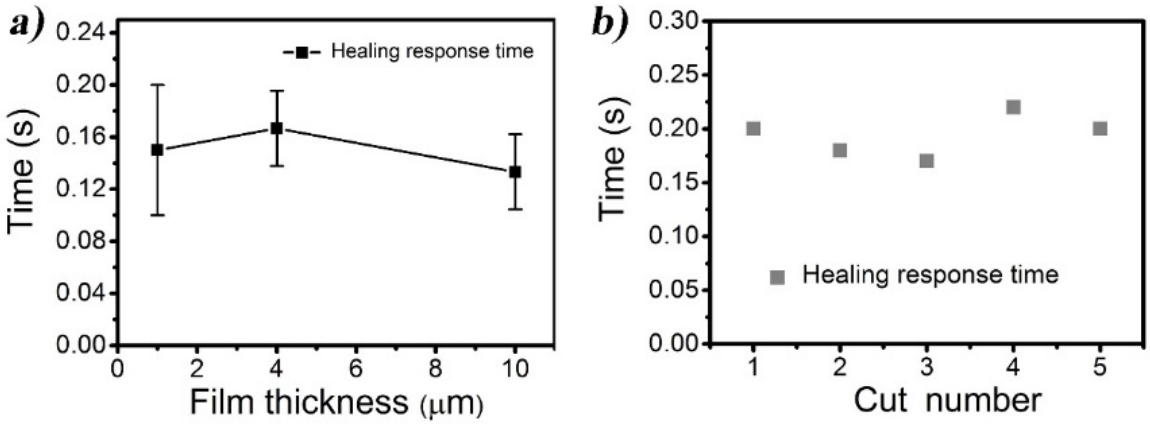

Figure S1. Healing of PEDOT:PSS films with different thicknesses and its repeatability. a) Healing response time comparison for PEDOT:PSS films (5 v/v% glycerol) with various thicknesses (the error bar represents standard deviation for three samples). Films of thickness less than 1 μm failed to instantly recover the current after the addition of water. b) Current healing time after each cut for five repeatable cuts. No significant increase of the healing time was observed.

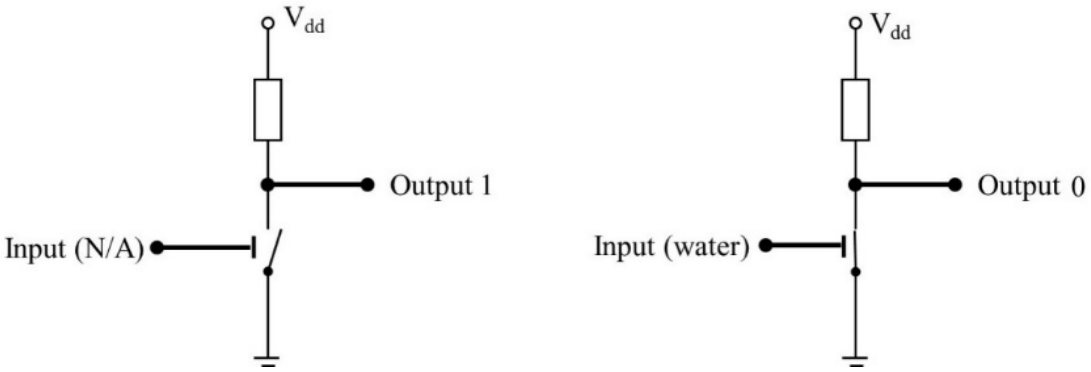

Figure S2. Water-healable PEDOT:PSS films as non-erasable inverters in circuits. The high output (1) changes to low output (0) after exposing the circuit to water.

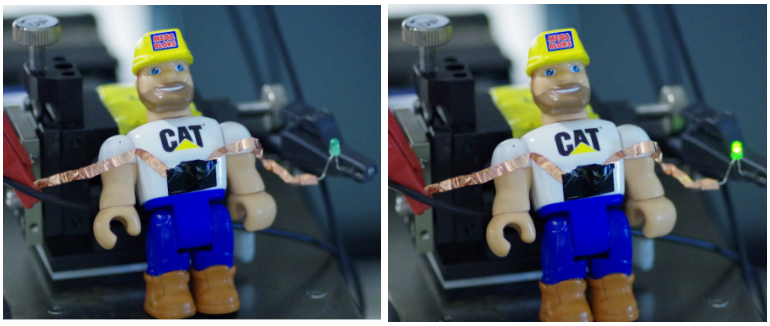

Figure S3. Demonstration of water-healable PEDOT:PSS film as water-enabled electric switch for life jacket or marine rescue. A PEDOT:PSS film was pasted on the toy man. Damaging the film with a razor blade interrupted the current flow (left) and the LED switched off. Once PEDOT:PSS was in contact with water (right), the electrical connection recovered and, as a result, switched the LED on.

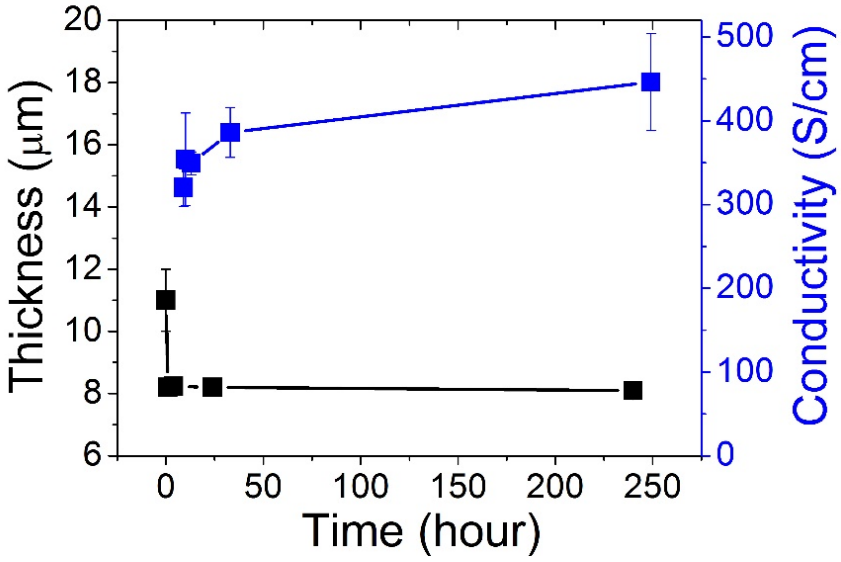

Figure S4. Thickness and conductivity change of PEDOT:PSS films (with 5 v/v% glycerol) when immersed in DI water for 10 days. The film thickness and conductivity after water immersion were measured after baking the wetted film on a hot plate at 120 °C for 3 minutes. The error bar represents standard deviation for three time measurements at different places of the sample.

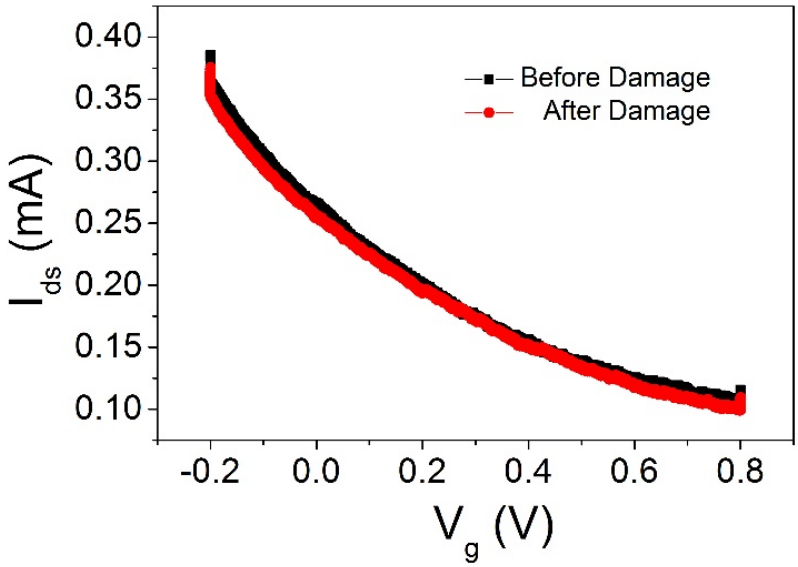

Figure S5. Transfer curves of OECTs with wet PEDOT:PSS film as channel. The PEDOT:PSS channel thickness is about 7 um. The channel width is 4 mm, and channel length is 8 mm. A glass well was pasted on top of the channel (with PDMS glue) to confine the electrolyte (10^{-2} M NaCl aqueous solution). Ag wire was immersed in the solution and used as the gate electrode. EGaIn was used as contact for source and drain electrodes. Before damage, the OECT source-drain current (I_{ds}) was measured as function of the gate voltage (V_g) using Agilent B2902A source-measure unit controlled by Labview software. Then, the channel was scratched in situ with a sharp tungsten tip and measured again. The source-drain voltage (V_{ds}) was fixed at 0.1 V.

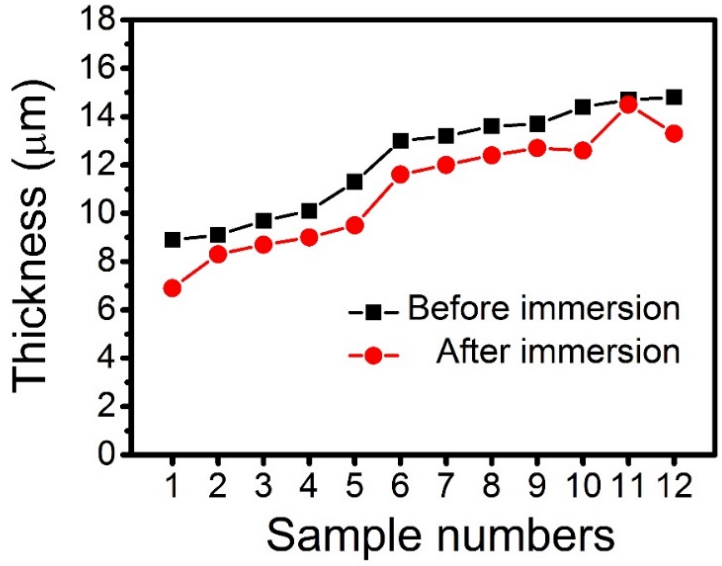

Figure S6. Thickness of PEDOT:PSS films (with 5 v/v% glycerol), with thickness ranging from 1 μm to 12 μm, before (black) and after water immersion for 1 minute (red). The film thickness after water immersion was measured after baking the wetted film on a hot plate at 120 °C for 3 minutes.

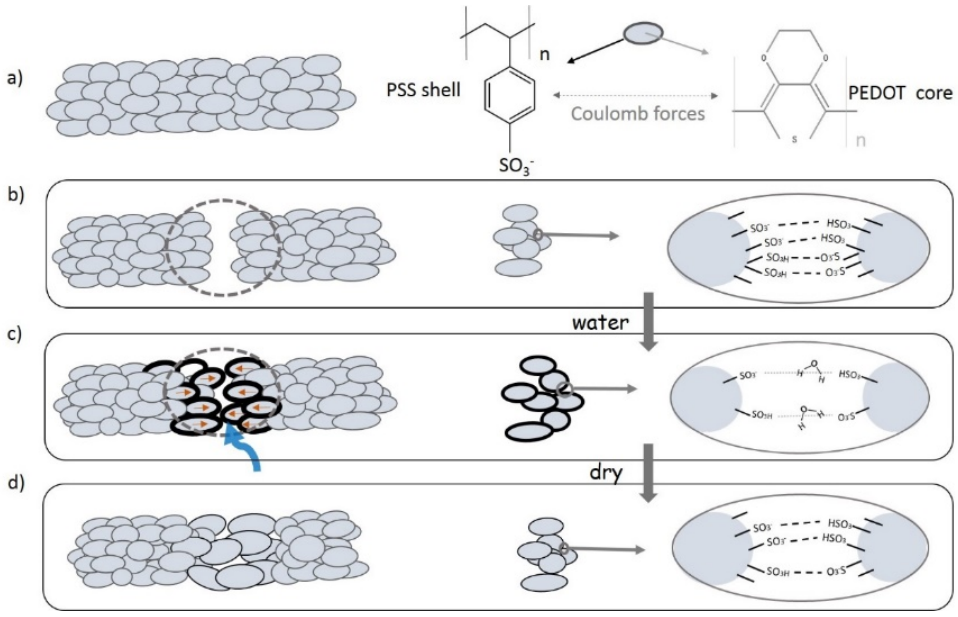

Figure S7. Tentative mechanism of water-enabled healing of PEDOT:PSS film. a) The PEDOT:PSS film consists of grains of PEDOT-rich core and PSS-rich shell linked by coulomb forces; b) the grains are connected by hydrogen bonds between the PSS^- shells; c) water induces PSS^- swelling (indicated by a thicker PSS^- shell) and the hydrogen bonds between the grains break increasing the grains' mobility; d) gaps are healed due to grain shifts and the hydrogen bonds are reformed.

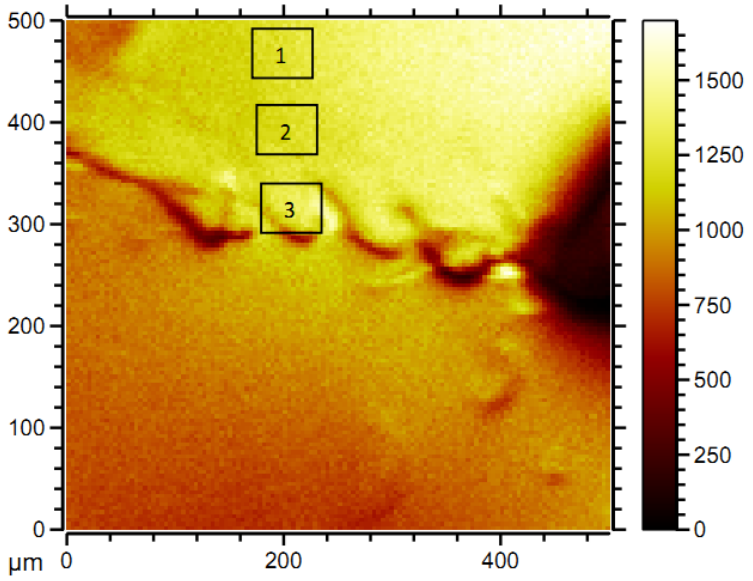

Table I Intensity detected for selected ions from regions extracted from mapping 1

Center of mass (u)	Assignment	Raw intensity (counts)			Intensity normalized to total ion intensity		
		Region 1	Region 2	Region 3	Region 1	Region 2	Region 3
15.9953	O-	22287	21903	21599	1.43E-01	1.44E-01	1.29E-01
23.9999	C_2-	3813	3639	3864	2.45E-02	2.40E-02	2.30E-02
25.0079	C_2H-	11230	11341	12434	7.21E-02	7.47E-02	7.40E-02
31.9713	S-	2599	2428	2514	1.67E-02	1.60E-02	1.50E-02
34.9682	Cl-	667	714	760	4.28E-03	4.70E-03	4.52E-03
39.9939	C_2O-	227	151	183	1.45E-03	9.96E-04	1.09E-03
43.9710	SiO-	19	18	13	1.22E-04	1.19E-04	7.74E-05
43.9710	CS-	19	18	13	1.22E-04	1.19E-04	7.74E-05
47.9647	SO-	1287	1262	1238	8.26E-03	8.31E-03	7.37E-03
55.9700	C_2S-	69	48	62	4.43E-04	3.16E-04	3.69E-04
59.9651	SiO_2-	63	64	94	4.05E-04	4.22E-04	5.60E-04
63.9598	SO_2-	1845	1770	1820	1.18E-02	1.17E-02	1.08E-02
67.9705	C_3S-	34	17	24	2.18E-04	1.12E-04	1.43E-04
79.9566	SO_3-	5226	4906	5827	3.36E-02	3.23E-02	3.47E-02
83.9996	C_4H_4S-	15	11	11	9.64E-05	7.25E-05	6.55E-05
110.0074	C_6H_6S-	6	4	6	3.85E-05	2.63E-05	3.57E-05
141.0005	C_6H_5SO_2-	2	2	2	1.28E-05	1.32E-05	1.19E-05
155.9849	C_6H_4SO_3-	367	297	361	2.35E-03	1.96E-03	2.15E-03

Figure S8. Time of flight secondary ion mass spectroscopy (TOF-SIMS) of PEDOT:PSS films. The top images shows the total ion mapping of the PEDOT:PSS film (500 µm x 500 µm). Regions 1, 2 and 3 indicate the areas from which the spectra were extracted and for which selected ion intensities are presented in Table I. Region 3 is the healed region. The highlighted ion $C_6H_5SO_2^-$ is the characteristic ion for PEDOT.

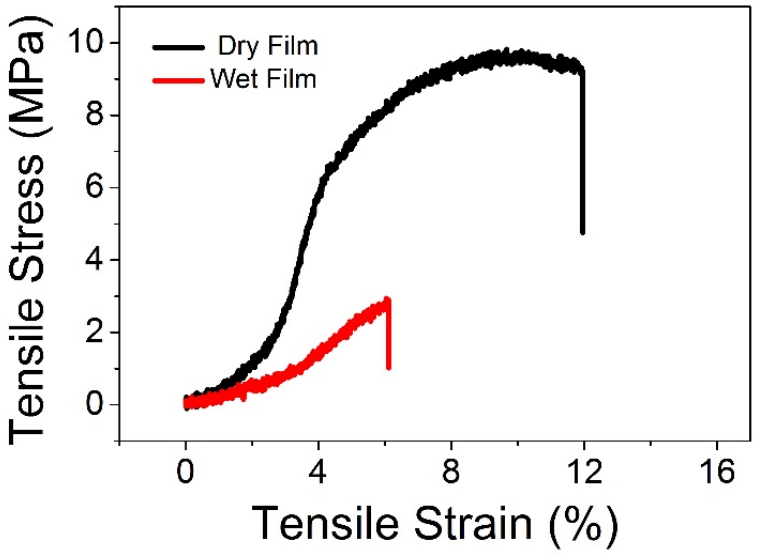

Figure S9. Strain-stress curves of PEDOT:PSS films before and after wetting. Wetting the PEDOT:PSS film causes a dramatic decrease in film tensile strength. The sample length is 1 cm and the strain rate is 1 mm/min. The thickness of PEDOT:PSS film is about 10 μm.

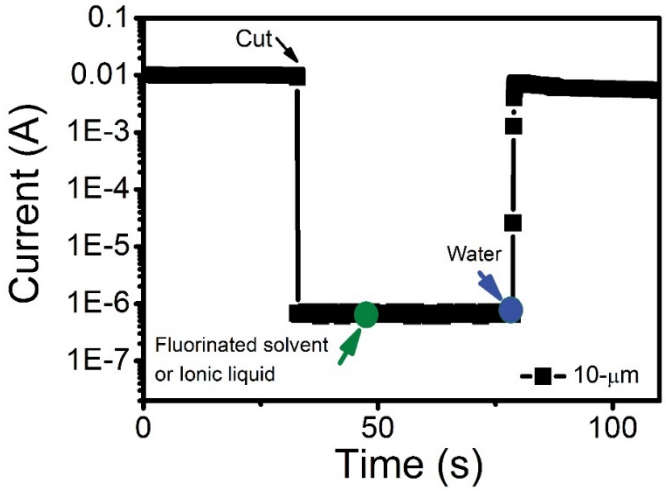

Figure S10. Fluorinated solvent and ionic liquid EMIM-TFSI failed to heal PEDOT:PSS films. Current change of a damaged PEDOT:PSS film (5 v/v% glycerol, 10 μm) after adding fluorinated solvent or ionic liquid EMIM-TFSI (green arrow), and then adding water (blue arrow) at the same damage place. The current remained stable after water evaporation.

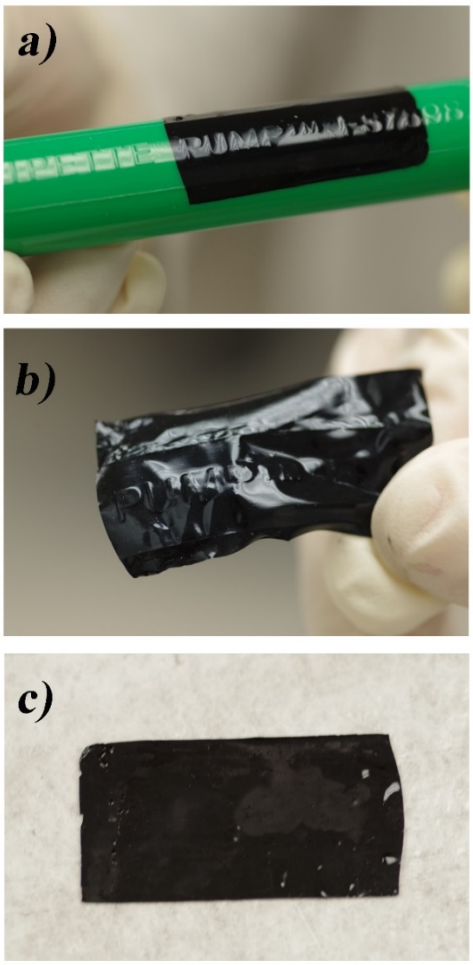

Figure S11. Moldable and erasable PEDOT:PSS films. a) laminating a wet PEDOT:PSS film on a cylinder with the word “PUMP”; b) delaminating the film transfers the word “PUMP” onto PEDOT:PSS and the “PUMP” shape remains after film dries; c) the word “PUMP” disappears after wetting the dry film in water, which demonstrates water erases the printed shape (“PUMP”) on PEDOT:PSS.

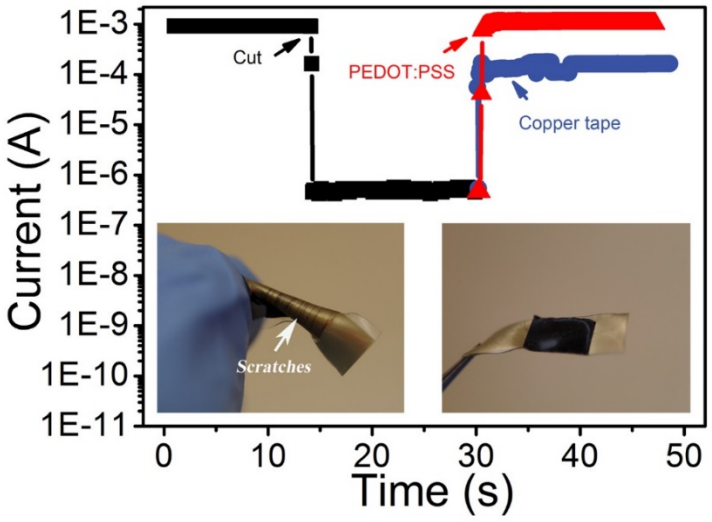

Figure S12. Damage repairing using PEDOT:PSS films. Use of PEDOT:PSS free-standing films to repair Au contacts. Current change of the 40 nm Au film deposited on PDMS (biased at 0.2 V) after scratching (black); after repairing by copper tape (blue); and after repairing by wet free-standing PEDOT:PSS (with 5 v/v% glycerol) (red). Inset: scratches of Au film and good PEDOT:PSS conformation on Au/PDMS substrate.

APPENDIX E – LIST OF PUBLICATIONS AT POLYTECHNIQUE MONTREAL NOT INCLUDED IN THE THESIS

1. F. Boubée de Gramont, **S. Zhang**, G. Tomasello, P. Kumar, A. Sarkissian, F. Cicoira, Highly stretchable electrospun conducting polymer nanofibers, Appl. Phys. Lett , 2017, 111, 093701.

2. P. Kumar, E. Di. Mauro, **S. Zhang**, A. Pezzella, F. Soavi, C. Santato, F. Cicoira, Melanin-based flexible supercapacitors, J. Mater. Chem. C, 2016, 4 (40), 9516-9525.

3. E. Di. Mauro, O. Carpentier, SIY. Sanchez, NI. Ignoumba, M. Lalancette-Jean, J. Lefebvre, **S. Zhang**, CFO. Graeff, F. Cicoira, C. Santato, Resistive Switching Controlled by the Hydration Level in Thin Films of the Biopigment Eumelanin, J. Mater. Chem. C, 2016, 4 (40), 9544-9553.

4. P. Kumar, Z. Yi, **S. Zhang**, A. Sekar, F. Soavi, F. Cicoira, Effect of channel thickness, electrolyte ions, and dissolved oxygen on the performance of organic electrochemical transistors, Appl. Phys. Lett, 2015, 107, 053303.

5. H. Tang*, P. Kumar*, **S. Zhang***, Z. Yi, GD. Crescenzo, C. Santato, F. Soavi, F. Cicoira, Conducting Polymer Transistors Making Use of Activated Carbon Gate Electrodes, ACS Appl. Mater. Interface, 2014, 7 (1), 969-973, ***Equally Contributed**.

6. X. Meng, **S. Zhang**, M. Barbosa, B. Baloukas, D. Chartrand, F. Cicoira and C. Santato, Electrolyte-gated phototransistors based on tungsten oxide films, Adv. Mater. Interfaces (Submitted).

7. **S. Zhang**, Y. Li, F. Cicoira, Intrinsically stretchable conducting polymer transistors (In preparation).

APPENDIX F – PARTICIPATION TO CONFERENCES

1. **S. Zhang**, and F. Cicoira, Flexible, stretchable and healable electronics, Oral, 67th Canadian Chemical Engineering Conference, 2017, Edmonton.

2. **S. Zhang**, and F. Cicoira, Water-enabled healing of conducting polymer films, Poster, NanoCanada, 2017, Montreal.

3. **S. Zhang**, F. Cicoira, Water-enabled healing of conducting polymer films, Poster, Surface Canada, 2017, Montreal.

4. **S. Zhang**, G. Tomasello, P. Kumar, F. Cicoira, Self-Healing Behavior of Conducting Polymer Films for Stretchable Bioelectronics, Oral, MRS Fall 2016, Boston.

5. **S. Zhang**, E. Hubis, P. Kumar, C. Girard, F. Cicoira, Stretchable organic bioelectronics devices, Oral, MRS Fall 2015, Boston.

6. **S. Zhang**, C. Girard, E. Hubis, P. Kumar, F. Cicoira, Flexible and highly stable organic electrochemical transistors, Oral, MRS Fall 2015, Boston.

7. **S. Zhang**, X. Meng, P. Kumar, H. Tang, F. Cicoira, Evolution of PEDOT:PSS in Organic Electrochemical Transistor, Poster, MRS Fall 2014, Boston.

8. **S. Zhang**, F. Cicoira, Processing of Conducting Polymer Thin Films for Organic Electrochemical Transistors, Oral, MRS Spring 2014, San Francisco.

APPENDIX G – SCHOLARSHIPS AND AWARDS RECEIVED AT POLYTECHNIQUE MONTREAL

1. Chinese Government Award for Outstanding Self-financed Students Abroad, 2016.

2. National Research Council Canada (NRC) Industrial Collaboration Award (Honorable Mention), 2015.

3. Vanier Canada Graduate Scholarships, NSERC, Canada Federal Government, 2014.

4. Le Fonds de recherche du Québec – Nature et technologies (FRQNT), Merit scholarship program for foreign students, (PBEEE-V1), 2014, declined.

5. Canada Mitacs Globalink Research Award, 2014.